Université d'Ottawa • University of Ottawa

PERMISSION DE REPRODUIRE ET DE DISTRIBUER LA THÈSE

PERMISSION TO REPRODUCE AND DISTRIBUTE THE THESIS

NOM DE L'AUTEUR / NAME OF AUTHOR:	ZHENG, Sheng
ADRESSE POSTALE / MAILING ADDRESS:	306-345 CLARENCE STREET OTTAWA ON K1N5R5
GRADE / DEGREE:	**ANNÉE D'OBTENTION / YEAR GRANTED**
M.A.Sc. (Chemical Engineering)	2003
TITRE DE LA THÈSE / TITLE OF THESIS: BIODIESEL PRODUCTION FROM WASTE FRYING OIL = CONVERSION MONITORING AND MODELING	

L'auteur permet, par la présente, la consultation et le prêt de cette thèse en conformité avec les règlements établis par le bibliothécaire en chef de l'Université d'Ottawa. L'auteur autorise aussi l'Université d'Ottawa, ses successeurs et cessionnaires, à reproduire cet exemplaire par photographie ou photocopie pour fins de prêt ou de vente au prix coûtant aux bibliothèques ou aux chercheurs qui en feront la demande.

Les droits de publication par tout autre moyen et pour vente au public demeureront la propriété de l'auteur de la thèse sous réserve des règlements de l'Université d'Ottawa en matière de publication de thèses.

The author hereby permits the consultation and the lending of this thesis pursuant to the regulations established by the Chief Librarian of the University of Ottawa. The author also authorizes the University of Ottawa, its successors and assignees, to make reproductions of this copy by photographic means or by photocopying and to lend or sell such reproductions at cost to libraries and to scholars requesting them.

The right to publish the thesis by other means and to sell it to the public is reserved to the author, subject to the regulations of the University of Ottawa governing the publication of theses.

N.B. LE MASCULIN COMPREND ÉGALEMENT LE FÉMININ

April 2, 2003

DATE

Sheng Zheng

(AUTEUR) SIGNATURE (AUTHOR)

Université d'Ottawa · University of Ottawa

Université d'Ottawa · University of Ottawa

FACULTÉ DES ÉTUDES SUPÉRIEURES ET POSTDOCTORALES

FACULTY OF GRADUATE AND POSTDOCTORAL STUDIES

ZHENG, Sheng

AUTEUR DE LA THÈSE - AUTHOR OF THESIS

M.A.Sc. (Chemical Engineering)

GRADE - DEGREE

Chemical Engineering

FACULTÉ, ÉCOLE, DÉPARTEMENT - FACULTY, SCHOOL, DEPARTMENT

TITRE DE LA THÈSE - TITLE OF THE THESIS

Biodiesel Production from Waste Frying Oil:
Conversion Monitoring and Modeling

Marc A. Dubé, David McLean and Morris Kates

DIRECTEUR DE LA THÈSE - THESIS SUPERVISOR

EXAMINATEURS DE LA THÈSE - THESIS EXAMINERS

K. Kennedy

A. Tremblay

J.-M. De Koninck, Ph.D.

LE DOYEN DE LA FACULTÉ DES ÉTUDES SUPÉRIEURES ET POSTDOCTORALES

SIGNATURE

DEAN OF THE FACULTY OF GRADUATE AND POSTDOCTORAL STUDIES

BIODIESEL PRODUCTION FROM WASTE FRYING OIL: CONVERSION MONITORING AND MODELING

by

Sheng Zheng

A thesis submitted to the Faculty of Graduate and Postdoctoral Studies in partial fulfillment of the requirements for the degree of

Master of Applied Science, Chemical Engineering

in the

DEPARTMENT OF CHEMICAL ENGINEERING

UNIVERSITY OF OTTAWA

Abstract

Biodiesel is a clean-burning substitute for petroleum-based diesel produced from virgin or waste vegetable oils and animal fats. One obstacle to the development of biodiesel is its high cost compared to petroleum diesel. Using waste frying oil instead of virgin oil can significantly reduce the high production cost. In our lab, promising preliminary results have indicated that transesterification of waste frying oil catalyzed by sulphuric acid has sufficient commercial feasibility to warrant further investigation.

In order to better understand the acid-catalyzed transesterification process and to optimize the process yield, an empirical study of the reaction kinetics was carried out. A mixture design for feed compositions at various temperatures was used to determine their effects on conversion rates and yields. Empirical models were built to describe the relationships of interest. Rate of mixing, feed composition and temperature were chosen as independent factors in this study. Intensity of mixing was found to have no significant effect on the yield over 100 rpm. The methanol to oil ratio and temperature were the most significant factors affecting the yield. Finally, a region of optimum operating conditions was determined from the models.

Analytical methods played an important role in our study. The extent of the reaction was followed off-line by gel permeation chromatography (GPC) and compared to results using an off-line infrared sensor based on attenuated total reflectance-Fourier transform infrared (ATR-FTIR) spectroscopy. The development, use and evaluation of the off-line method were discussed. The reproducibility of both methods was found to be excellent ($\leq$ 1%); data obtained from both methods were found to be reliable. Finally, a comparison of the two methods showed good agreement (within 2%) in the monitoring of the transesterification reaction.

Résumé

Le biodiesel est un substitut de combustion sensible à l'environnement pour le diesel à base pétrolière, qui est produit à partir d'huiles végétales et de graisses animales vierges ou superflues. Un obstacle à la commercialisation du biodiesel est son coût plus élevé comparativement au diesel à base pétrolière. L'utilisation de l'huile de cuisine superflue au lieu de l'huile vierge peut réduire de façon significative le coût de production élevé. Dans notre laboratoire, des résultats préliminaires prometteurs ont indiqué que la transestérification de l'huile de cuisine superflue par l'acide sulfurique possède suffisamment de faisabilité commerciale pour justifier d'avantage de recherche.

Pour mieux comprendre le procédé de transestérification catalysé d'acide et d'optimiser le rendement du procédé, une étude empirique de la cinétique de réaction a été effectuée. Une conception de mélange de compositions à l'entrée à diverses températures a été employée pour déterminer leurs effets sur les taux de conversion et les rendements. Des modèles empiriques ont été établis pour décrire les relations d'intérêt. Le taux de mélange, la composition à l'entrée et la température ont été choisis comme facteurs indépendants pour les fins de cette étude. Il a été observé que le taux de mélange n'avait aucun effet significatif sur le rendement au-delà de 100 rpm. Le ratio méthanol:huile et la température étaient les facteurs les plus importants affectant le rendement. Finalement, une région de conditions d'opération optimale a été déterminée à partir des modèles.

Les méthodes analytiques ont joué un rôle important dans notre étude. Le progrès de la réaction était suivi hors-ligne en utilisant la chromatographie de perméation de gel (gel permeation chromatography, GPC) et comparé aux résultats utilisant une sonde infrarouge hors-ligne basée sur la spectroscopie réflectivité totale atténuée – transformation infrarouge Fourier (attenuated total reflectance – Fourier transform infrared, ATR-FTIR). L'élaboration, l'utilisation et l'évaluation de la méthode hors-ligne ont été discutées. La reproductibilité des deux méthodes s'est avérée excellente ($\leq 1\%$); il a été conclu que les données obtenues à partir des deux méthodes sont fiables. Finalement, une comparaison des deux méthodes a démontré une bonne concordance dans la surveillance de la réaction de transestérification.

Statement of Contributions of Collaborators

I hereby declare that I am the sole author of this thesis. The experimental design, experiments, data analyses and the associated model building were all performed by myself.

My supervisors, Professors Marc A. Dubé, David D. McLean and Morris Kates, provided editorial comments to my written work and devoted supervision throughout my Master of Applied Science research.

Signature: 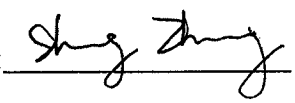

Date: April. 2, 2003

Acknowledgements

Many people have contributed to my thesis. First and foremost I would like to thank my supervisors Dr. Marc A. Dubé, Dr. David D. McLean and Dr. Morris Kates, for their endless care and patient supervision, and for giving their superb and creative suggestions and extensive criticism throughout my research.

I would also like to thank our great team, Hong Hua, Marc Laplante, Yi Zhang, Stéphane Roberge and Renata Jovanović, for their support and encouragement, and for the wonderful time we have shared together.

I am grateful for the help from the Chemical Engineering Department technical support staff Louis Tremblay, Franco Ziroldo and Gerard Nina for their patient help with my experiments. I owe special thanks to Louis, without whose help, none of my experiments could have been carried out.

I would like to thank the support staff and other professors, as well as the Dept. of Chemical Engineering for their help during my Master's study.

Finally I would like to express my grateful thanks to my family and friends, without whose unquestioning support, my work would not be possible.

Table of Contents

List of Tables

List of Figures

Abbreviations and Nomenclature

^{1}H NMR	proton nuclear magnetic resonance
a, *b*	model parameters
ATR-FTIR	attenuated total reflectance-Fourier transform infrared
D_a	diameter of the impeller (mm)
DG	diglyceride
DiComp	diamond-composite
E(Y)	expected values of the response variable
F	*F* distribution is a distribution used most commonly in analysis of variance
FAAE	fatty acid alkyl ester
FAME	fatty acid methyl ester
FFA	free fatty acid
GC	gas chromatography
GPC	gel permeation chromatography
HPLC	high performance liquid chromatography
IR	infrared
k	overall reaction rate of the transesterification
LC-GC	liquid chromatography with gas chromatography
MG	monoglyceride
n	number of observations in a model
n	rotational speed of the impeller (round/s)
N	numbers of moles (mol)

N_{Re}	Reynolds number as defined in Equation 4.12
NIR	near infrared
NMR	nuclear magnetic resonance
p	number of parameter estimates in a model
PTFE	polytetrafluoroethylene
R	ratio used to check the adequacy of a model
Q	ratio used to compare two models using extra sum square test
R^2	proportion of the total variation that explained by a model
SEC	size-exclusion chromatography
SSres	sum of square of residuals
t	reaction time (min)
t_0	lag time of a reaction (min)
$t_{1/2}$	time to reach ½ of the maximum obtainable conversion (min)
T	coded value of the reaction temperature (arbitrary unit)
TG	triglyceride
THF	tetrahydrofuran
TLC	thin layer chromatography
w	difference between the off-line ATR-FTIR and GPC analyses (molar fractional conversion)
x	initial fractional molar composition of the reaction mixture
X	fractional molar conversion
X_{240}	conversion of a reaction at 240 min (molar fraction)
X_{max}	maximum obtainable conversion of a reaction (molar fraction)

Y	estimated responses
Z	matrix
β	model parameters
μ	viscosity of fluid (Pa·s)
ν	degree of freedom
ρ	density of a fluid (kg/m^3)
$\hat{\rho}$	estimated correlation matrix of a model
σ^2	variance

CHAPTER 1

INTRODUCTION

1.1 Biodiesel

Biodiesel is a clean-burning diesel fuel produced from vegetable oils, animal fats, or waste grease. Its chemical structure is that of methyl esters of fatty acids. Due to diminishing petroleum reserves and environmental consequences of exhaust gases from petroleum-derived fuels, such as gasoline and diesel, biodiesel has attracted attention during the past decade as a renewable and environmentally friendly fuel.

Using renewable resources as fuel is not a new practice. In 1895, Dr. Rudolf Diesel first developed the diesel engine with the full intention of running it on a variety of fuels, including vegetable oil. Work on plant-derived fuel expanded during World War II due to fuel shortages, and interest in biodiesel revived in the late 1970's during the "energy crisis".

Because biodiesel is made entirely from vegetable oil or animal fats, it is renewable, biodegradable, and does not contain any sulphur, aromatic hydrocarbons, metals or crude oil residues. Moreover, because biodiesel is plant-derived, it helps to reduce the greenhouse effect. A 1998 biodiesel lifecycle study, jointly sponsored by the US Department of Energy and the US Department of Agriculture (National biodiesel board, www.biodiesel.org), concluded biodiesel reduces net CO_2 emissions by 78 percent compared to petroleum diesel (Sheehan et al., 1998). This is due to biodiesel's closed carbon cycle. The CO_2 released into the atmosphere when biodiesel is burned is recycled by growing plants, which are later processed into fuel. In addition, the emissions of

blended biodiesel with petroleum diesel can also be reduced. Sheehan et al. (1998) found that the B-20 (20% biodiesel/80% conventional #2 diesel blend) reduces net CO_2 emission by 16%. Thus biodiesel reduces green house gas emissions and helps mitigate "global warming". Biodiesel is better than petroleum diesel for the environment because it has lower emissions compared to petroleum diesel. According to research at the Southwest Research Institute, compared with low-sulphur No. 2 diesel, B-20 with an oxidation catalyst reduced particulate matter by 45%, total hydrocarbons by 65%, and carbon monoxide by 41% (Von Wedel, 1999). Biodiesel is the only alternative fuel to fully comply with the health effects testing requirements of the Clean Air Act (National Biodiesel Board, www.biodiesel.org). Since it is made domestically from renewable resources such as soybeans, its use decreases our dependence on foreign oil and contributes to our own economy.

Like petroleum diesel, biodiesel operates in compression-ignition engines, such as private vehicles, industrial fleet trucks, off-road and farm equipment, boat engines and generators. Essentially no engine modifications are required, and biodiesel maintains the payload capacity and range of diesel. Because biodiesel is oxygenated, it is a better lubricant than diesel fuel, and increases the life of engines. Diesel engines combust biodiesel more completely than petroleum diesel (National Biodiesel Board). The flash point (the point at which fuel ignites) of biodiesel in its pure form is more than 149°C (300°F) compared to about 52°C (125°F) for regular No. 2 diesel. This makes biodiesel the safest fuel to use, handle and store. With its relatively low emission profile, it is an ideal fuel for use in sensitive environments, such as marine areas, national parks and forests, and heavily polluted cities.

One problem with biodiesel is its high cost largely due to the high cost of virgin oil. At present, the price of biodiesel is about 1.4-2.4 US $/US gal, compared with 1.0-1.5 US $/US gal for petroleum diesel (Coltrain, 2002). The cost of biodiesel could be significantly reduced by the use of waste frying oil (Zhang et al., 2002). Several successful studies have been done on the production of biodiesel from waste oils or animal fats (Nye et al., 1983; Watanabe et al, 2001). Experiments in our laboratory (Ripmeester, 1998; McBride, 1999) showed that waste frying oil could reach 100% conversion to biodiesel within a reasonable time period (about 3 hrs at 70°C) through transesterification with an excess of methanol (methanol: oil ratio was 250:1) catalyzed by sulphuric acid.

Every year in Japan, thousands of tons of waste edible oil are discharged into the environment; only half of this amount is estimated to be recycled as animal feed or as raw material for lubricant and paint (Watanabe et al., 2001). Production of biodiesel from waste oil and grease provides a clean way to avoid the environmental damage and reduce CO_2 emission. Many countries have become aware of the problem of global warming and have started to take action to reduce greenhouse gases. Currently, biodiesel is being used in public transportation in Europe, Japan and North America (Watanabe et al., 2001). Several local governments in Japan began using biodiesel derived from waste frying oil for public transportation. Here in Canada, the federal government has already set its goal to increase production of biodiesel to 500 million litres to reach its Kyoto target for reducing greenhouse gas emissions (Thompson, 2002). Ontario dropped all provincial tax on biodiesel in its budget in June 2002, and a provincial committee has recommended all diesels in Ontario should contain at least some biodiesel by 2006 (CBC Newsworld,

2002). In Montreal, a "biobus" project was launched in May 2002; the eventual goal of the project is to have the city buses use biodiesel derived from recycled sub-food-grade vegetable oil and animal fats for fuel (CBC Newsworld, 2002).

Biodiesel production is now commercialized in many countries. The first industrial plant in the world with a biodiesel production capacity of 10,000 tons per year went into operation in Australia in 1991 (Agarwal and Das, 2001). In Ireland, two pilot projects on the use of biodiesel in commercial vehicles were reported (Agarwal and Das, 2001). In the U.S and Japan, biodiesel has also been commercialized since the 1990s. In Austria, about 6,000 tons of methyl esters from waste frying oil have been produced per year and used successfully as a 100% fuel substitute in a series of different vehicles (Mittelbach et al., 2001).

1.2 Transesterification

Currently, most of the commercially available biodiesel is produced by transesterification. Transesterification is an exchange reaction between an alcohol and an ester catalyzed by acid or alkali catalysts. The reaction consists of transforming triglyceride (TG) into fatty acid alkyl esters (FAAE), in the presence of an alcohol and an alkaline or acidic catalyst with glycerol as a major by-product. In Figure 1.1, ***R***s represent typical fatty acid hydrocarbon chains (14-20 carbon atoms, 0-2 double bonds), and ***X*** represents the alcohol alkyl group.

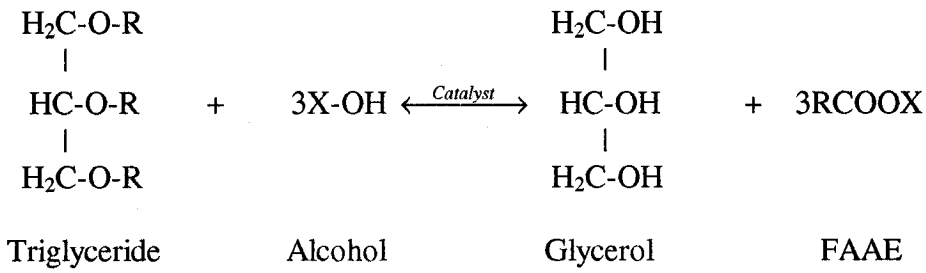

Figure 1.1 Stoichiometric reaction for the conversion of a TG into FAAE.

The transesterification reaction is a three-step reaction as follows

Triglyceride (TG) + X-OH $\xleftrightarrow{Catalyst}$ Diglyceride (DG) + RCOOX

Diglyceride (DG) + X-OH $\xleftrightarrow{Catalyst}$ Monoglyceride (MG) + RCOOX

Monoglyceride (MG)+ X-OH $\xleftrightarrow{Catalyst}$ Glycerol (GL) + RCOOX

Since most of the fatty acid methyl esters (FAME, a.k.a. biodiesel) produced commercially today are made by the alkali-catalyzed reaction from high quality virgin oil, the cost of biodiesel is relatively higher than petroleum-based diesel. In order to reduce the production cost and make it competitive with petroleum diesel, low cost feedstocks, such as non-edible oils and waste frying oils, could be used to make biodiesel. However, the relatively higher amount of free fatty acids in waste frying oil, may result in the production of soap in the presence of the alkali catalyst. Thus, an additional step to remove the free fatty acids (FFA) or soap from the reaction mixture may be required.

Acid catalysts showed many advantages when used in the transesterification of waste cooking oils compared to alkali catalysts (Canakci and Van Gerpen, 1999). With the acid catalyst, the reaction is simplified to a single step. However, one drawback is the requirement for the reactor to withstand an acidic environment, which would increase the production cost of biodiesel. An economic assessment by Zhang et al. (2001) was carried

out on four different continuous processes with different types of oil (virgin vs. waste) and catalysts (acid vs. alkali). The study showed that although the alkali-catalyzed process using virgin oil has the lowest capital investment cost, the cost of using virgin oil leads to a high total manufacturing cost. When waste frying oil is used in the alkali-catalyzed process, a pre-treatment unit is required to reduce the content of free fatty acid. Thus the cost associated with the pre-treatment unit would balance the credit of using waste frying oil. In contrast, the acid-catalyzed process using waste frying oil did not require a pre-treatment step and had the lowest total manufacturing cost, and the highest profit in operating a biodiesel plant.

1.3 Analytical Methods

1.3.1 Gel Permeation Chromatography

Gel permeation chromatography (GPC), or size-exclusion chromatography (SEC) - separates components on the basis of their hydrodynamic size. It allows obtaining the molecular weights of the components as well as their molecular weight distribution. Separation is achieved by the use of columns packed with porous "gel" particles. Those particles do not interact with the sample molecules. The molecules diffuse from the mobile liquid phase into the stationary gel phase. Molecules smaller than the pore size can enter the particles and therefore have a longer path and longer residence or retention time in the column than larger molecules that cannot enter the particles. Molecules having different sizes and shapes therefore have different total residence times in the column. Molecules larger than the pore size can not enter the pores and will elute first and molecules that are smaller than the pore size can enter all pores and have the longest

residence time on the column and will elute later. GPC has been primarily used for the fractionation and mass analysis of high molecular weight species such as polymers and proteins.

The composition of the transesterification products, in terms of TG, DG, MG, FFA, glycerol and FAME can be readily determined by GPC. GPC analysis time is short (about 10-30 minutes) and sample preparation is straightforward.

1.3.2 ATR-FTIR Spectroscopy

ATR-FTIR spectroscopy is an analytical technique used to identify organic (and in some cases inorganic) materials. This technique measures the absorption of various infrared light wavelengths by the material of interest. These infrared absorption bands identify specific molecular components and structures. Absorption bands in the range of 1500 - 4000 wavenumbers are due to typical functional groups (e.g. -OH, C=O, N-H, CH_3, etc.). The region between 1500 - 4000 wavenumbers is referred to as the fingerprint region. Absorption bands in this region are generally due to intra-molecular phenomena, and are highly specific for each material. The specificity of these bands allows identifying the material. When used in the reactions, time-dependent or temperature-dependent kinetic profiles may be derived by monitoring continuously at a characteristic fixed wavenumber the absorption intensity of a functional group, which is either associated with a particular reactant or attributed to a product, this is called in-line monitoring. The monitoring can also be done off-line.

ATR-FTIR spectroscopy has been widely used in qualitative and quantitative analysis of organic compounds. It is routinely used to estimate the identity and concentration of absorbing species in multicomponent system.

ATR-FTIR spectroscopy has received attention for use in the qualitative and quantitative analysis of the oil and fats (Yang and Irudayaraj, 2001; Verleyen et al., 2001). It is sensitive, rapid, easy to handle, and very cost-effective compared with other methods.

1.4 Objectives

The objectives of this thesis are to carry out an empirical study of the acid-catalyzed transesterification from waste frying oil, using GPC and ATR-FTIR spectroscopy; also to compare and assess the suitability of ATR-FTIR spectroscopy and GPC methods for the study of acid-catalyzed transesterification of waste frying oil, and to evaluate the possibility of monitoring the transesterification in-line using ATR-FTIR spectroscopy. The reliability of data obtained from the analytical methods, and the reproducibility of the methods were investigated. A mixture design (Box et al., 1978) for feed compositions at various temperatures was used to determine their effects on conversion rates and yields. Finally, empirical models were used to describe the relationships of interest and to obtain the region of optimum reaction conditions.

1.5 Thesis Outline

The second chapter of this thesis provides a literature review of biodiesel research and kinetic studies. The thesis also includes two manuscripts to be submitted for publication in refereed journals. The first manuscript, which forms Chapter 3 of the thesis, discusses the analytical techniques used to monitor the reaction kinetics both off-line and in-line. Chapter 4, the second manuscript, contains the results of our kinetic

study and model development. Chapter 5 contains a brief summary discussion of the entire thesis, concluding remarks and recommendations for future work. Finally, references and an appendix containing charts and graphs are included.

1.6 References

Agarwal, A. K. and L. M. Das, "Biodiesel Development and Characterization for Use as a Fuel in Compression Ignition Engines", J. Eng. Gas Turb.& Power **123**, 440-447 (2001).

Box, G. E. P., W.G. Hunter and J. S. Hunter, "Statistics for experimenters : an introduction to design, data analysis, and model building", Wiley, New York (1978).

Canakci, K., J. Van Gerpen, "Biodiesel Production via Acid Catalysis", Transactions of the ASAE **42**, 1230-1210 (1999).

Coltrain, D., "Biodiesel: Is It Worth Considering", 2002 Risk and Profit Conference, Manhattan, Kansas (2002).

CBC Newsworld, "Canadian inventors, governments aim to cut costs of biodiesel" CBC News Online (June 28, 2002).

Darnoko, D., M. Cheryan, and E.G. Perkins, "Analysis of Vegetable Oil Transesterification Productions by Gel Permeation Chromatography", J. Liq. Chrom. & Rel. Technol. **23**, 2327-2335 (2000).

McBride, N., "Modeling the Production of Biodiesel from Waste Frying Oil", B.A.Sc graduate thesis (unpublished), 1999.

Mittelbach, M. and Gangl, S., "Long Storage Stability of Biodiesel Made from Rapeseed and Used Frying Oil", J. Am. Oil Chem. Soc.**78**, 573-577 (2001).

Nye, M.J., T.W. Williamson, S. Deshpande, J.H. Schrader and W.H. Snively, "Conversion of Used Frying Oil to Diesel Fuel by Transesterification: Preliminary Test", J. Am. Oil Chem. Soc. **60**, 1598-1601 (1983).

Ripmeester, W., "Modeling the Production of Biodiesel from Waste Frying Oil", B.A.Sc graduate thesis (unpublished), 1998.

Sheehan, J., V., Camobreco, J., Duffield, M., Graboski, and H., Shapouri, "Life-cycle inventory of biodiesel and petroleum diesel for use in an urban bus". Report: NREL/SR-580-24089, http://www.ott.doe.gov/biofuels/lifecycle_pdf.html (1998).

Thompson, J., CBC Newsworld, "Canada's new plan for Kyoto", CBC News Online (Nov. 21, 2002).

Verleyen, T., R.Verhe, A. Cano, A. Huyhebaert, and W.De Greyt, "Influence of Triacylglycerol Characteristics on the Determination of Free Fatty Acids in Vegetable Oils by Fourier Transform Infrared Spectroscopy", J. Am. Oil Chem. Soc.**78**, 981-984 (2001).

Von Wedel, R., "Technical Handbook for Marine Biodiesel In Recreational Boats", National Biodiesel Board, http://www.biodiesel.org (1999).

Watanabe, Y., Y. Shimada, A. Sugihara and Y. Tominaga, " Enzymatic Conversion of Waste Edible Oil to Biodiesel Fuel in a Fixed-bed Bioreactor", J. Am. Oil Chem. Soc. **78**, 703-707 (2001).

Yang, H., and J. Irudayaraj, "Comparison of Near-Infrared, Fourier Transform-Infrared and Fourier Transform-Raman Methods for Determining Olive Pomace oil Adulteration in Extra Virgin Olive Oil", J. Am. Oil Chem. Soc.**78**, 889-895 (2001).

Zhang, Y., M.A. Dubé, D.D. McLean, and M. Kates, "Biodiesel Production from Waste Cooking oil: Process Design and Technological Assessment", Bioresource Technol. (to be published).

CHAPTER 2

LITERATURE REVIEW

2.1 Analytical Methods

Many analytical methods have been employed in biodiesel research, such as: gas chromatography (GC) (Freedman et al., 1986; Peterson, 1991; Lechner et al., 1997; Mittlebach, 1996), liquid chromatography with gas chromatography (LC-GC) (Plank and Lorbeer, 1995), thin layer chromatography (TLC) (Freedman et al., 1984), high performance liquid chromatography (HPLC) (Mittlebach, 1996; Noureddini and Zhu, 1997; Holčapek, 1999), nuclear magnetic resonance (NMR) spectroscopy (Knothe, 2000), near infrared (NIR) spectroscopy (Knothe, 1999; Knothe, 2000) and gel permeation chromatography (GPC) (Darnoko et al., 2000).

GC has found wide application in the analysis of triglyceride (TG) or complex mixtures containing acylglycerols (Lechner et al., 1997). Freedman et al. (1986) first applied GC for their study of soybean oil transesterification. GC is also generally regarded as the most precise and the reproducible method (Plank and Lorbeer, 1995). However, the accuracy of GC analysis can be influenced by factors such as baseline drift, overlapping signals, etc (Knothe, 2000). GC also requires derivatization of samples, which is laborious and time- and reagent-consuming.

LC-GC was also applied to the analysis of sterols in biodiesel from derived different vegetable oils (Knothe, 2000). Lechner et al. (1997) developed a reliable on-line LC-GC quantification of monoglyceride (MG), diglyceride (DG), and TG. However, they

also mentioned the methods didn't work well on the analysis of fuel derived from waste frying oil, which contained large amounts of unidentified dimerization products.

TLC is a simple method using simple sample preparation (Freedman et al., 1984; Kates, 1986). TLC is basically a qualitative method, quantification being difficult. TLC has therefore not been used extensively for quantitative analyses of oils. HPLC is less time- and reagent-consuming compared with GC (Knothe, 2000). Trathnigg and Mittelbach (1990) first developed an isocratic solvent system on a cyano-modified silica column coupled to two GPC columns. The system was useful for quantitation of various degrees of transesterification conversion. Holčapek et al. (1999) carried out an extensive study on transesterification using different detection methods; they found that the sensitivity and linearity of each detection method varied with the individual TG. HPLC was not used in our study because of availability.

NMR spectroscopy was first used for determining the yield of the transesterification of rapeseed oil with methanol (Gelbard et al., 1995). It is precise but it is useful mainly for identification and not quantitative analysis. NIR spectroscopy has attracted a lot of attention recently because it provides a possible method of rapid, easy to handle, and cost-effective monitoring of the transesterification reaction and of biodiesel fuel quality (Knothe, 2000). At 6005 cm^{-1} and at 4425-4430 cm^{-1}, the absorbance of methyl esters was stronger than that of TG, which were used in the conversion monitoring of the transesterification; the monitoring results from NIR spectroscopy were also compared with ^{1}H NMR, the results of the two methods showed good agreement (Knothe, 2000). NIR spectroscopy and ^{1}H NMR were also used for determining the blend level of mixtures of biodiesel with conventional diesel (Knothe, 2001). However, there are no

reports about whether the NIR spectroscopy can identify other components in the transesterification, such as DG and MG, and nor whether an in-line monitoring of the transesterification reaction can be carried out by NIR spectroscopy.

Among these analytical methods GPC appears to be the most promising. Darnoko et al. (2000 a) reported excellent linearity of calibration curves for the mass calculation of MG, DG, TG, and methyl esters components, and the method showed good reproducibility. Their analysis of mixtures of these standards with different compositions showed a relative standard deviation of 0.27% - 3.87%. In the kinetic study of the alkali-catalyzed palm oil transesterification in a batch reactor, Darnoko et al. (2000 b) used GPC for their analysis. It proved to be effective in the composition analysis of transesterification.

ATR-FTIR spectroscopy is a method newly employed in the analysis of vegetable oils. Currently, published reports show that it is mostly employed in the qualitative assessment of vegetable oil. It has been used in the determination of free fatty acids in vegetable oils (Verleyen et al., 2001) and of olive pomace oil adulteration in extra virgin oil and showed good prediction of the adulteration (Yang and Irudayaraj, 2001). Recently, ATR-FTIR spectroscopy has been used in the determination of soap in refined vegetable oils (Mirghani, et al, 2002). Small differences in structure can be detected and quantitated, which makes it useful in the study of biodiesel production. The methyl ester displays different absorbance from TG at 1378 cm^{-1}, which can be calibrated and used for determining the composition of TG and methyl ester. The structures of DG and MG, however, are too similar to that of TG, and thus cannot be distinguished from TG. With

the development of ATR-FTIR technology, the extent of the reaction should easily be monitored. It is sensitive, rapid, and very cost-effective compared to other methods.

2.2 Oil Transesterification

The use of vegetable oil directly as diesel fuel has been shown to be unsatisfactory and impractical, mostly due to the high viscosity of the oil (Ma and Hanna, 1999). Four well-known techniques are available to reduce the viscosity level of vegetable oils, namely dilution, pyrolysis, micro-emulsion, and transesterification. Dilution can be accomplished with solvents like ethanol or petroleum diesel fuel. Pyrolysis refers to the chemical change induced by the action of heat. Micro-emulsion refers to a system consisting of a liquid dispersed with or without an emulsifier in an immiscible liquid. However, transesterification is the common choice, which results in a fuel with similar properties to petroleum diesel fuel.

There are three basic routes to methyl ester production from oils and fats through transesterification:

1. Alkali-catalyzed transesterification of the oil with an alcohol.
2. Acid-catalyzed transesterification of the oil with an alcohol.
3. Enzymatic transesterification of the oil with an alcohol by lipase.

Most enzymatic transesterification processes use immobilized lipase as catalyst to be able to reuse the lipase (Fukuda et al., 2001; Hsu et al., 2001). High conversion can be achieved at relatively low temperatures from virgin oils or waste oils (at about 50°C) (Hsu et al., 2001). Removal of the catalyst is less difficult than that of alkali-catalyzed and acid-catalyzed processes. One drawback is the generally high cost of enzymes. It is

well known that water content in the system affects the activity of the enzyme, thus there is a requirement for low water content in the system (Iso et al., 2001). The recycling of enzymes is also a potential factor that affects the production of biodiesel. The search for efficient lipases and cost of their production has not been optimized yet (Hsu et al., 2001).

Alkalis used in the production of biodiesel include NaOH, KOH, carbonates, and alkoxides such as sodium methoxide, sodium ethoxide, and sodium butoxide. The alcohols include methanol, ethanol, 1-butanol, etc. Alkali-catalyzed transesterification proceeds much faster than that catalyzed by acid catalyst (Freedman, 1984), thus it is the one most used commercially. Considerable research has been done on biodiesel made from vegetable oil or waste oils using alkali catalysts. Types of oils include palm oil, soybean oil, sunflower oil, coconut oil, rapeseed oil and tung oil. Effects of moisture and free fatty acids, effect of molar ratio of alcohol to oil, effect of catalyst type and concentration, and effect of mixing have been investigated. The majority of biodiesel today is produced by alkali-catalyzed transesterification with methanol. With the alkali-catalyst, reaction time is relatively short and minimal side reactions occur. However, the vegetable oil and alcohol must be substantially anhydrous because the presence of water promotes saponification. The soap formed lowers the yield of esters and renders the separation of esters, methanol, and glycerol by water washing difficult. In addition, low free fatty acid content in TG is required for alkali-catalyzed transesterification (Freedman et al., 1984).

Freedman et al. (1982) reported a 98% yield of methyl ester in 1 hour using alkali catalysts such as sodium hydroxide or sodium methoxide with alcohols such as methanol,

ethanol, and 1-butanol. Freedman et al. (1984) investigated the effect of the molar ratio of the alcohol to oil, type of catalyst (base vs. acid), temperature and degree of refinement of the oil on the yield of biodiesel. For the alkali-catalyzed reaction, the effect of alcohol to oil ratio was found to be the most important variable affecting the yield, the highest yield being observed at a 6:1 molar ratio. It was found that the temperature had a significant effect on the yield early in the reaction; however, after 4 hr, it no longer had an impact on the yield. They also compared the alkali-catalyzed alcoholysis with the acid-catalyzed alcoholysis. It was pointed out in their study that the acid catalysts would be more effective when the degree of refinement of oil was low, and for oils that had a high free fatty acid content.

Noureddini and Zhu (1998) studied the kinetics of alkali-catalyzed methanolysis of soybean oil, and the effect of mixing and temperature on the reaction rate. The mixing effect was found to be more significant during the initial slow stage of the reaction. The effect of mixing became insignificant when the reaction rate was dominated by the temperature. They proposed a reaction mechanism consisting of an initial mass transfer-controlled stage followed by a kinetically controlled stage. The later stage was found to be second-order.

Darnoko and Cheryan (2000 b) studied the kinetics of palm oil transesterification (alkali-catalyzed) in a batch reactor; the effect of temperature and catalyst concentration on the reaction rate was investigated. They found higher temperatures ($\geq$ 50°C) did not reduce the time to reach maximal conversion; during the late stage of the reaction, the conversion of triglycerides to diglycerides, and monoglycerides were second order.

Although the acid-catalyzed transesterification is much slower than the alkali-catalyzed one, it is considered to be more suitable for oils that have relatively high amounts of free fatty acid and water (Freedman et al., 1984). As early as 1945, Keim suggested that if more water and free fatty acids are in the oil, acid-catalyzed transesterification could be used. When waste frying oil is used in the alkali-catalyzed transesterification, saponification is even more prevalent due to its higher free fatty acid content (Ahn et al., 1995). The acid-catalyzed process thus avoids the difficult and costly soap-separation step. However, due to its slow reaction rate compared to the alkali-catalyzed process, high alcohol to oil ratios are necessary to promote the conversion of oil to fatty acid methyl ester (FAME, a.k.a. biodiesel). Few reports were found on the production of biodiesel using acid catalysts.

Freedman et al. (1986) studied the transesterification kinetics of soybean oil with various alcohols in the presence of acid and base catalysts. They found that the conversion with lower alcohol to oil ratios was not satisfactory. Nye et al. (1983) reported that acid catalysts could also produce ethyl esters from waste frying oil in ethanol.

Canaki and Van Gerpen (1999) studied the acid-catalyzed transesterification of soybean oil. The effect of several variables on the reaction was investigated. The molar ratio of alcohol to oil, temperature, catalyst amount, reaction time, water and free fatty acid content were examined. In their study, water was found to strongly inhibit the ester-formation reaction; the concentration of water in the reaction mixture should be less than 0.5%. Therefore water formed by the esterification of free fatty acids would limit their presence in the oil to 5%. This study was carried out on a small scale, and the reaction contents were stirred by a magnetic stirrer. The early stages of the transesterification were

known to be mass transfer dominated, although these results might have been different if the reactions were carried out on a larger scale with improved mixing.

Ripmeester (1998) and McBride (1999) used an acid catalyst for the transesterification of waste frying oil (canola oil) with methanol. They found that nearly 100% FAME was formed in 3 hours with a feed composition of 98.1 mol% methanol, 1.5 mol% sulfuric acid and 0.4 mol% oil. They concluded that a large excess of methanol was the driving force for the reaction.

Another interesting study was that of Kusdiana and Saka (2000) reporting on the kinetics of rapeseed oil transesterification (without catalyst) in supercritical methanol. Batch transesterifications were carried out at supercritical conditions with different supercritical temperatures (200°C to 500°C) and methanol to oil ratios. The conversion of oil was found to increase dramatically in the supercritical state, and a reaction temperature of 350°C was considered as the best condition with the methanol to oil ratio being 42.

Among the numerous published studies on biodiesel, only a few are concerned with the kinetics of the transesterification of vegetable oil, and most of them were done with alkali catalysts. Because of poor reproducibility or low precision of the analytical methods, few kinetic studies have been carried out on biodiesel production. Rather, studies on the emission, fuel performance, physical properties, and environmental benefits of biodiesel have dominated the literature. A systematic conversion monitoring and modeling of the acid-catalyzed transesterification will provide a means to estimate the optimal conditions for better yields of biodiesel, and are essential for the future development of biodiesel production. That is precisely the purpose of our research.

2.3 References

Ahn, E., M. Koncar, M. Mittelbach and R. Marr, "A Low-waste Process for the Production of Biodiesel", Separation Science and Technology **30**, 2021-2033 (1995).

Canakci, K. and J. Van Gerpen, "Biodiesel Production via Acid Catalysis", Transactions of the ASAE **42**, 1230-1210 (1999).

Colthup, N. B., and L.H. Daly, "Introduction to Infrared and Raman Spectroscopy, 3rd Edition", Academic Press Inc., San Diego, Chapter 9(1990).

Coltrain, D., "Biodiesel: Is It Worth Considering", 2002 Risk and Profit Conference, Manhattan, Kansas (2002)

Connemann, J. and J. Fischer, "Biodiesel in Europe 2000: Biodiesel Processing Technologies and Future Market Development", National Biodiesel Board report, http://www.biodiesel.org (1999).

Darnoko, D., M. Cheryan, and E.G. Perkins, "Analysis of Vegetable Oil Transesterification Productions by Gel Permeation Chromatography", J. Liq. Chrom. & Rel. Technol. **23**, 2327-2335 (2000 a).

Darnoko, D., and M. Cheryan, "Kinetics of Palm Oil Transesterification in a Batch Reactor", J. Am. Oil Chem. Soc. **77**, 1263-1267 (2000 b).

Freedman, B., E.H. Pryde and T.L. Mounts, "Variables Affecting the Yields of Fatty Esters from Transesterified Vegetable Oils", J. Am. Oil Chem. Soc. **61**, 1638-1643 (1984).

Freedman, B., R.O. Butterfield and E. H. Pryde, "Transesterification Kinetics of Soybean Oil", J. Am. Oil Chem. Soc. **63**, 1375-1380 (1985).

Freedman, B., W. F. Kwolek, and E. H. Pryde, "Quantitation in the Analysis of Transesterified Soybean Oil by Capillary Gas Chromatography", J. Am. Oil Chem. Soc. **63**, 1370-1375 (1986).

Fukuda, H., A. Kondo, and H. Noda, "Review: Biodiesel Fuel Production by Transesterification of Oils", J. Biosc. Bioeng. **92**, 405-416 (2001).

Gelbard, G., O. Brès, R.M.Vargas, E. Vielfaure, and U.F. Schuchardt. "1H Nulear Magnetic Resonance Determination of the Yield of the Transesterification of Rapeseed Oil with Methanol", J. Am. Oil Chem. Soc. **72**, 1239-1241 (1995).

Goodacre, R., and E. Anklam, "Fourier Transform Infrared Spectroscopy and Chemometrics as a Tool for the Rapid Detection of Other Vegetable Fats Mixed in Cocoa Butter", J. Am. Oil Chem. Soc. **78**, 993-1000 (2001).

Holčapek, M., P. Jandera, J. Fischer, and B. Prokeš, "Analytical Monitoring of the Production of Biodiesel by High Performance Liquid Chromatography with Various Detection Methods", J. Chromatogr. A. **858,** 13-31 (1999).

Hsu, A.-F., K. C. Jones, W. N. Marmer, and T. A. Foglia, "Immobilized Lipase-catalyzed Production of Alkyl Esters of Restaurant Grease as Biodiesel", J. Am. Oil Chem. Soc. **78**, 585–588 (2001).

Iso, M., B. Chen, M. Eguchi, T. Kudo and S. Shrestha, "Production of Biodiesel Fuel from Triglycerides and Alcohol Using Immobilized Lipase", J. Molec. Catal. B: Enzymatic **16**, 53-58 (2001)

Kates, M., "Techniques in Lipidology 2nd ed.", Elsevier, Amsterdam, (1986).

Keim., G.I. "Process for treatment of Fatty glycerides", US Patent **2**, 381-601 (1945).

Knothe, G., "Rapid Monitoring of Transesterification and Assessing Biodiesel Fuel Quality by Near-Infrared Spectroscopy Using a Fibre-Optic Probe", J. Am. Oil Chem. Soc. **76**, 795-800 (1999).

Knothe, G., "Monitoring a Processing Transesterification Reaction by Fiber-Optic Near Infrared Spectroscopy with Correlation to 1H Nuclear Magnetic Resonance Spectroscopy", J. Am. Oil Chem. Soc. **77**, 489-493 (2000).

Knothe, G., " Determining the Blend Level of Mixtures of Biodiesel with Conventional Diesel Fuel by Fiber-Optic Near-Infrared Spectroscopy and ^{1}H Nuclear Magnetic Resonance Spectroscopy", J. Am. Oil Chem. Soc. **78**, 1025-1028 (2001)

Kusdiana, D., S. Saka, "Kinetics of Transesterification in Rapeseed Oil to Biodiesel Fuel as Treated in Supercritical Methanol", Fuel **80**, 693-698 (2000).

Lechner, M., C. Bauer-Plank, and E. Lorbeer, "Determination of Acylglycerols in Vegetable Oil Methyl Esters by On-line Normal Phase LC-GC", J. High Resol. Chromatogr. **20**, 581-585 (1997).

Lin-Vien, D., N.B. Colthup, W.G. Fateley, and J.G. Grasselli, "The Handbook of Infrared and Raman Characteristic Frequencies of Organic Molecules", ACADAMIC PRESS, San Diego (1991).

Ma, F. and M.A. Hanna, "Biodiesel production: a review", Bioresource Technol. **70**, 1-15 (1999).

McBride, N., "Modeling the Production of Biodiesel from Waste Frying Oil", B.A.Sc graduate thesis (unpublished), 1999.

Mirghani, M.E.S., Y.B. Che Man, S. Jinap, B. S. Baharin, and J. Bakar, "FTIR Spectroscopic Determination of Soap in Refined Vegetable Oils", J. Am. Oil Chem. Soc. **79**, 111-116 (2002).

Mittelbach, M., "Diesel Fuel Derived from Vegetable Oils, V [1]: "Gas Chromatographic Determination of Free Glycerol in Transesterified Vegetable Oil", Chromatographia **37**, 623-626 (1993).

Mittelbach, M, G. Roth, and A. Bergmann, "Simultaneous Gas Chromatographic Determination of Methanol and Free Glycerol in Biodiesel", Chromatographia **42**, 431-434 (1996).

Mittelbach, M. and S. Gangl, "Long Storage Stability of Biodiesel Made from Rapeseed and Used Frying Oil", J. Am. Oil Chem. Soc. **78**, 573-577 (2001).

Noureddini, H. and D. Zhu, "Kinetics of Transesterification of Soybean Oil", J. Am. Oil Chem. Soc. **74**, 1457-1463 (1997).

Nye, M.J., T.W. Williamson, S. Deshpande, J.H. Schrader and W.H. Snively, "Conversion of Used Frying Oil to Diesel Fuel by Transesterification: Preliminary Test", J. Am. Oil Chem. Soc. **60**, 1598-1601 (1983).

Peterson, C.L., M. Feldman, R. Korus, and D.L. Auld, "Batch Type Transesterification Process for Winter Rape Oil", ASAE **91**, 711-716 (1991).

Plank, C. and E. Lorbeer, "Simultaneous Determination of Glycerol, and MG, DG and TG in Vegetable Oil Methyl Esters by Capillary Gas Chromatography", J. Chromatogr. A. **697**, 461-468 (1995).

Plank, C. and E. Lorbeer. " On-line Liquid Chromatography/ Gas Chromatography for the Analysis of Free and Esterified Sterols in Vegetable Oil Methyl Esters Used as Diesel Fuel Substitutes", J. Chromatogr. A. **683**, 95-104 (1994).

Ripmeester, W., "Modeling the Production of Biodiesel from Waste Frying Oil", B.A.Sc graduate thesis (unpublished), 1998.

Verleyen, T., R.Verhe, A. Cano, A. Huyhebaert, and W.De Greyt, "Influence of Triacylglycerol Characteristics on the Determination of Free Fatty Acids in Vegetable Oils by Fourier Transform Infrared Spectroscopy", J. Am. Oil Chem. Soc. **78**, 981-984 (2001).

Yang, H., and J. Irudayaraj, "Comparison of Near-Infrared, Fourier Transform-Infrared and Fourier Transform-Raman Methods for Determining Olive Pomace oil Adulteration in Extra Virgin Olive Oil", J. Am. Oil Chem. Soc. **78**, 889-895 (2001).

Zhang, Y., M.A. Dubé, D. D. McLean and M. Kates, , "Biodiesel Production from Waste Cooking Oil: Economic Assessment and Sensitivity Analysis", Bioresource Technol. (to be submitted, 2002).

CHAPTER 3

MONITORING BIODIESEL PRODUCTION USING ATR-FTIR SPECTROSCOPY AND GPC (PAPER 1)

Sheng Zheng[1], Marc A. Dubé[1*], David D. McLean[1], Morris Kates[2]

[1]Dept. of Chemical Engineering, [2]Dept. of Biochemistry

University of Ottawa, 161 Louis Pasteur St., Ottawa, ON Canada K1N 6N5

Abstract

Gel permeation chromatography (GPC) and attenuated total reflectance-Fourier Transform infrared (ATR-FTIR) spectroscopy were used to monitor the production of biodiesel from waste frying oil. To evaluate the reliability and reproducibility of the methods, a quantitative analysis of mixtures of standards was carried out using both methods. A series of nested experimental designs were used to evaluate the reproducibility of procedures in both methods, as well as the sources of variability. The reproducibility of both methods was found to be excellent ($\leq 1\%$); and data obtained from both methods were found to be reliable. Finally, a comparison of the two methods showed good agreement for monitoring of the transesterification reaction.

Keywords: Biodiesel, acid-catalyzed transesterification, GPC, ATR-FTIR spectroscopy, waste frying oil.

---

* to whom correspondence should be addressed.

3.1 Introduction

Appropriate analytical methods are very important to the research of acid-catalyzed transesterification of triglycerides (TG, major component of waste frying oil). Because three step-reactions are theoretically involved in the transesterification, step-reaction products such as diglycerides (DG) and monoglycerides (MG) are always mixed together with the final product, fatty acid methyl esters (FAME, a.k.a. biodiesel). Of most concern is a means to measure the yield of biodiesel. In addition, due to the presence of the step-reaction by-products, a means to identify and quantify the various reaction components is necessary. The analytical method should also be precise, accurate, of short analysis time, and easy to use.

Many analytical methods have been used in the study of biodiesel transesterification, including gas chromatography (GC) (Freedman et al., 1986; Peterson, 1991; Mittlebach, 1993; Lechner et al., 1997; Mittlebach et al., 1996), liquid chromatography with gas chromatography (LC-GC)(Plank and Lorbeer, 1995; Lechner et al., 1997), thin layer chromatography (TLC) (Freedman et al., 1984), high performance liquid chromatography (HPLC) (Mittlebach, 1996; Noureddini and Zhu, 1997; Holčapek, 1999), nuclear magnetic resonance (NMR) spectroscopy (Knothe, 2000), and near infrared (NIR) spectroscopy (Knothe, 1999; Knothe, 2000).

Among these analytical methods, GC has been the most widely used due to its accuracy in quantifying not only TG and FAME, but also the intermediate reaction products: DG and MG. HPLC has also been found useful for quantifying the conversion of oil to FAME in the reaction. TLC and NMR spectroscopy have tended to be less reliable for qualitative purposes. More recently, near-infrared (NIR) spectroscopy was

used to monitor transesterification and assess fuel quality (Knothe, 1999; Knothe, 2000). The basis for quantification was that, at 6005 cm^{-1}, and also between 4425-4430 cm^{-1}, the methyl esters displayed peaks while TG only exhibited shoulders (Knothe, 1999). These monitoring results were also correlated with ^{1}H NMR spectroscopy and, the results of the two methods showed good agreement (Knothe, 2000). The two methods have also been used for the determination of the blend level of mixtures of biodiesel with conventional diesel (Knothe, 2001). However, there was no indication as to whether NIR spectroscopy could be used to identify the other components in the transesterification.

Of the numerous analytical methods, GPC and ATR-FTIR spectroscopy have shown good promise. GPC, or size–exclusion chromatography (SEC), separates components on the basis of their hydrodynamic size. Recently, Darnoko et al. (2000 a) developed a GPC method for the simultaneous analysis of palm oil transesterification products. Sample preparation involved only neutralization and dilution. Analysis of mixtures of standards with different compositions showed a relative standard deviation between 0.27% and 3.87%. The same method was also used for their kinetic study of palm oil transesterification in a batch reactor to investigate the effect of temperature and catalyst concentration on the reaction rate (Darnoko et al., 2000 b). The method was found to be effective in the analysis of the extent of the reaction.

ATR-FITR spectroscopy is considered to be an attractive analytical method primarily because of the ease, rapidity, and cost of analysis. ATR-FTIR spectroscopy has been used to identify organic (and in some cases inorganic) materials. This technique measures the absorption of various infrared light wavelengths by the material of interest. These infrared absorption bands are used to identify specific molecular components and

structures. Absorption bands in the range of 4000 to 1500 wavenumbers are typically due to functional groups (e.g. -OH, C=O, N-H, CH_3, etc.). The absorption of an infrared band is linearly proportional to the concentration of species giving rise to that band. It has been used for the determination of free fatty acids (FFA) in vegetable oils (Verleyen et al., 2001), and in examining olive pomace oil adulteration in extra virgin oil, showing good prediction of the adulteration (Yang and Irudayaraj, 2001). Recently, ATR-FTIR spectroscopy has been used in the determination of soap amounts in refined vegetable oils (Mirghani, et al, 2002). No reports on the monitoring of transesterification were found.

The objectives of this study were to compare and assess the suitability of ATR-FTIR spectroscopy and GPC methods for the conversion monitoring of acid-catalyzed transesterification of waste frying oil, and to evaluate the possibility of monitoring the transesterification in-line using ATR-FTIR spectroscopy. Furthermore, the reliability of the data and the reproducibility of the methods were investigated using a series of nested designs (Box et al., 1978).

3.2 Experimental Method

3.2.1 Procedures

Methanol (reagent grade, ACP Chemicals Inc.), sulfuric acid (ACS grade, BDH Chemicals Inc.), and waste canola oil (from a local restaurant, Sam's University Tavern) were used in the experiments. The FFA in oil was determined by GPC to be ~6 wt%. The oil was untreated and directly used in the transesterification.

All experiments were carried out at both 70°C and 80°C in a jacketed 5L stainless steel reactor. It was suggested volume of the reactants would not exceed 70% of volume of the reactor. The impeller used was a two-plate turbine impeller. The rotational speed of the impeller was set at 400 rpm. Pressure was allowed to vary (for 70°C range from 10 to 13 psi, and for 80°C from 24 to 28 psi) when the set point of the temperature was changed. All the experiments were conducted for 4 hrs. Nine feed compositions were chosen according to the experimental design shown in Table 3.1. All of the experiments and the sample analysis were carried out in random order to minimize any potential experimental errors.

Methanol and sulfuric acid were premixed and cooled to room temperature before use. This mixture was charged into the reactor, and the reactor was sealed, pressurized and the mechanical stirrer was started. The mixture was heated to the reaction temperature (70°C or 80°C) and the cooling water for the condenser was switched on. Oil was separately measured and preheated to 70°C, then was fed to the reactor with a liquid pump. The reaction was timed as soon as the oil was all pumped in (usually less than 1 minute).

Table 3.1 Feed compositions of experiments

	Composition (mol%)			Total
Expt.	Methanol	Acid	Oil	Volume (L)
1	98.1	1.5	0.4	2.24
2	95.6	3.5	0.9	2.56
3	94.6	3.5	1.9	2.31
4	96.5	1.5	2.0	2.29
5	96.9	2.5	0.6	2.37
6	95.1	1.5	3.4	2.53
7	95.6	2.5	1.9	2.64
8	97.3	1.5	1.2	2.28
9*	96.2	2.5	1.3	2.73

* Replicated experiment

Ten 5 mL samples were taken for each experiment and placed in 16 mL vials with plastic caps. To each sample was added about 1 mL distilled water to stop the reaction immediately, then 5 mL petroleum ether. The upper layer was retained, then washed with 1-2 mL of a methanol and distilled water mixture (10 volume% H_2O). The upper layer of the subsequent mixture was retained and was left in a fume hood to evaporate any remaining solvent. The sample was then placed in a vacuum oven at room temperature overnight. The samples were then refrigerated at -20°C until analysis. The method was shown to be effective, and no acid residuals were found in the sample (see Appendix A-1). All of the samples were analyzed for conversion by both GPC and off-line ATR-FTIR spectroscopy.

3.2.2 Product Characterization

Gel Permeation Chromatography

A Waters Corp. GPC system consisting of an HPLC pump, a controller, and a differential refractive index detector was used. Waters Millennium 32^{TM} software (Waters) was used for analysis. The columns used were two 300 x 7.5 mm Phenogel columns of 3 μm and 100 Å pore size (Phenomenex, Torrance, CA) connected in series. The mobile phase was HPLC grade tetrahydrofuran (THF) at a flow rate of 1 mL/ min at 38°C. The sample injection loop was 200-μL with a running time of 25 min.

THF was used to make a 20 mg/mL solution of the sample. 10 μL of the solution was injected into the 200-μL loop. Other concentrations and injection volumes were tested but they resulted in poorer separation of TG and DG (Appendix A-3). Prior to injection, the solutions were filtered through a 0.2 μm polytetrafluoroethylene (PTFE) syringe filter.

A calibration curve was generated from 6 standards: triolein (TG), diolein (DG), monoolein (MG), methyl oleate (FAME), oleic acid (the majority type of FFA present in the waste frying oil), and glycerol. The injection masses were plotted against the peak areas (see Appendix A-2). Each standard was injected 3 times at 5 different concentrations. The calibration curves of the standard solutions showed good linearity. The retention time of the standards are shown in Table 3.2. While the retention time of a standard sometimes varied from injection to injection, the relative retention times remained constant (Table 3.2). Figure 3.1 shows a typical chromatograph of a mixture of standards (note: sample concentration was 0.3925 mg/mL TG, 0.1235 mg/mL DG, 0.0722mg/mL MG, 0.0075 mg/mL oleic acid, 1mg/mL FAME and 0.085 mg/mL glycerol and injection volume was 200 μL).

Table 3.2 Retention time of standards

Standard	Retention time (min)	Relative retention time
Triolein (TG)	12.20	1
Diolein (DG)	12.64	1.04
Monoolein (MG)	13.47	1.10
Oleic acid (FFA)	14.15	1.16
Methyl oleate (FAME)	14.26	1.17
Glycerol	15.34	1.26

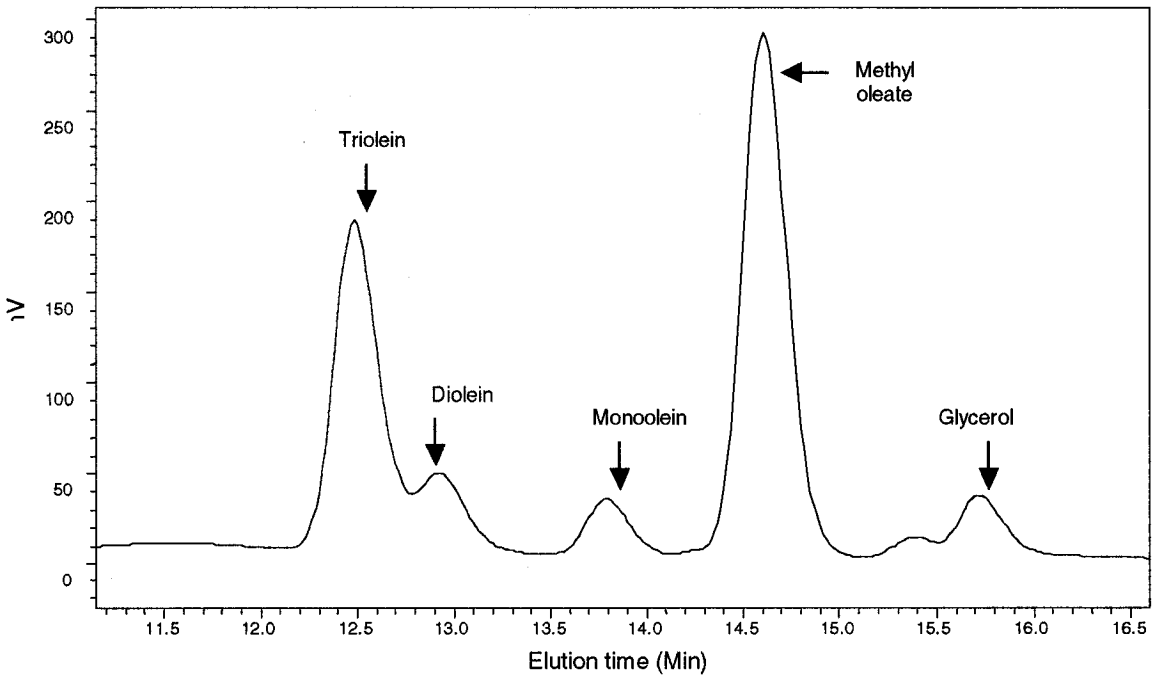

Figure 3.1 GPC plot of mixture of standards.

For the calculation of fractional conversion, it was assumed that the reactor was well mixed, and that the reaction stopped once the sample was taken from the reactor. Thus, the fractional conversion of oil to FAME in the sample was taken to represent the actual conversion in the reactor.

The oil to FAME conversion at time t can be calculated from sample analyses

$$X = \frac{N_{oil(t=0)} - N_{oil(t=t)}}{N_{oil(t=0)}} \tag{3.1}$$

where X is the fractional molar conversion, $N_{oil(t=0)}$ is the original number of moles of oil (or TG equivalents) in the sample. $N_{oil(t=t)}$, or $N_{TG(t=t)}$ is the number of moles of TG left in the sample. The original total moles of oil was therefore calculated from the TG

equivalents amounts of DG, MG, FFA and FAME present in the sample using the calibration curves (see Appendix A-2):

$$N_{oil(t=0)} = 2/3\ N_{DG(t=t)} + 1/3N_{MG\,(t=t)} + 1/3N_{FFA(t=t)} + 1/3N_{FAME(t=t)} + N_{TG(t=t)} \qquad (3.2)$$

where $N_{DG(t=t)}$, $N_{MG(t=t)}$, $N_{FFA(t=t)}$, $N_{TG(t=t)}$ and $N_{FAME(t=t)}$ represent the number of moles of DG, MG, FFA, TG and FAME at time *t*, respectively.

ATR-FTIR Spectroscopy

The reaction was monitored both in-line and off-line using an ATR-FTIR spectrometer-the ReactIR 1000^{TM} (ASI Applied Systems Inc.). The device employs light conduit technology, which consists of 6 mirrors and 3 tubes that provide a purged (with filtered air) path through which the infrared beam travels to a remote sampling device and back to a detector. The sampling device has a diamond-composite (DiComp) insertion probe with a stainless steel body (18.42 cm length, 1.59 cm diameter) and a 6-reflection bilayer ATR element with a diamond surface element (6 mm diameter, 0.25 mm thickness) at the top.

The probe was inserted into the reactor to monitor the transesterification reaction in-line. All spectra were scanned 64 times and recorded at a resolution of 8 cm^{-1}. The in-line monitoring of the transesterification was not successful. A diminishing peak was not found. Instead, a rising peak at 1437 cm^{-1} (associated with the $-OCH_3$ group in FAME) was used to monitor the reaction. However, the large excess of methanol used in the experiments diluted the samples, pushing the abilities of the ReactIR 1000 to its limit. Therefore in-line monitoring was not used.

Samples were prepared and used for off-line ATR-FTIR measurements. For off-line analysis, a few drops (about 0.1 mL) of sample were placed on the probe tip. Spectra were recorded at a resolution of 8 cm^{-1}. There were 64 scans, and less than 1 min was required to collect a spectrum. Ambient air was routinely used as the background. Figure 3.2 shows a typical spectrum of waste frying oil.

The basis for monitoring the reaction is the determination of characteristic peaks that represent a functional group associated with the transesterification. According to Beer's Law, the concentration of a component is proportional to absorbance, which can be measured by the peak height. The absorbance at 1378 cm^{-1}, which is attributed to the symmetric deformation of the terminal CH_3 group in TG, DG, MG, and FAME, was used in the off-line ATR-FTIR monitoring. Figure 3.3 shows the changes in the absorbance of waste frying oil during the course of a transesterification. Thus, the conversion of oil to FAME of a sample at time t can be defined by a decrease in peak height during the reaction. It was noticed that the absorbance of FAME alone at 1378 cm^{-1} was very weak but non-zero due to the presence of the terminal CH_3 group in the structure of FAME. Therefore, all peak heights were adjusted for the peak height of FAME. Thus, the fractional molar conversion of oil to FAME was written as

$$X = \frac{PeakHeight^{*}_{(t=0)} - PeakHeight^{*}_{(t=t)}}{PeakHeight^{*}_{(t=0)}} \tag{3.3}$$

where X is the molar fraction conversion and

$$Peak\ Height\ * = Peak\ Height - Peak\ Height\ of\ FAME \tag{3.4}$$

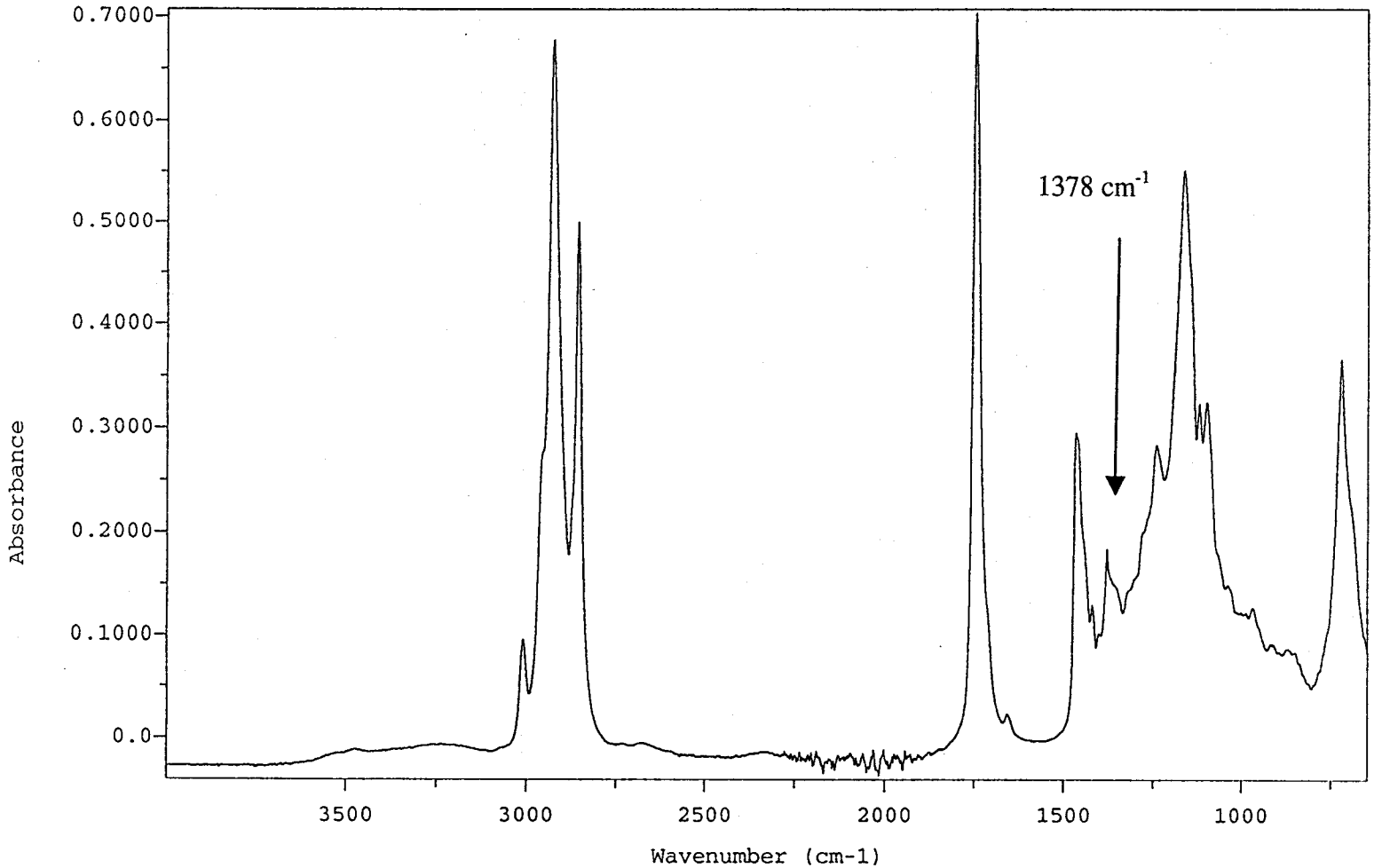

Figure 3.2 ATR-FTIR spectra of waste frying oil using air as background.

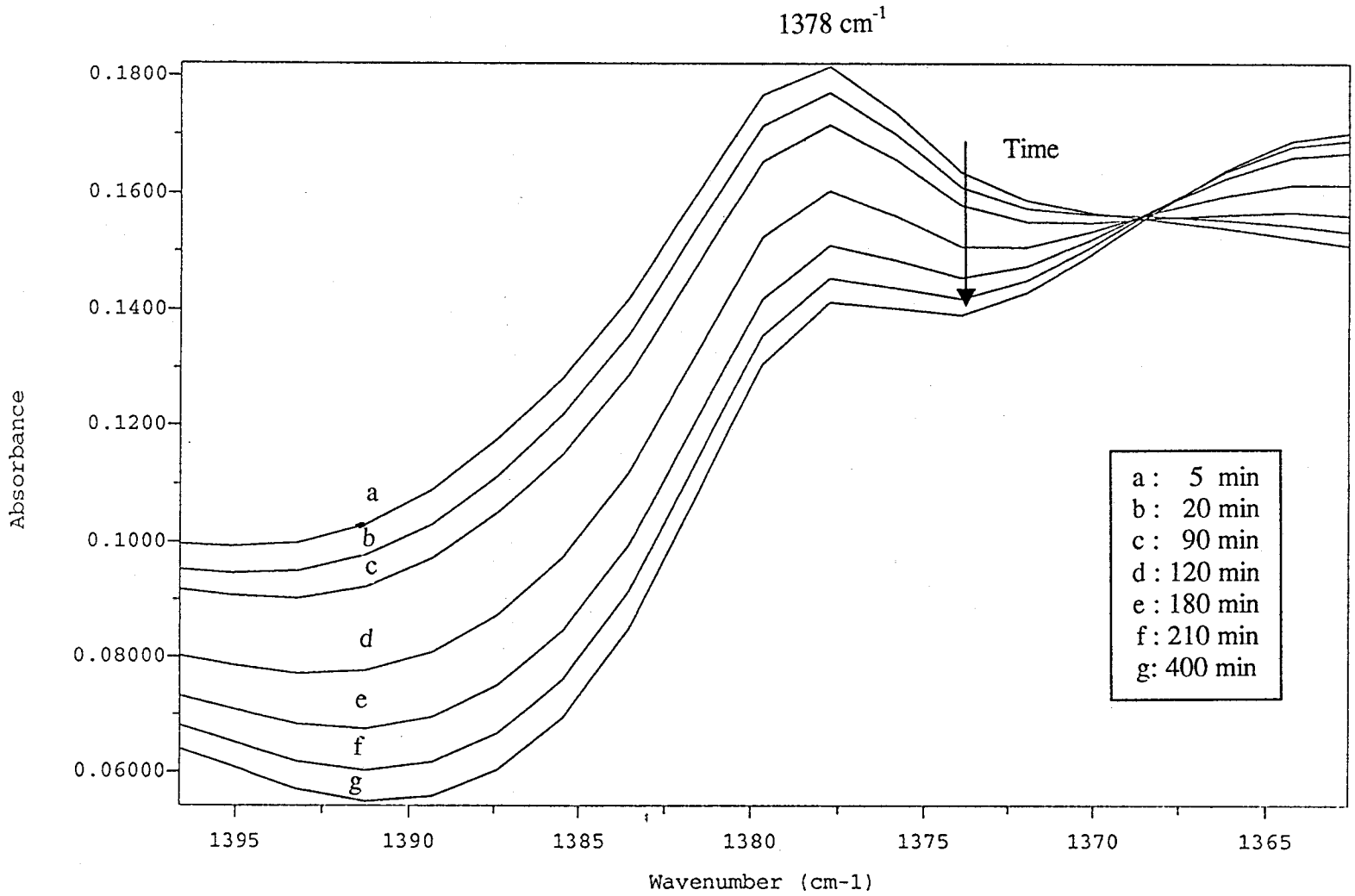

Figure 3.3 Changes in the absorbance at 1378 cm^{-1} of waste frying oil during the course of a transesterification.

3.3 Results and Discussion

3.3.1 Analysis of Mixtures of Standards

Gel Permeation Chromatography

A typical GPC plot of a sample taken from the biodiesel transesterification is shown in Figure 3.4. In this particular sample, only TG, DG and FAME were found. The presence of any MG was below the detection limit of the GPC. The original oil was composed of about 82 wt % TG, 12 % DG, and 6 % FFA.

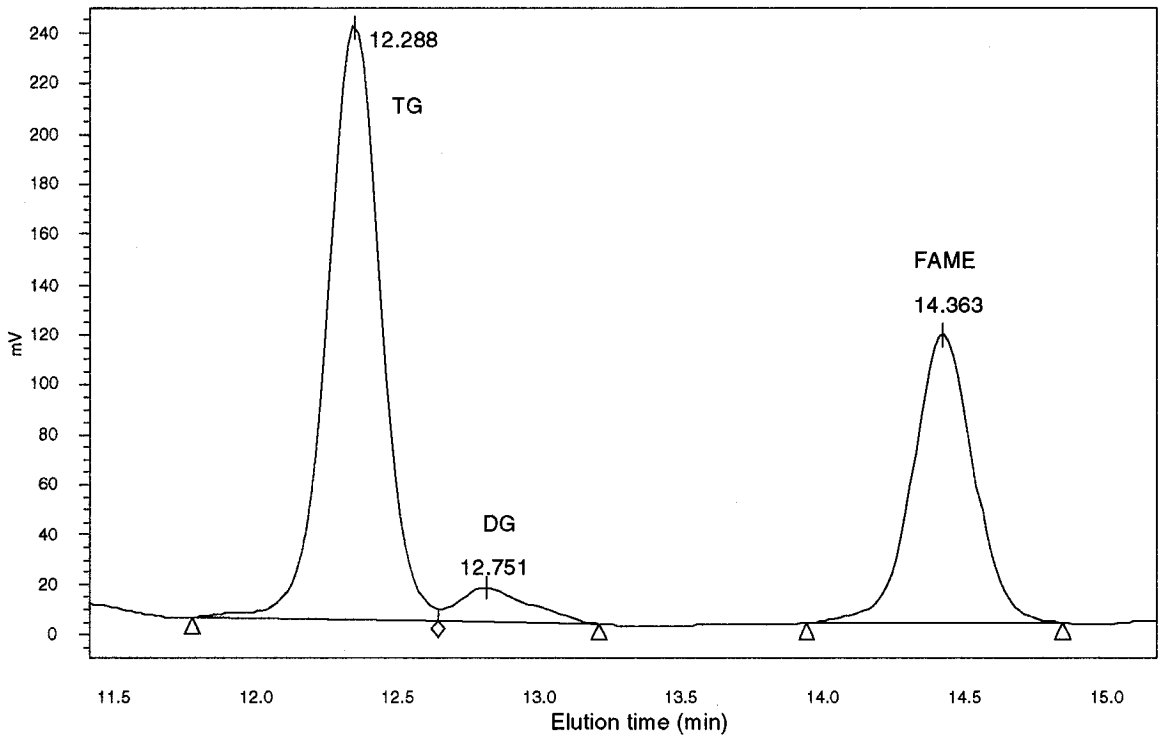

Figure 3.4 GPC plot of a sample taken from Experiment #9 at 180 min (feed composition: 96.2 mol% MeOH, 2.5% acid and 1.3% oil, at 70°C).

The retention times of the oleic acid (a major component of FFA) and FAME were very close to each other (see Table 3.2), the presence of FFA in the sample could have been masked by the FAME peak. Early samples (as early as 0.5 min) taken from the

reaction were examined specifically for the presence of FFA. It appeared that there was no FFA in any of our samples, and it is assumed that it was totally converted to FAME because of the large excess of methanol used in our study. Most glycerol was removed in the washing step of our sample preparation. Thus, little glycerol was found in the GPC chromatogram. The separation of TG and DG appeared to be incomplete and some peak overlap was present in most of the samples.

Three mixtures of known amounts of triolein, diolein, monoolein, and methyl oleate were injected 5 times each into the GPC (Mixture 1: 70.9 wt% triolein, 10.8% diolein, 4.7 % monoolein and 13.6 % methyl oleate; Mixture 2: 23.4 wt% triolein, 5.3% diolein, and 71.3% methyl oleate; Mixture 3: 19.4 wt% triolein, 14.8% diolein, 25.0 % monoolein and 40.8 % methyl oleate). Based on preliminary GPC results of early transesterification experiments, glycerol and oleic acid were added to the mixture standards.

Figure 3.5 shows a typical GPC chromatogram of Mixture 3. The analysis of the mixture is shown in Table 3.3. It was found that the reproducibility of the method was very good. The standard error of 5 injections was smaller than 10^{-4} (see Table 3.3). The measured molar fraction of each component was compared to its actual molar fraction. For FAME and monoolein, the difference between the measured and actual weight fractions was less than 5%. However, for triolein and diolein, differences were significant. This was because of the slight overlap of the TG and DG peaks. In addition, the integration limits of the peaks were manually selected because the GPC software could not set the limits automatically. In this study, because there was always vastly more TG than DG present in the samples, the amount of TG was usually underestimated and that of DG was overestimated, as shown in Table 3.3. However, it was found that the

recovery of TG and DG was a linear function of the TG: DG molar ratio (see Figure 3.6). The recovery of TG and DG was therefore corrected for all of the reaction samples according to the TG: DG ratio (Figure 3.6), and the revised recovery data were adequate (see Table 3.3). Similar analyses of the other two mixtures of standards are given in Appendix A-4.

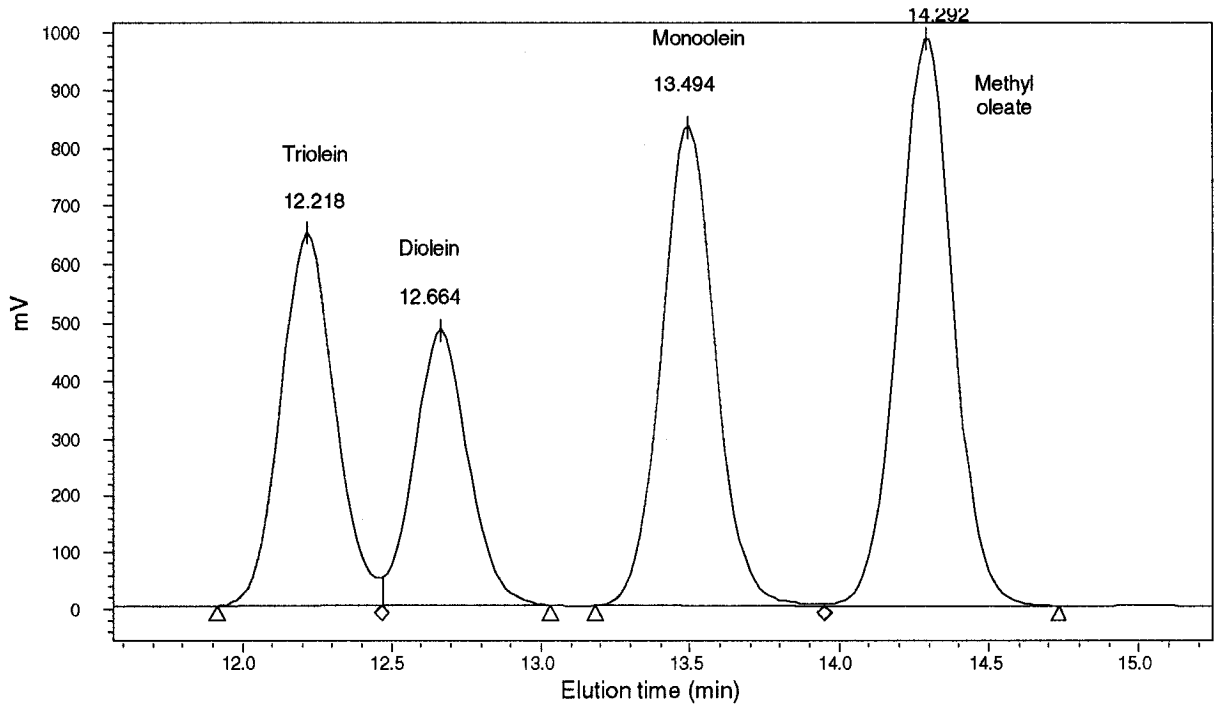

Figure 3.5 GPC chromatogram of Mixture 3 (composition: 19.4 wt% triolein, 14.8% diolein, 25.0 % monoolein and 40.8 % methyl oleate).

From Figure 3.6, it is seen that with an increase in the TG: DG molar ratio, the recovery of TG approached 1. At the same time, the analysis of DG became less reliable with the increase in the TG: DG ratio. However, in our study, DG was not of major concern. Furthermore, in the samples taken from our experiments, the amount of DG was always typically low, and the highest concentration of DG was always detected at the

beginning of the reaction. After 2 hrs, the amount of DG was almost negligible, thus the analysis of samples taken at the end of a reaction (see Figure 3.7) could be considered highly reliable. The data obtained from GPC were suitable for our conversion monitoring and modeling (Zheng et al., 2003), because only the final samples were used for model building.

Table 3.3 GPC analysis of one mixture of standards

Injections	Weight fraction			
	Triolein	Diolein	Monoolein	Methyl oleate
Inj#1	0.176	0.156	0.247	0.421
Inj#2	0.176	0.156	0.247	0.421
Inj#3	0.175	0.157	0.247	0.421
Inj#4	0.176	0.157	0.247	0.421
Inj#5	0.176	0.157	0.247	0.421
Mean	0.176	0.157	0.247	0.421
Standard error	$< 10^{-4}$	$< 10^{-4}$	$< 10^{-4}$	$< 10^{-4}$
Actual	0.194	0.148	0.250	0.408
Deviation	-0.018	0.009	-0.003	0.013
Relative deviation	-0.093	0.060	-0.013	0.031
Recovery (%)	87.39	113.42	98.74	103.10
Revised recovery (%)	**100.44**	**100.39**	98.74	103.10

As mentioned earlier, Darnoko et al. (2000) developed a GPC method for the study of the alkali-catalyzed transesterification of palm oil. Two pLgel columns (300 × 7.6 mm, and pore size was 50 Å) were used. Likely as a result of the lower methanol to oil ratios used in their work, the amounts of MG found in their samples were significant. A slightly different sample preparation was employed and glycerol was present in their samples. Judging by the GPC traces shown in their work, despite the use of lower pore size columns, their separation of TG and DG were similar to those in the present study. However, problems of poor recovery of TG and DG were not reported.

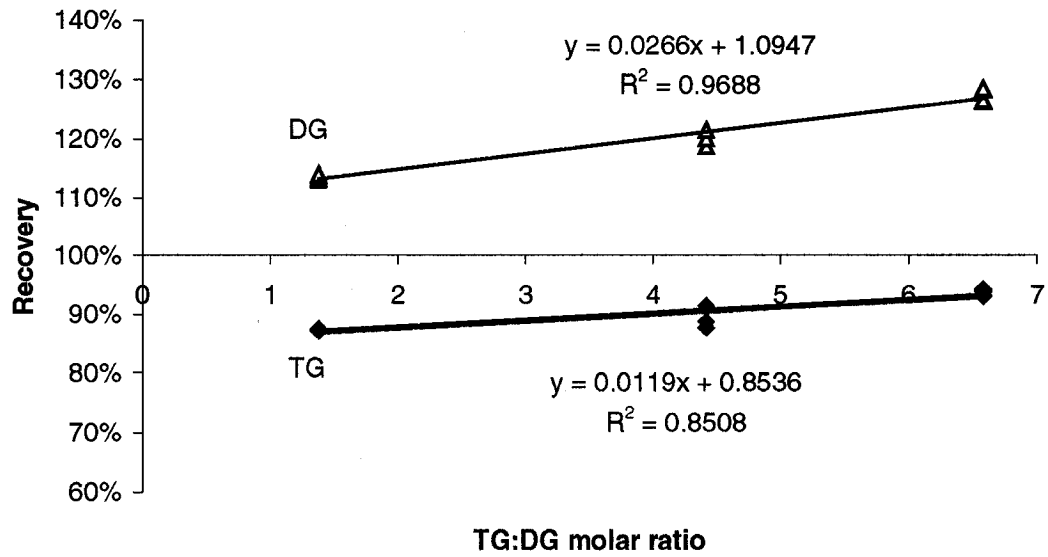

Figure 3.6 Recovery (%) of TG and DG as a function of TG: DG molar ratio.

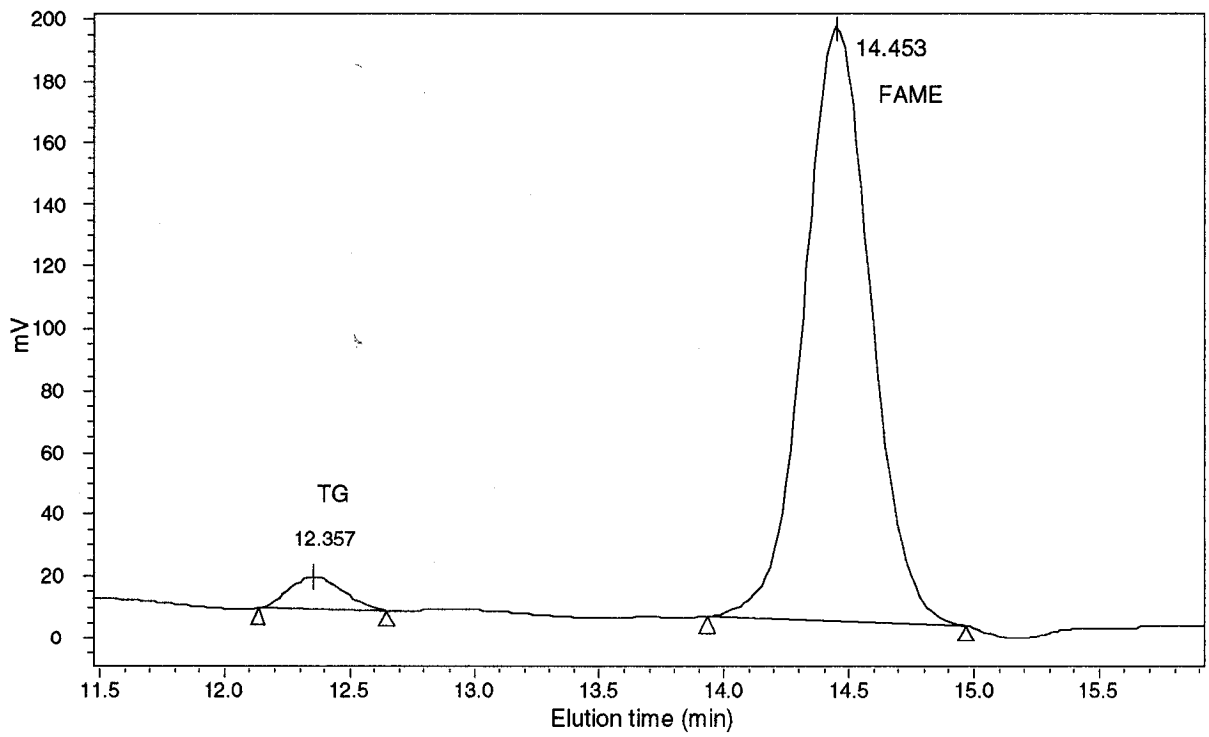

Figure 3.7 A typical sample taken at the end of a transesterification (Expt. # 9 at 80°C, taken at 180 min).

ATR-FTIR Spectroscopy

Five standard mixtures of differing compositions (compositions of the 5 standards are given in Table 3.4) were examined using off-line ATR-FTIR spectroscopy. Each standard was analyzed 3 times. It was found that the measurement-to-measurement variation was very small: the standard error of the analyses was less than 10^{-5}, showing very good reproducibility. The predicted conversions of the 5 standards were consistent with the known compositions (see Table 3.4 and Figure 3.8).

Table 3.4 Off-line ATR-FTIR spectroscopy analysis of the standard mixtures

	Injection	Measured conversion (molar fraction)	Mean	Standard error	Relative deviation	Actual conversion (molar fraction)
	S#1-1	0.110				0.100
M#1	S#1-2	0.113	0.112	1.87×10^{-6}	1.67×10^{-5}	0.100
	S#1-3	0.112				0.100
	S#2-1	0.247				0.250
M#2	S#2-2	0.245	0.246	2.13×10^{-6}	8.66×10^{-6}	0.250
	S#2-3	0.245				0.250
	S#3-1	0.521				0.500
M#3	S#3-2	0.527	0.526	2.27×10^{-5}	4.32×10^{-5}	0.500
	S#3-3	0.530				0.500
	S#4-1	0.756				0.750
M#4	S#4-2	0.762	0.761	1.58×10^{-5}	2.08×10^{-5}	0.750
	S#4-3	0.763				0.750
	S#5-1	0.891				0.900
M#5	S#5-2	0.892	0.893	6.35×10^{-6}	7.11×10^{-6}	0.900
	S#5-3	0.896				0.900

As a result, a calibration curve was not required for the off-line ATR-FTIR analysis, thus greatly simplifying the analysis. The analysis time was short (1- 2 minutes per sample). One disadvantage of the technique was the fact that the structures of DG and MG are very similar to that of TG, and thus they couldn't be identified and quantified by off-line ATR-FTIR spectroscopy. Although it did not have a significant impact on our biodiesel study because the amounts of DG and MG were low in our samples (see Figure 3.7), application of off-line technique to samples containing large amounts of DG and MG would not be feasible. Nonetheless, ATR-FTIR spectroscopy still can provide reliable information in a very short time frame.

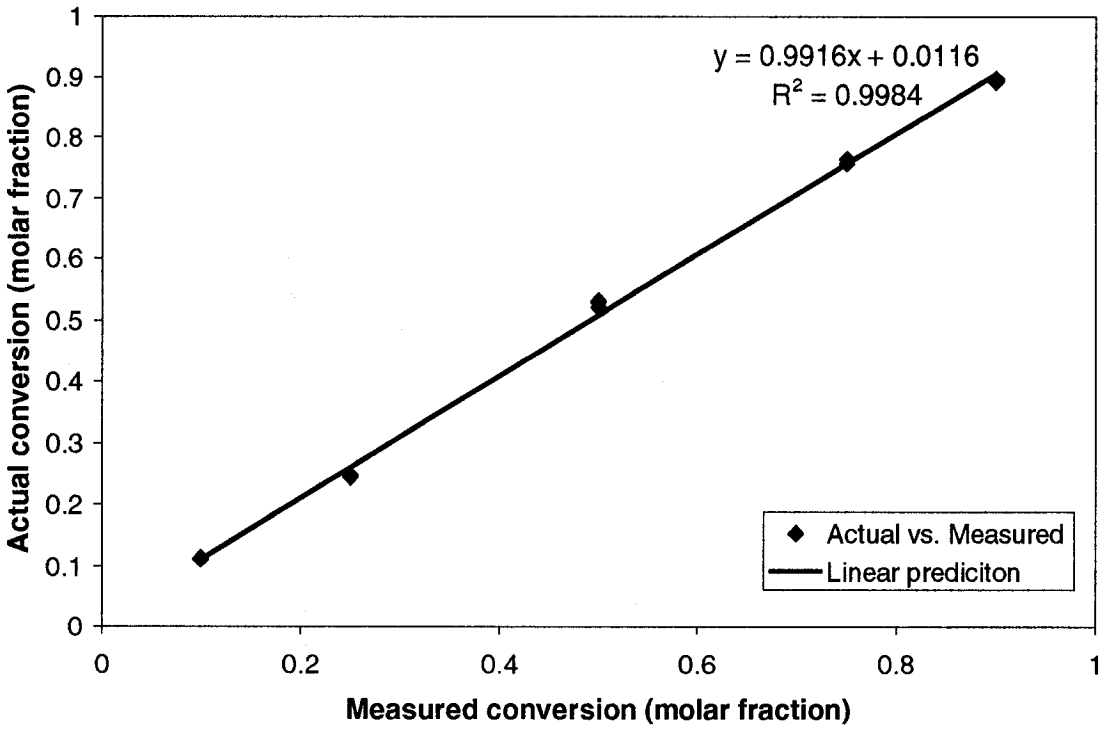

Figure 3.8 Conversions measured by ATR-FTIR analysis vs. actual conversion

3.3.2 Comparison of ATR-FTIR Spectroscopy to GPC Analyses

In both GPC and ATR-FTIR spectroscopy, multiple steps were used in the analysis: sampling from the reactor, sample preparation, and for GPC only, sample dilution. A series of nested designs were used to try to identify the most significant sources of variability.

Five mixtures of oil and FAME (see Table 3.5) were used in the nested design. Three samples were taken from each of the mixtures and analyzed by both GPC and ATR-FTIR. For GPC analysis, 3 dilutions were made for each of the 5 mixtures, and for each dilution, 3 repeat injections were made for a total of 45 measurements. For ATR-FTIR spectroscopy, 3 samples were taken from each of the 5 mixtures, and 3 repeat measurements were carried out for each sample for a total of 45 measurements. The variances at each level were calculated, and a total variance was obtained (see Tables 3.6 and 3.7). In Table 3.6, σ^2_m and σ^2_C each represent the measurement-to-measurement and composition-to- composition variation in off-line ATR-FTIR spectroscopy, respectively. $\sigma^2_m/(\sigma^2_m+\sigma^2_C)$ and $\sigma^2_C/(\sigma^2_m+\sigma^2_C)$ represent the proportion that the two variations contributed to the total variation, respectively. In Table 3.7, σ^2_I and σ^2_D each represent the injection-to-injection and dilution-to-dilution variation in GPC, respectively. None of the variations shown in Tables 3.6 and 3.7 was found to contribute to the total variation in each method. Variations were also found randomly distributed between the two levels, indicating that neither the sample preparation nor the analysis itself was the major source of variation. The total variations of the 5 mixtures were also small (all smaller than 10^{-4}), thus reinforcing the idea that both methods give highly repeatable measurements.

Table 3.5 Compositions of mixtures used in the nested design

Mixture	Moles	
	mol% Oil	mol% FAME
M#1	89.0	11.0
M#2	76.0	24.0
M#3	45.0	55.0
M#4	25.0	75.0
M#5	10.0	90.0

Table 3.6 ATR-FTIR spectroscopy results of the nested design

Mixture	σ^2_m	σ^2_C	$\sigma^2_m+\sigma^2_C$	$\sigma^2_m/(\sigma^2_m+\sigma^2_C)$	$\sigma^2_T/(\sigma^2_m+\sigma^2_C)$
M#1	5.22×10^{-6}	8.60×10^{-6}	1.38×10^{-5}	37.77%	62.23%
M#2	0	4.67×10^{-6}	4.67×10^{-6}	0.00%	100.00%
M#3	3.35×10^{-5}	7.73×10^{-6}	4.13×10^{-5}	81.26%	18.74%
M#4	9.69×10^{-5}	2.85×10^{-6}	9.98×10^{-5}	97.14%	2.86%
M#5	8.67×10^{-6}	6.51×10^{-6}	1.52×10^{-5}	57.13%	42.87%

Table 3.7 GPC results of the nested design

Mixture	σ^2_I	σ^2_D	$\sigma^2_I+\sigma^2_D$	$\sigma^2_I/(\sigma^2_I+\sigma^2_D)$	$\sigma^2_D/(\sigma^2_I+\sigma^2_D)$
M#1	4.06×10^{-6}	1.23×10^{-5}	1.23×10^{-5}	33.09%	66.91%
M#2	2.44×10^{-7}	2.29×10^{-6}	2.53×10^{-6}	9.62%	90.38%
M#3	2.71×10^{-6}	1.29×10^{-6}	4.00×10^{-6}	67.78%	32.22%
M#4	1.33×10^{-5}	6.54×10^{-5}	7.87×10^{-5}	16.85%	83.15%
M#5	1.27×10^{-5}	0	1.27×10^{-5}	100.00%	0.00%

A paired comparison was carried out between the results of the composition analyses from the two analytical methods. For the five mixtures of standards, a 95% confidence interval calculated for the difference in conversion measurements between the two methods was found to be: [-0.0114, 0.0001]. This indicates that no significant difference between the two methods exists. A comparison of all the results from the nested design using GPC vs. that of off-line ATR-FTIR spectroscopy is shown in Figure 3.9. R^2 was found to be 0.9968, showing good consistency of the two analyses.

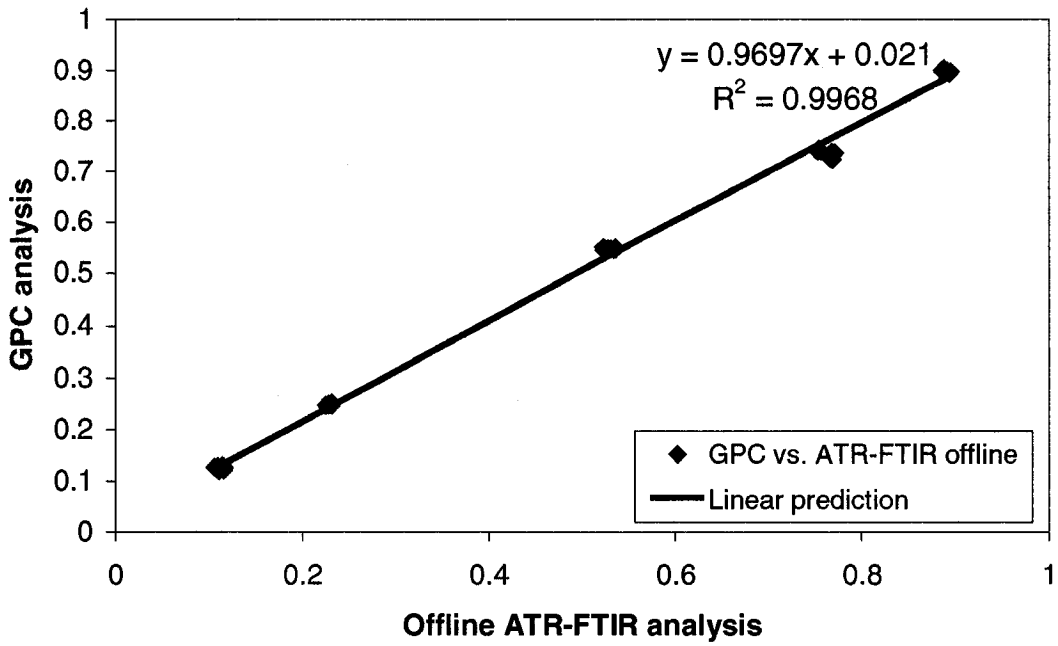

Figure 3.9 GPC vs. off-line ATR-FTIR analysis in the nested design

All of the experiments listed in Table 3.1 were analyzed by both ATR-FTIR spectroscopy and GPC. A paired comparison was carried out for each of the experiments to compare the differences between the two methods. 95 and 99% confidence intervals were calculated for the differences (see Appendix Table A-6) and were found to be: [0.008838, 0.02219] and [0.006740, 0.02429], respectively. Although both of these

intervals didn't include 0, results from individual experiments revealed that most of the individual confidence intervals of the differences did include 0 (12 out of 20 for the 95% confidence level, and15 out of 20 for the 99% level). It was also found that most of the inconsistencies in the two analytical methods occurred when the FAME conversions were low. Nine out of ten of the reactions with high FAME content (>80%) showed good agreement between the methods. An overall comparison of all the analysis points is shown in Figure 3.10, the R^2 value was found to be 0.9738, again indicating good agreement of the two analyses. Furthermore, because the differences were actually very small (<0.01), these two analytical methods can still be considered equal.

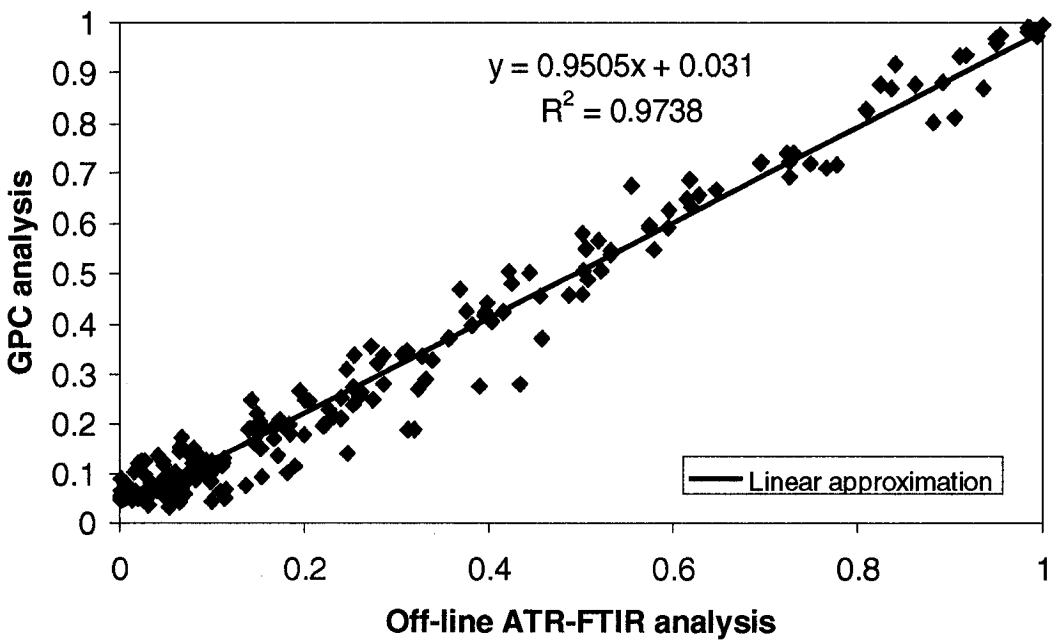

Figure 3.10 GPC vs. off-line ATR-FTIR analysis in all experiments

3.4 Conclusions

Two analytical methods: ATR-FTIR spectroscopy and GPC were investigated for their suitability and accuracy in the conversion monitoring of the acid-catalyzed biodiesel production from waste frying oil.

GPC was found to be reliable for the conversion monitoring of the transesterification reaction. Sample recovery using this method was examined by injecting mixtures of standards and was found to be reliable. The reproducibility of the results was found to be excellent. The standard error of the repeated injections was smaller than 10^{-4}. Furthermore, the analysis time was short (25 min per sample), and sample preparation was simple.

Although identification of DG and MG was not possible using ATR-FTIR spectroscopy, the method was shown to be effective in measuring the conversion of oil to FAME. The accuracy and repeatability of off-line ATR-FTIR spectroscopy was found to be excellent by analyzing standard mixtures of oil and FAME. The reproducibility of the method was excellent: the relative standard deviation of repeated tests was less than 10^{-4}. It provided a very cost effective rapid check for oil to FAME conversion: the analysis time for the off-line method was very short (1-2 minute per sample), and sample preparation was also easy. A diminishing peak at 1378 cm^{-1} was used in the off-line monitoring of the transesterification, and a calibration curve was not required, thus simplifying the analyses.

A series of nested designs was used to determine the most significant sources of variation in both methods. The results showed that, for both methods, none of the variation examined was significant, and the total variability of the two methods was very

small, indicating very good reproducibility. Using the data collected for the nested designs, a comparison of all the measurements using both methods showed that they were in good agreement: the difference between the two methods was found not to be significant at a 95% confidence level.

All of the experiments were analyzed both by GPC and off-line ATR-FTIR spectroscopy. A comparison of the measurements of the two methods was made for every experiment, and 95% and 99% confidence intervals were calculated for the differences. It was found that, on an experiment to experiment basis, most of the differences were not significant, and the overall comparison of all GPC and off-line ATR-FTIR spectroscopy measurements showed that the two analytical methods were in good agreement: the differences between the analyses being less than 2%.

3.5 References

Box, G. E. P., W.G. Hunter and J. S. Hunter, "Statistics for experimenters : an introduction to design, data analysis, and model building", Wiley, New York (1978).

Colthup, N. B., and L.H. Daly, "Introduction to Infrared and Raman Spectroscopy, 3rd Edition", Academic Press, San Diego (1990).

Darnoko, D., M. Cheryan, and E.G. Perkins, "Analysis of Vegetable Oil Transesterification Productions by Gel Permeation Chromatography", J. Liq. Chrom. & Rel. Technol. **23**, 2327-2335 (2000 a).

Darnoko, D., and M. Cheryan, "Kinetics of Palm Oil Transesterification in a Batch Reactor", J. Am. Oil Chem. Soc. **77**, 1263-1267 (2000 b).

Freedman, B., E.H. Pryde and T.L. Mounts, "Variables Affecting the Yields of Fatty Esters from Transesterified Vegetable Oils", J. Am. Oil Chem. Soc. **61**, 1638-1643 (1984).

Freedman, B., R.O. Butterfield and E. H. Pryde, "Transesterification Kinetics of Soybean Oil", J. Am. Oil Chem. Soc. **63**, 1375-1380 (1985).

Freedman, B., W. F. Kwolek, and E. H. Pryde, "Quantitation in the Analysis of Transesterified Soybean Oil by Capillary Gas Chromatography", J. Am. Oil Chem. Soc. **63**, 1370-1375 (1986).

Goodacre, R., and E. Anklam, "Fourier Transform Infrared Spectroscopy and Chemometrics as a Tool for the Rapid Detection of Other Vegetable Fats Mixed in Cocoa Butter", J. Am. Oil Chem. Soc. **78**, 993-1000 (2001).

Jovanovic R., and M.A. Dubé, Monitoring of butyl acrylate and vinyl acetate homo- and copolymerizations in toluene. J. Appl. Polym. Sci. **82**, 2958-2977 (2001).

Holčapek, M., P. Jandera, J. Fischer, and B. Prokeš, "Analytical Monitoring of the Production of Biodiesel by High Performance Liquid Chromatography with Various Detection Methods", J. Chromatogr. A. **858**, 13-31 (1999).

Kates, M., "Techniques in Lipidology 2nd ed.", Elsevier, Amsterdam, 1986.

Knothe, G., Rapid Monitoring of Transesterification and Assessing Biodiesel Fuel Quality by Near-Infrared Spectroscopy Using a Fibre-Optic Probe", J. Am. Oil Chem. Soc. **76**, 795-800 (1999).

Knothe, G., "Monitoring a Processing Transesterification Reaction by Fiber-Optic Near Infrared Spectroscopy with Correlation to ^{1}H Nuclear Magnetic Resonance Spectroscopy", J. Am. Oil Chem. Soc. **77**, 489-493 (2000).

Knothe, G., " Determining the Blend Level of Mixtures of Biodiesel with Conventional Diesel Fuel by Fiber-Optic Near-Infrared Spectroscopy and ^{1}H Nuclear Magnetic Resonance Spectroscopy", J. Am. Oil Chem. Soc. **78**, 1025-1028 (2001)

Koenig, J.L., "Spectroscopy of Polymers, 2nd Edition", Elsevier Science Inc., New York (1999).

Lechner, M., C. Bauer-Plank, and E. Lorbeer, "Determination of Acylglycerols in Vegetable Oil Methyl Esters by On-line Normal Phase LC-GC", J. High Resol. Chromatogr. **20**, 581-585 (1997).

Lin-Vien, D., N.B. Colthup, W.G. Fateley, and J.G. Grasselli, "The Handbook of Infrared and Raman Characteristic Frequencies of Organic Molecules", ACADAMIC PRESS, San Diego (1991).

Mirghani, M.E.S., Y.B. Che Man, S. Jinap, B. S. Baharin, and J. Bakar, "FTIR Spectroscopic Determination of Soap in Refined Vegetable Oils", J. Am. Oil Chem. Soc. **79**, 111-116 (2002).

Mittelbach, M., "Diesel Fuel Derived from Vegetable Oils, V [1]: Gas Chromatographic Determination of Free Glycerol in Transesterified Vegetable Oil", Chromatographia **37**, 623-626 (1993).

Mittelbach, M, G. Roth, and A. Bergmann, "Simultaneous Gas Chromatographic Determination of Methanol and Free Glycerol in Biodiesel", Chromatographia **42**, 431-434 (1996).

Mittelbach, M. and S. Gangl, "Long Storage Stability of Biodiesel Made from Rapeseed and Used Frying Oil", J. Am. Oil Soc. Chem.**78**, 573-577 (2001).

Noureddini, H. and D. Zhu, "Kinetics of Transesterification of Soybean Oil", J. Am. Oil Chem. Soc. **74**, 1457-1463 (1997).

Peterson, C.L., M. Feldman, R. Korus, and D.L. Auld, "Batch Type Transesterification Process for Winter Rape Oil", ASAE **91**, 711-716 (1991).

Plank, C. and E. Lorbeer, "Simultaneous Determination of Glycerol, and MG, DG and TG in Vegetable Oil Methyl Esters by Capillary Gas Chromatography", J. Chromatogr. A. **697**, 461-468 (1995).

Plank, C. and E. Lorbeer. " On-line Liquid Chromatography/ Gas Chromatography for the Analysis of Free and Esterified Sterols in Vegetable Oil Methyl Esters Used as Diesel Fuel Substitutes", J. Chromatogr. A. **683**, 95-104 (1994).

Verleyen, T., R.Verhe, A. Cano, A. Huyhebaert, and W.De Greyt, "Influence of Triacylglycerol Characteristics on the Determination of Free Fatty acids in Vegetable Oils by Fourier Transform Infrared Spectroscopy", J. Am. Oil Chem. Soc. **78**, 981-984 (2001).

Yang, H., and J. Irudayaraj, "Comparison of Near-Infrared, Fourier Transform-Infrared and Fourier Transform-Raman Methods for Determining Olive Pomace oil Adulteration in Extra Virgin Olive Oil", J. Am. Oil Soc. Chem.**78**, 889-895 (2001).

CHAPTER 4

MODELING THE ACID-CATALYZED PRODUCTION OF BIODIESEL FROM WASTE FRYING OIL (PAPER 2)

Sheng Zheng[1], Marc A. Dubé[1*], David D. McLean[1], Morris Kates[2]

[1]Dept. of Chemical Engineering, [2]Dept. of Biochemistry

University of Ottawa, 161 Louis Pasteur St., Ottawa, ON Canada K1N 6N5

Abstract

An empirical study of the acid-catalyzed methanolysis of waste frying oil was carried out to investigate the process and optimize biodiesel yield. Rate of mixing, feed composition and temperature were chosen as independent factors in this study. A mixture experimental design was used to determine the effect of feed compositions on oil conversion and yield of fatty acid methyl ester (FAME, a.k.a biodiesel). Empirical models were built to determine the effect of each factor on biodiesel yield. Intensity of mixing was found to have no significant effect on the yield over 100 rpm. The methanol to oil ratio and temperature were the most significant factors affecting the yield. Finally, a region of optimum operating conditions was determined from the models over our experimental design space.

Keywords: Biodiesel; waste frying oil; acid-catalyzed transesterification; empirical modeling.

---

* to whom correspondence should be addressed.

4.1 Introduction

Biodiesel is a clean burning alternative diesel fuel, produced from domestic, renewable resources, such as vegetable oils and animal grease. Its chemical structure is that of the fatty acid alkyl esters (FAAE). It is renewable, biodegradable, non-flammable, non-toxic, and its use results in no net increase in green house gases emissions. Its relatively low emission profile, makes it an ideal fuel for use in sensitive environments such as marine areas, national parks and forests, and heavily polluted cities.

Because biodiesel is made mostly from high quality virgin oil, the cost of biodiesel is higher than petroleum based diesel. Currently, the price of biodiesel is about 1.4-2.4 US $/US gal, compared with 1.0-1.5 US $/US gal for petroleum diesel (Coltrain, 2002). In order to reduce production costs and make it competitive with petroleum diesel, low cost feedstocks, such as non-edible oils and waste frying oils are being used to make biodiesel. Economic analysis also shows that the acid-catalyzed process is an attractive competitor with the alkali-catalyzed process (Zhang et al., 2002).

Acid catalysts show many advantages when used in the transesterification of waste cooking oils compared to alkali catalysts (Canakci and Van Gerpen, 1999). The removal of free fatty acid (FFA) prior to the reaction is not required in the acid-catalyzed process. It was also found that, although the acid-catalyzed reaction required a longer reaction time and a higher temperature than the alkali-catalyzed reaction, the acid catalysts were more effective when the amount of free fatty acid was higher than 1%(Freedman et al, 1984; Liu, 1994).

Transesterification kinetics for vegetable oils has been reported in a few studies. Freedman et al. (1984) investigated the effect of molar ratio of the alcohol to oil, type of catalyst (base vs. acid), temperature and degree of refinement of the oil on the yield of biodiesel. They reported that the temperature had a significant effect on the yield early in the reaction. It was pointed out in their study that the acid catalysts would be more effective when the degree of refinement of oil was low, and for oils that had a high free fatty acid content. Noureddini and Zhu (1997) studied the kinetics of alkali-catalyzed methanolysis of soybean oil, and the effect of mixing and temperature on the reaction rate. The mixing effect was found to be more significant during the initial slow reaction rate region of the reaction. Mixing became insignificant at high temperatures where the reaction rate was faster.

Canakci and Van Gerpen (1999) studied the acid-catalyzed transesterification of soybean oil. It was found in their study that the methanol to oil ratio was a key element to increase the conversion. The completeness of ester formation increased with higher amounts of catalyst and higher temperatures. They also found that the transesterification was strongly inhibited by the presence of water in the oil phase.

There are no reported kinetic studies of the acid-catalyzed transesterification of waste frying oil. In order to better understand the process, and optimize the biodiesel yield from waste frying oil, it is important to identify and quantify the effect of some important factors that affect the yield of biodiesel, and build kinetic models of the transesterification to understand the reaction mechanism. Thus the objectives of this study were to investigate the effect of feed compositions, temperature, and mixing on the acid-catalyzed transesterification of waste frying oil by building empirical models of the

reaction. A mixture design (Box et al., 1978) was used in the model building to efficiently gather information on the effect of feed composition. The reaction conditions were then optimized to achieve maximum conversion.

4.2 Materials and Methods

4.2.1 Experimental Design

Three factors were investigated: the effect of mixing, feed composition and temperature. The maximum obtainable conversion of oil to biodiesel (X_{max}), conversion at 240 min (X_{240}), overall reaction rate (k), and the time to reach 50% of the maximum obtainable conversion ($t_{1/2}$) were chosen as the response variables.

A constrained mixture design (see Figure 4.1) was used to efficiently collect data to build empirical models describing the effects of composition on the response variables. The overall factor space for the three components is given by a two dimensional equilateral triangle. Other constraints on the compositions are also indicated. In order to push the equilibrium reaction towards 100% conversion, a minimum molar ratio of methanol to oil of 50:1 was required, which was much higher than stoichiometry requires. To prevent the scorching of oil by the acid, the molar ratio of sulfuric acid to oil was limited to 4:1. This was accomplished with an acid concentration in the range of 1.5 and 3.5 mol% (Ripmeester, 1998; McBride, 1999).

Experiments were carried out at the nine feed compositions consisting of the vertices, midpoints of the boundaries, and centre point of the constrained region (see Figure 4.1). Actual compositions of the nine runs are shown in Table 4.1. Experiments

with the feed compositions in Table 4.1 were carried out at both 70°C and 80°C. One replicate (Expt.#9, Table 4.1) was carried out at the centre point at both temperatures to obtain estimates of reproducibility.

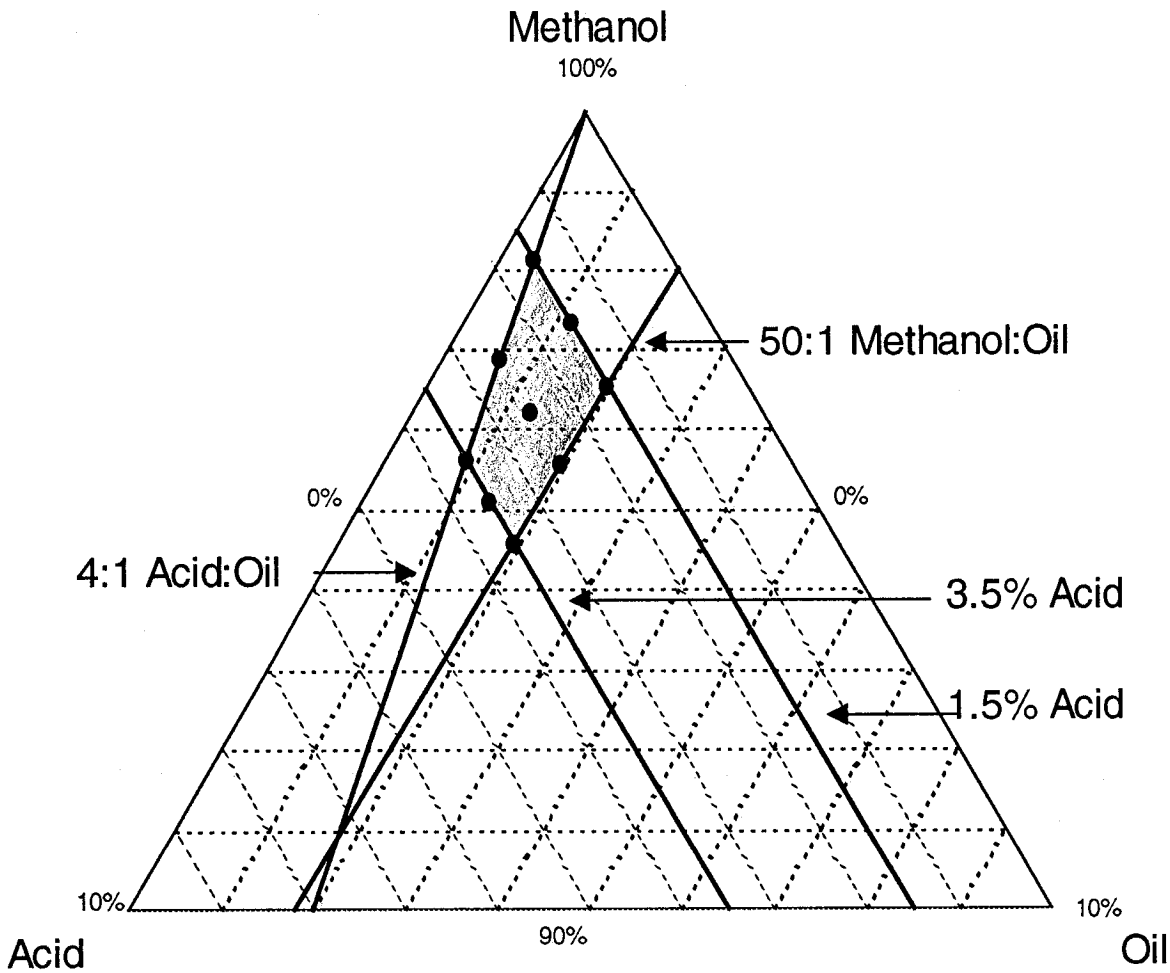

Figure 4.1 Constrained mixture design region (shaded).

(• – run compositions)

Table 4.1 Feed compositions of experiments used in the model building

Expt.	Composition (mole %)		
	Methanol	Acid	Oil
1	98.1	1.5	0.4
2	95.6	3.5	0.9
3	94.6	3.5	1.9
4	96.5	1.5	2.0
5	96.9	2.5	0.6
6	95.1	1.5	3.4
7	95.6	2.5	1.9
8	97.3	1.5	1.2
9*	96.2	2.5	1.3

* Replicated experiment

A series of experiments was also carried out at the center point of the mixture design with different mixing intensities to investigate the effect of mixing. Three stirring speeds were chosen according to the operating range of the equipment, which were 100 rpm, 400 rpm, and 600 rpm.

Models were built to describe the mixed effect of feed composition and temperature. The effect of feed composition was described by the first or second order models, given respectively by

$$E(Y) = a_{MeOH}x_{MeOH} + a_{Oil}x_{Oil} + a_{Acid}x_{Acid} \tag{4.1}$$

and $E(Y) = a_{MeOH}x_{MeOH} + a_{Oil}x_{Oil} + a_{Acid}x_{Acid} + a_{MeOH,Oil}x_{MeOH}x_{Oil} + a_{MeOH,Acid}x_{MeOH}x_{Acid}$

$$+ a_{Oil,Acid}x_{Oil}x_{Acid} \tag{4.2}$$

where x represents the initial fractional molar composition of the reaction mixture, subject to the constraint

$$x_{MeOH} + x_{Oil} + x_{Acid} = 1 \tag{4.3}$$

$E(Y)$ represents the expected value of the response variable, namely, the maximum obtainable conversion (X_{max}), the conversion at 240 min (X_{240}), the overall reaction rate

(k), and the time to reach 50% of the maximum obtainable conversion ($t_{1/2}$). The a's are the model parameters. The effect of temperature was described by the first order model given by

$$E(Y) = \beta_0 + \beta_1 T \tag{4.4}$$

where T represents the coded value of the reaction temperature given by

$$T = \frac{Temperature(^\circ C) - 75}{5} \tag{4.5}$$

and β_0 and β_1 are parameters.

Effects of both temperature and feed composition, were described by the combined first order model

$$E(Y) = (\beta_0 + \beta_1 T)(a_{MeOH} x_{MeOH} + a_{Oil} x_{Oil} + a_{Acid} x_{Acid}) \tag{4.6}$$

and the combined first order temperature and second order composition model

$$E(Y) = (a_{MeOH} x_{MeOH} + a_{Oil} x_{Oil} + a_{Acid} x_{Acid} + a_{MeOH,Oil} x_{MeOH} x_{Oil} + a_{MeOH,Acid} x_{MeOH} x_{Acid} + a_{Oil,Acid} x_{Oil} x_{Acid})(\beta_0 + \beta_1 T) \tag{4.7}$$

4.2.2 Experimental Procedures

Apparatus

The batch reactor used in the transesterification was a 5-litre stainless steel jacketed reactor, equipped with an internal cooling coil. The reactor contents were stirred by a propeller turbine agitator. A condenser using cold tap water was available to condense the methanol vapour. The overall temperature of the reactor was controlled using LabView™ software.

The reaction was monitored off-line using an attenuated total reflectance-Fourier transform infrared (ATR-FTIR) spectrometer, the ReactIR™ 1000 (ASI Applied System, Inc.). All spectra were scanned 64 times and recorded at a resolution of 8 cm^{-1}. The extent of reaction was also measured by gel permeation chromatography (GPC) on samples taken during the reaction. The apparatus of ATR-FTIR spectroscopy and GPC were described in detail by Zheng et al. (2003).

Procedures

Methanol (reagent grade, ACP Chemicals Inc.), sulfuric acid (ACS grade, BDH Chemicals Inc.), used canola oil (from a local restaurant, Sam's University Tavern) were used in the experiments. The FFA content of the oil was determined by GPC to be 6 wt%. The oil was not further treated and directly used in the transesterification.

Methanol and sulfuric acid were premixed and cooled to room temperature before use. This mixture was charged into the reactor, and the reactor was sealed, pressurized and the mechanical stirrer was started. The mixture was heated to the reaction temperature (70°C or 80°C) and the cooling water for the condenser was switched on. Oil was separately measured and preheated to 70°C, then was fed to the reactor with a liquid pump. Pressure was allowed to vary (for 70°C range from 10 to 13 psi, and for 80°C from 24 to 28 psi) when the set point of the temperature was changed. The reaction was timed as soon as the oil was all pumped in (usually less than 1 minute). The total reaction time for all experiments was set to 4 hrs.

Ten 5 mL samples were collected throughout the reaction. The sample preparations were also discussed in detail by Zheng et al. (2003). All the samples were analyzed by both GPC and off-line ATR-FTIR spectroscopy.

For GPC analysis, a calibration curve was generated from 6 standards: triolein (TG), diolein (DG), monoolein (MG), methyl oleate (FAME), oleic acid (FFA), and glycerol. The injection masses were plotted against the peak area (see Appendix A-2). Each standard was injected 3 times at 5 different concentrations. Samples were diluted with THF to make a 20 mg/mL solution and analyzed for TG, diglyceride, MG, and methyl ester content by GPC, and 10 μL of the solution was injected into the 200 μL loop. Prior to injection, the sample solutions were filtered through a 0.45 μm PTFE syringe filter to remove any particles and high molecular weight insolubles.

It was assumed that at time t, the oil to FAME conversion in a sample taken from a transesterification represented the actual oil to FAME conversion in the reaction. The fractional conversion of oil to FAME at time t was calculated as follows

$$X = \frac{N_{oil(t=0)} - N_{oil(t=t)}}{N_{oil(t=0)}} \tag{4.8}$$

where X is the fractional molar conversion, $N_{oil(t=0)}$ is the original number of moles of oil as TG equivalents in the sample, and $N_{oil(t=t)}$, or $N_{TG(t=t)}$, is the number of moles of TG left in the sample. The original total moles of oil $N_{oil(t=0)}$ was therefore calculated from the TG equivalents amounts of TG, DG, MG, FFA and FAME present in the sample at time t

$$N_{oil(t=0)} = N_{TGE(t=0)}$$

$$= 2/3\, N_{DG(t=t)} + 1/3 N_{MG(t=t)} + 1/3 N_{FFA(t=t)} + 1/3 N_{FAME(t=t)} + N_{TG(t=t)} \tag{4.9}$$

where $N_{TGE(t=0)}$ is the number of moles of TG equivalents present in the sample, and $N_{DG(t=t)}$, $N_{MG(t=t)}$, $N_{FFA(t=t)}$, $N_{FAME(t=t)}$ and $N_{TG(t=t)}$ represent the number of moles of DG, MG, FFA and FAME at time t, respectively. The moles of each component was

determined from the calibration curve. The details were discussed in the previous paper (Zheng et al., 2003).

Samples were also analyzed by off-line ATR-FTIR spectroscopy to determine the percentage of oil to biodiesel conversions. The absorbance at 1378 cm^{-1}, which could be attributed to the symmetric deformation of the terminal CH_3 group in TG, DG, MG, and FAME, was used in the off-line ATR-FTIR monitoring. For off-line analysis, a few drops (about 0.1 mL) of sample were placed on the probe tip. Ambient air was routinely used as the background. Spectra were recorded at a resolution of 8 cm^{-1}. There were 64 scans, and less than 1 min was required to collect a spectrum. Thus the fractional molar conversion of oil to FAME can be written as:

$$X = \frac{PeakHeight^*_{(t=0)} - PeakHeight^*_{(t=t)}}{PeakHeight^*_{(t=0)}} \tag{4.10}$$

where X is the molar fraction conversion and

$$Peak\ Height\ ^* = Peak\ Height - Peak\ Height\ of\ FAME \tag{4.11}$$

It was found that the conversion data of the two methods of analysis were equally reliable (Zheng et al., 2003). The data from GPC analyses were used for model building because they included results for all components.

4.3 Results and Discussion

A typical plot of the weight fraction of each component versus time is shown in Figure 4.2. The original oil was composed of about 82 wt% TG, 12% DG, and 6% free fatty acid. As shown in Figure 4.2, the weight fraction of biodiesel reached 96.7% after 4 hrs. After a further 2 hr 20 min of reaction time, 98.9% was reached. During the reaction, a negligible amount of MG was detected. A possible explanation for this is that the large

excess of methanol used in the reaction increased the methanolysis rate of MG more than that of DG and TG. It is of interest that in alkali-catalyzed transesterification, the conversion of MG to fatty acid methyl ester (FAME, a.k.a. biodiesel) was found to be faster than other 2 step reactions (Darnoko and Cheyan, 2000). The amount of DG continually decreased during the reaction, and the DG almost disappeared by the end of the reaction. The free fatty acid in the waste frying oil was likely converted to FAME very rapidly because the earliest sample (at 0.5 min) did not show the presence of free fatty acid. Thus, the presence of free fatty acid in waste frying oil is not found to be a problem in the acid-catalyzed transesterification.

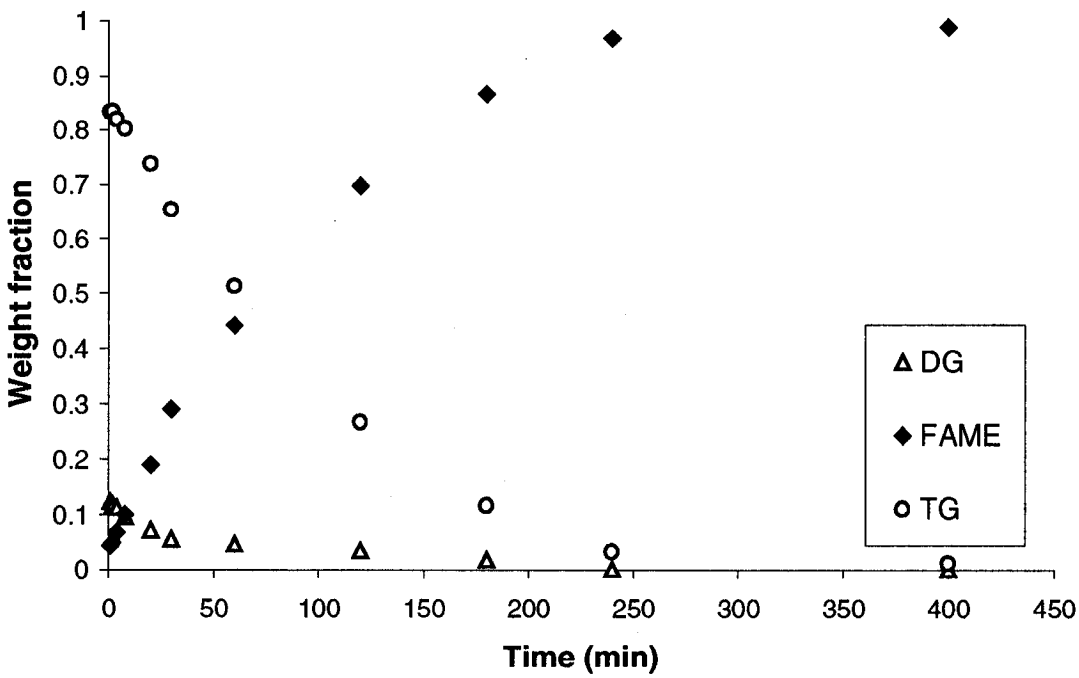

Figure 4.2 The reaction mixture composition vs. time during the transesterification of waste frying oil at 80°C; stirring speed = 400 rpm; feed composition: 96.2mol% methanol, 2.5% acid, and 1.5% oil.

4.3.1 The Effect of Mixing

Three different mixing intensities were used to investigate the effect of mixing on the kinetic behaviour. The rotational speed of the impeller was set at 100, 400, and 600 rpm. The mixing intensity can also be expressed by the Reynolds number (N_{Re})

$$N_{\mathrm{Re}} = \frac{nD_a^{\,2}\rho}{\mu} \tag{4.12}$$

where n is the rotational speed of the impeller, D_a is the diameter of the impeller, and ρ and μ are the fluid density and viscosity. The Reynolds numbers for the three stirring speeds were estimated to range from 6000-12000. Thus at these three mixing intensities, the flow in the reactor was turbulent flow.

No significant difference in conversion was found between the three mixing intensities (Figure 4.3). A possible reason was that the system was initially two-phased at room temperature, but at 80°C methanol and oil were found to be partly miscible. Also the viscosity of the mixture decreased when the temperature was increased. Another contributing factor was that the large excess of methanol used in the reaction also served to reduce the viscosity. Due to the incomplete solubility of oil in methanol, the small oil droplets were surrounded by methanol during stirring. Although the stirring speed was increased from 100 rpm to 600 rpm, the increase in mixing intensity was likely inadequate to break the droplets further into smaller sizes and thus, the contact area of the two phases was not changed, and consequently, the three experiment finally reached the same conversion. Therefore, a stirring speed of 400 rpm was routinely used in all of the experiments.

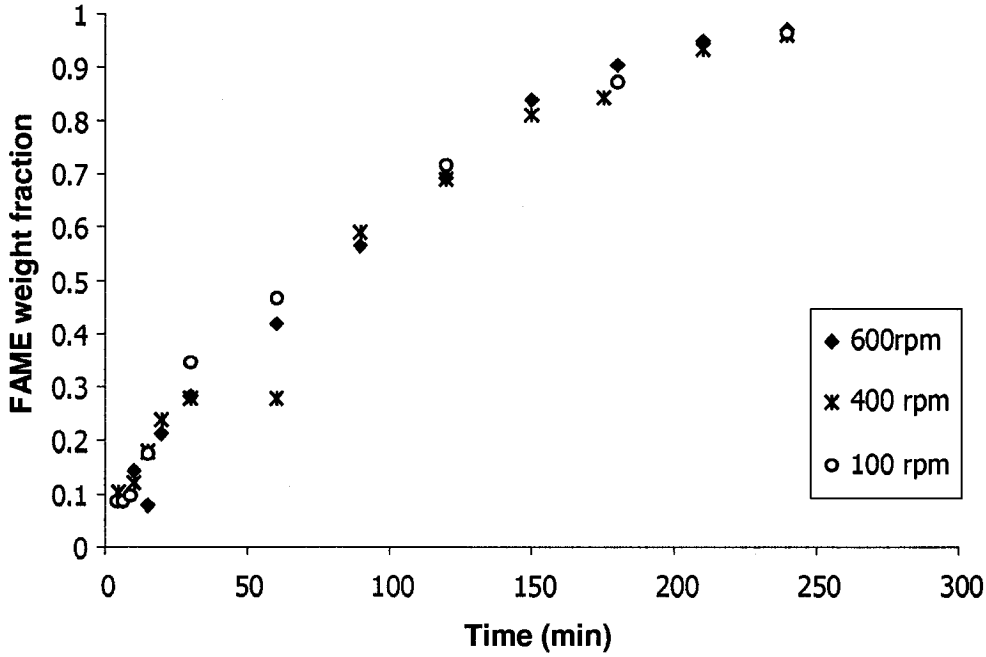

Figure 4.3 The effect of mixing and time on the weight fraction yield of FAME at 80 °C, with feed composition: 96.2 mol% MeOH, 2.5% acid and 0.7% oil.

4.3.2 The Effect of Feed Composition and Temperature

The methanol to oil ratio is known to be an important factor in biodiesel production (Freedman et al., 1984). The stoichiometric molar ratio of methanol to oil is 3:1 in order to make 3 moles of FAME from 1 mole of oil. The acid-catalyzed transesterification is an equilibrium reaction. The molar ratio used in practical production must be higher than the stoichoimetic requirement in order to drive the reaction to completion. The methanol to oil ratio used in our study was in the range of 50:1 to 250:1. As mentioned previously, two temperatures and three acid concentrations were used in the mixture design. The conversion of oil reached at 240 min was plotted as a function of methanol to oil ratio at

three acid concentrations and at 70°C and 80°C (Figure 4.4). Note that most of the reactions did not reach equilibrium at 240 min.

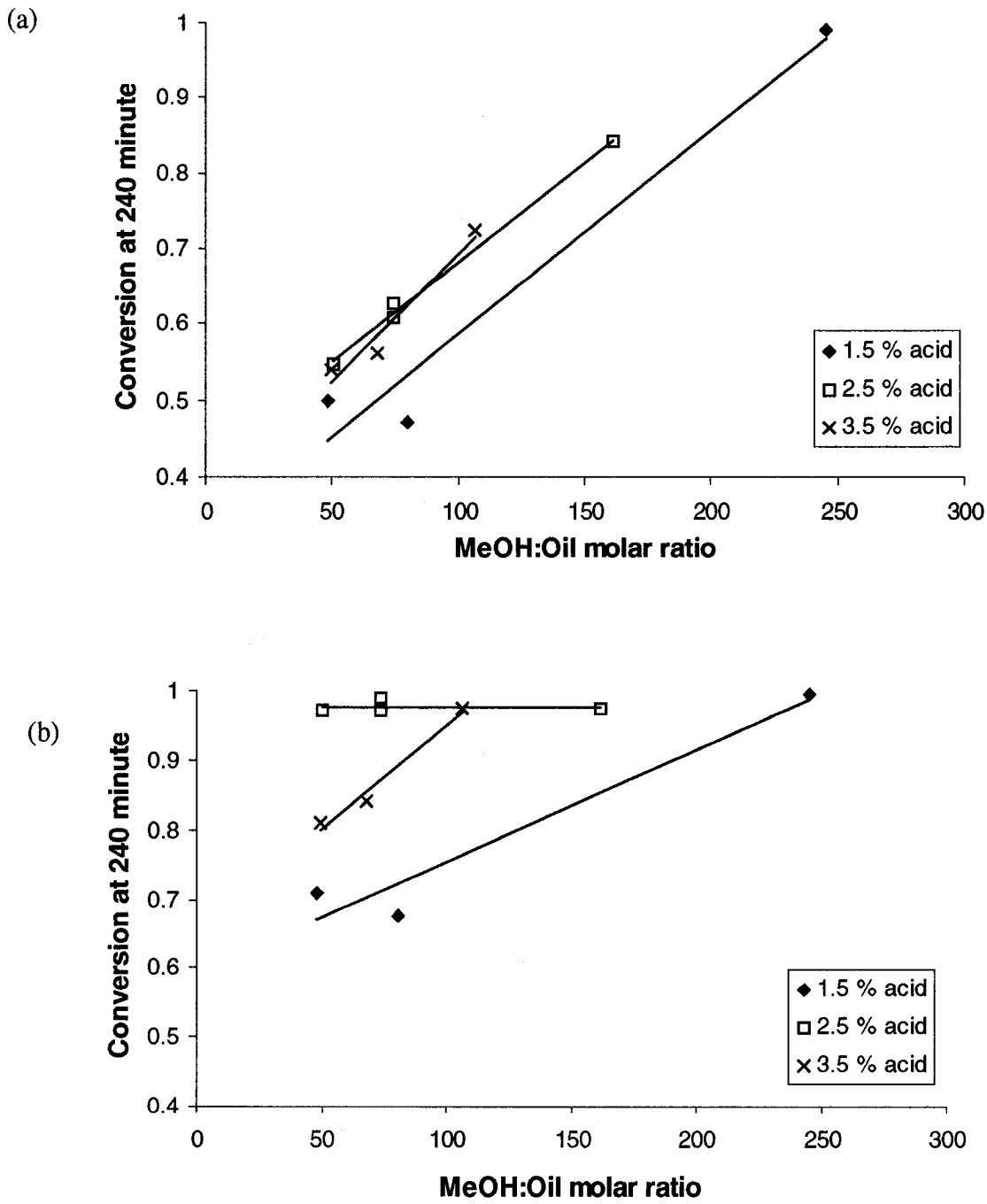

Figure 4.4 Conversion as a function of methanol to oil ratio at 70°C (a) and 80°C (b) with different acid concentrations.

The methanol to oil ratio appeared to have a linear effect on the conversion at 70°C at all acid concentrations studied, the conversion increased when increasing the methanol to oil ratio. The conversion increased with increasing the acid concentration from 1.5% to 2.5% but did not change at 3.5% acid. It was seen that at 70°C, the methanol to oil ratio was a key element to increase the conversion, conversion generally increased significantly with increasing the methanol to oil ratio.

At 80°C, the methanol to oil ratio appeared to have no effect at 2.5% acid but for both 1.5% and 3.5% acid, resulted in increases in conversion (see Figure 4.4 b). Experiments carried out at 2.5% acid concentration all reached high conversions. The relationship between the conversion and methanol to oil ratio appeared to be non-linear but more complex.

Temperature also had a significant effect on the reaction rate. Figure 4.5 shows typical conversion versus time results for a given initial composition at 70°C and 80°C. Under the same reaction conditions, the conversion increased significantly at the higher temperature indicating a strong effect of temperature on reaction rate.

4.3.3 Modeling the Effects of Temperature and Initial Composition

Models were built to describe the combined effects of temperature and feed composition on four responses the maximum obtainable conversion (X_{max}), conversion at 240 min (X_{240}), overall reaction rate (k), and the time to reach 50% of maximum obtainable conversion ($t_{1/2}$). All the model building was conducted using *Microsoft Excel.*

Conversions for each experimental run were plotted against reaction time and a non-linear first-order conversion model

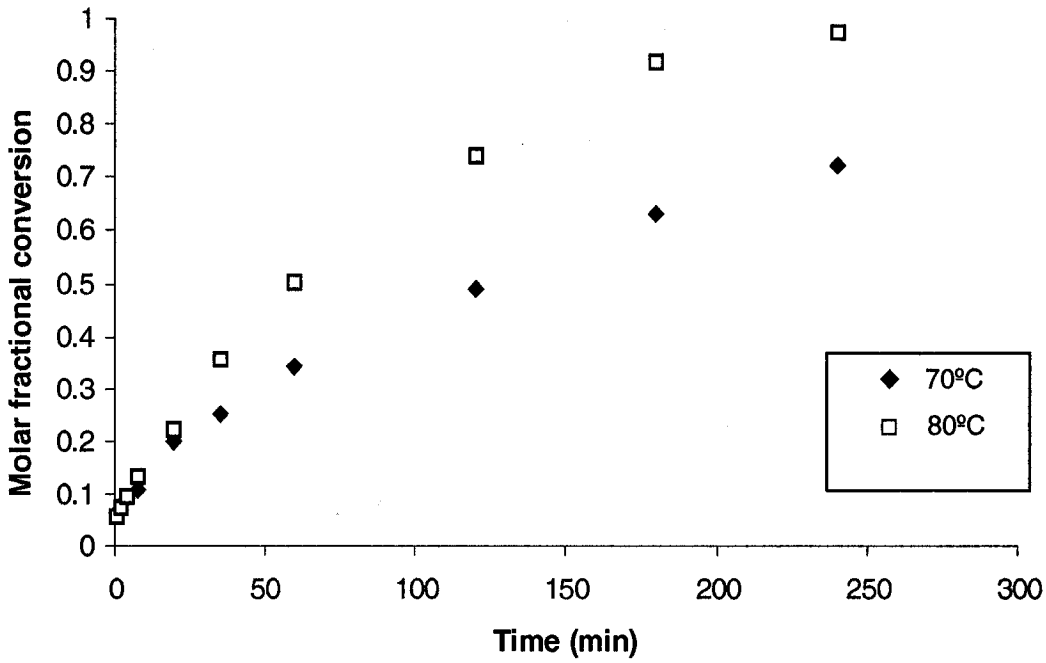

Figure 4.5 Effect of temperature on conversion over time (initial composition: 95.6 mol%, 3.5% acid, 0.9% oil).

$$X = X_{max}(1-\exp(-k\cdot(t-t_0))) \tag{4.13}$$

where t is the reaction time, X is the molar fractional conversion of oil at time t, and t_0 is the lag time in the reaction, was fitted to the data to determine the values of X_{max} and k in each plot. The value of $t_{1/2}$ can be determined by

$$t_{1/2} = \frac{\ln 2}{k} \tag{4.14}$$

The model was fitted to the experiment data using *Microsoft Excel*. For example, for an experiment with a feed composition of 98.1 mol% MeOH, 1.5% acid and 0.4% oil at 80°C, the TG to FAME conversions were first determined by sample analyses. The conversion data were then fed to the model and the values of X_{max}, k, t_0 and $t_{1/2}$ were determined using the software to be 1, 0.026 min^{-1}, 0 and 26.7 min. A constraint of $X_{max} \leq$

1 was applied to all the experiment data. The response vs. model fit of the model prediction was plotted in Figure 4.7.

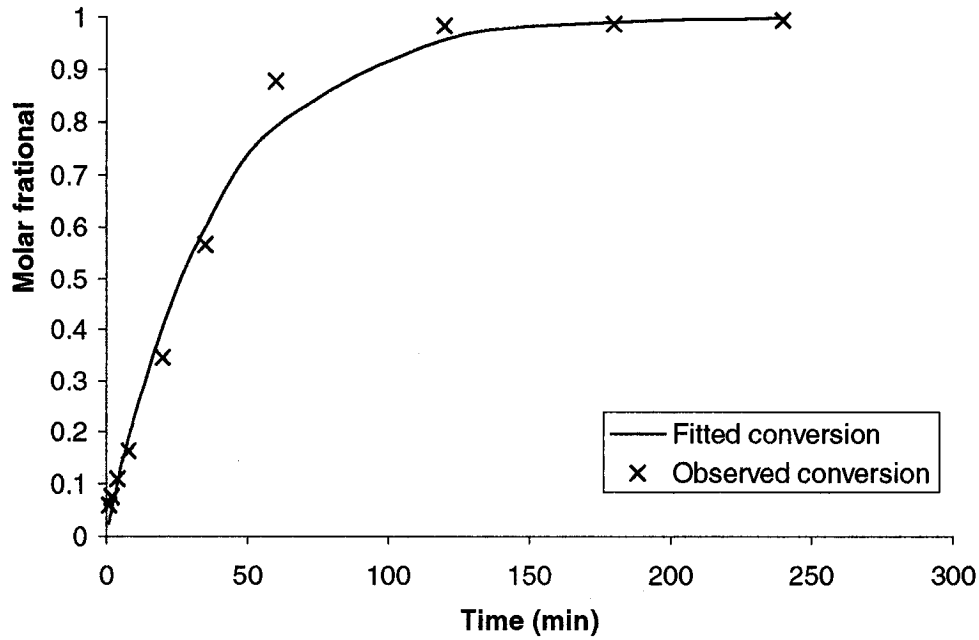

Figure 4.6 Observed and predicted conversion over time (Initial conditions: temperature: 80°C; feed composition: 98.1 mol% MeOH, 1.5% acid and 0.4% oil).

The confidence intervals of X_{max}, X_{240}, $t_{1/2}$ and k were calculated (Appendix A-7) and found to be [0.9926,1.0074], [0.9835,1.0044], [0.0003, 0.05] and [0.30, 53.01], respectively. The $t_{1/2}$ and k were found to have more variability than X_{max} and X_{240}, thus appeared to be unreliable.

The results of all the model fittings are given in Table 4.2. The lag time, t_0 was found to be 0 for all experiments carried out, and thus, is not shown in Table 4.2. The precisions of $t_{1/2}$ and k were found to be poor, thus the reliability of these data should be considered. The confidence intervals of X_{max}, X_{240} were also examined and the values of X_{max} and X_{240} were considered to be highly reliable.

Table 4.2 Mixture design with response data

Exp	x_{acid} (mol%)	x_{oil} (mol%)	T(°C)	95% confidence intervals for estimated responses			
				X_{max}	X_{240}	$t_{1/2}$ (min)	k (min^{-1})
1	0.015	0.004	70	1.0000 ± 0.0450	0.9898 ± 0.0104	59.97 ± 38.89	0.0116 ± 0.0075
2	0.035	0.009	70	0.7420 ± 0.0419	0.7226 ± 0.0104	63.10 ± 44.79	0.0110 ± 0.0078
3	0.035	0.019	70	0.5278 ± 0.0494	0.5393 ± 0.0104	58.69 ± 57.26	0.0118 ± 0.0115
4	0.015	0.02	70	0.4933 ± 0.0455	0.4600 ± 0.0104	81.08 ± 81.55	0.0085 ± 0.0086
5	0.025	0.006	70	1.0000 ± 0.0437	0.8695 ± 0.0104	79.36 ± 53.46	0.0087 ± 0.0059
6	0.035	0.014	70	0.6063 ± 0.0499	0.5960 ± 0.0104	70.62 ± 67.87	0.0098 ± 0.0094
7	0.015	0.012	70	0.3909 ± 0.0311	0.5060 ± 0.0104	37.48 ± 23.40	0.0185 ± 0.0115
8	0.025	0.019	70	0.6000 ± 0.0341	0.5923 ± 0.0104	49.52 ± 29.84	0.0140 ± 0.0084
9	0.025	0.013	70	0.7131 ± 0.0562	0.6473 ± 0.0104	81.65 ± 84.47	0.0085 ± 0.0088
10	0.025	0.013	70	0.6925 ± 0.0623	0.6651 ± 0.0104	72.20 ± 81.56	0.0096 ± 0.0108
11	0.015	0.004	80	1.0000 ± 0.0074	0.9940 ± 0.0104	26.65 ± 26.36	0.0260 ± 0.0257
12	0.035	0.009	80	1.0000 ± 0.0299	0.9742 ± 0.0104	56.06 ± 23.73	0.0124 ± 0.0052
13	0.035	0.019	80	0.9022 ± 0.0335	0.8108 ± 0.0104	78.74 ± 42.83	0.0088 ± 0.0048
14	0.015	0.02	80	0.7852 ± 0.0319	0.7103 ± 0.0104	73.33 ± 40.01	0.0095 ± 0.0052
15	0.025	0.006	80	1.0000 ± 0.0153	0.9892 ± 0.0104	41.10 ± 8.12	0.0169 ± 0.0033
16	0.035	0.014	80	1.0000 ± 0.1019	0.8770 ± 0.0104	100.40 ± 167.20	0.0069 ± 0.0115
17	0.015	0.012	80	0.7767 ± 0.0624	0.7185 ± 0.0104	71.96 ± 76.80	0.0096 ± 0.0103
18	0.025	0.019	80	1.0000 ± 0.0380	0.9716 ± 0.0104	68.36 ± 38.68	0.0101 ± 0.0057
19	0.025	0.013	80	1.0000 ± 0.0487	0.9581 ± 0.0104	68.94 ± 50.46	0.0101 ± 0.0074
20	0.025	0.013	80	1.0000 ± 0.0174	0.9885 ± 0.0104	63.19 ± 17.50	0.0110 ± 0.0030

Models for X_{max}, X_{240}, k and $t_{1/2}$

The first and second order models were built on the four responses: X_{max}, X_{240}, k and $t_{1/2}$. The residuals of those models were examined for any lack of fit. A lack-of-fit test (Box et al., 1978) was carried out for each of the models, and a comparison of the first and second order model using extra sum square (ESS) test (Box et al., 1978) was carried out (Details are included in Appendices A-7 to A-10).

For the X_{max} and X_{240} models, the second order models provided a better fit than the first order models. The second order models were then simplified by removing terms that did not make a significant contribution to the fit based on ESS test (see Appendix A-7 and A-8).

The fitted reduced second order X_{max} model with least parameters was

$$E(Y) = 0.46 + 69.53\, x_{acid} - 75.92\, x_{oil} - 0.182T + 45.21\, x_{oil}T + 1243\, x_{acid}^2 + 2277\, x_{oil}^2 - 1380\, x_{oil}^2 T \quad (4.15)$$

and the fitted reduced second order X_{240} model with least parameters was

$$E(Y) = 0.53 + 58.87\, x_{acid} - 66.46\, x_{oil} + 0.12\, T - 1070\, x_{acid}^2 + 1882\, x_{oil}^2 \quad (4.16)$$

Unlike the X_{max} and X_{240} models, the first order k and $t_{1/2}$ models were found to be adequate (see Appendix A-9 and A-10). However the precisions of the model parameters was very poor such as the confidence interval for each parameter included zero as a plausible true value. As a result of the high correlations among the parameters (Appendix A-11), terms should be removed from the model were difficult. Consequently, no further modeling of the k and $t_{1/2}$ were attempted. The first order k model was

$$E(Y) = 0.029 - 0.56\, x_{acid} - 1.02\, x_{oil} + 0.009\, T + 30.50\, x_{acid}\, x_{oil} - 0.15\, x_{acid}\, T - 0.56\, x_{oil}T + 7.45\, x_{acid}\, x_{oil}T \quad (4.17)$$

and the first order $t_{1/2}$ model was

$$E(Y) = 11.84 + 1744\, x_{acid} + 3228\, x_{oil} - 8.27\, T - 9.19\times10^{4}\, x_{acid}\, x_{oil} - 408\, x_{acid}\, T + 245\, x_{oil} T + 5.13\times10^{4}\, x_{acid}\, x_{oil} T \quad (4.18)$$

The observed versus the predicted values of the X_{max} and X_{240} models are plotted in Figures 4.7- 4.8. Approximately 95% confidence intervals for the parameters in the models along with results of lack of fit, sum square of residuals and ESS test are given in Table 4.3.

It was noticed that for the reduced second order X_{max} and X_{240} models, R^2 values were still 0.9516 and 0.8780 (Figure 4.7 and 4.8), respectively, indicating the reduced models still explained a large fraction of the variability of the data. The lack of fit test showed that the reduced second order X_{max} model displayed lack of fit (Table 4.3). One reason for this was that the restriction that the maximum observed value of X_{max} must equal one while no such restriction exists in the model. Pure error variance might not be a good approach to assess the adequacy of the model. The X_{240} model appeared to be more convincing than the X_{max} model, because the 95% confidence intervals (Table 4.2) showed that the X_{240} model appeared to have less variability than the X_{max} model.

Although the X_{max} and X_{240} models were simplified, the models were complex and found to be very difficult to interpret as a result of interaction and quadratic terms. In order to better interpret the models, contours of predicted values of X_{max} and X_{240} were plotted against feed compositions at different temperatures (Figures 4.9 and 4.10).

Table 4.3 Statistical results of the 2nd order reduced X_{max} and X_{240} models, and the 1st order k and $t_{1/2}$ models

Variables	95% confidence intervals of the coefficients			
	X_{max} model	X_{240} model	k model	$t_{1/2}$ model
Intercept	0.46 ± 0.34	0.53 ± 0.45	0.03 ± 0.01	12 ± 72
x_{acid}	69.53 ± 29.42	58.87 ± 38.25	-0.56 ± 0.63	1745 ± 3126
x_{oil}	-75.93 ± 30.10	-66.46 ± 39.13	-1.02 ± 1.03	3228 ± 5121
T	-0.18 ± 0.16	0.12 ± 0.04	0.009 ± 0.014	-8.27 ± 72
$x_{acid}*x_{oil}$	----------	----------	30.50 ± 44.00	$(-9.2 \pm 21.9) \times 10^4$
x_{acid}*T	----------	----------	-0.15 ± 0.63	-408 ± 3126
x_{oil}*T	45.21 ± 27.34	----------	-0.56 ± 1.03	245± 5121
$x_{acid}*x_{oil}$*T	----------	----------	7.45 ± 44.00	$(5.1 \pm 2.2) \times 10^4$
x_{acid}^2	-1243 ± 578	-1069 ± 751	----------	----------
x_{oil}^2	2276 ± 1184	1881 ± 1539	----------	----------
x_{acid}^2*T	----------	----------	----------	----------
x_{oil}^2*T	-1380 ± 1083	----------	----------	----------
Statistical Results	X_{max} model	X_{240} model	k model	$t_{1/2}$ model
SSres	0.0389	0.0792	1.23×10^{-4}	3823
$\hat{\sigma}^2$ (ν=2)	0.000106	0.00054	2.63×10^{-6}	246.5
Lack of fit test	R = 60.86 > $F_{10, 2, 0.05}$ = 19.40 Lack of fit	R = 11.11 < $F_{12, 2, 0.05}$ = 19.41 No lack of fit	R = 4.47 < $F_{10, 2, 0.05}$ = 19.40 No lack of fit	R = 1.24 < $F_{10, 2, 0.05}$ = 19.40 No lack of fit
Compared with 2nd order full model	Q = 6.15 < $F_{4, 2, 0.05}$ = 19.25 Differences are not significant	Q = 13.64 < $F_{6, 2, 0.05}$ = 19.33 Differences are not significant	Q = 8.66 < $F_{4, 2, 0.05}$ = 19.25 Differences are not significant	Q = 1.71 < $F_{4, 2, 0.05}$ = 19.25 Differences are not significant

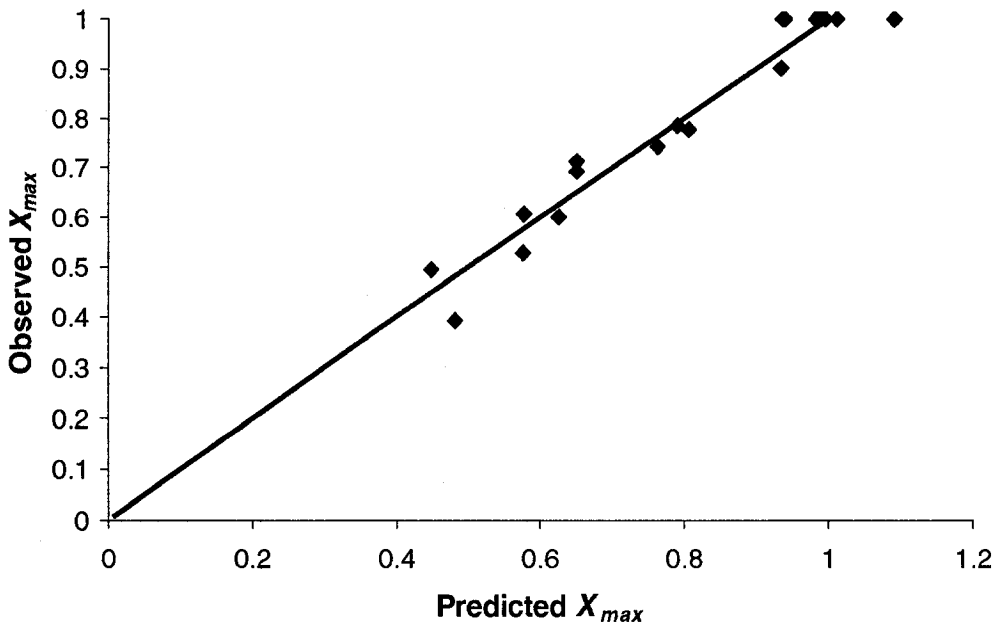

Figure 4.7 Observed X_{max} vs. predicted X_{max} for the reduced 2nd order X_{max} model.

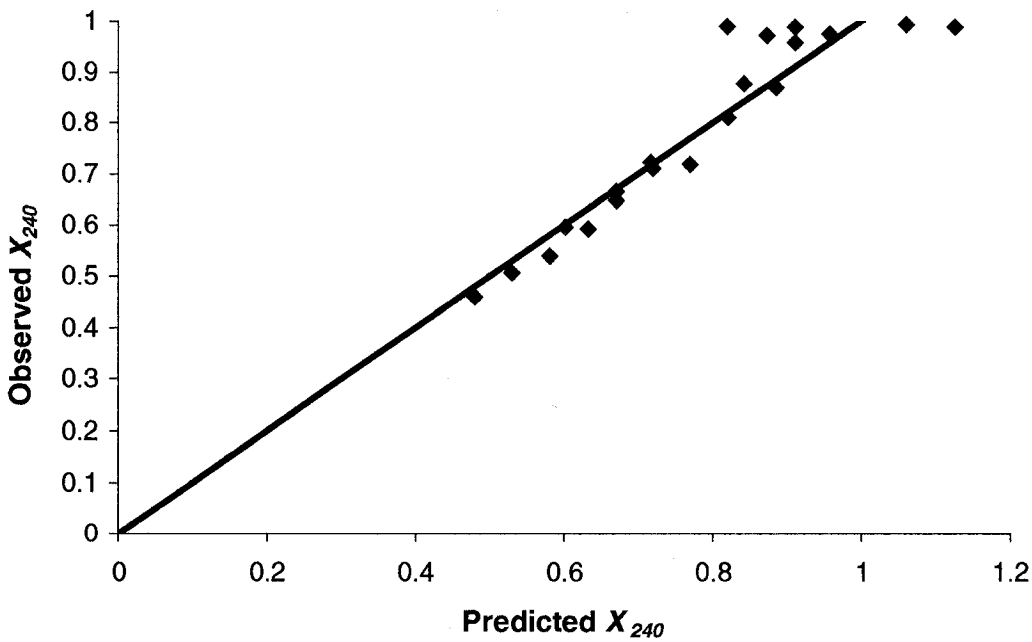

Figure 4.8 Observed X_{240} vs. predicted X_{240} for the reduced 2nd order X_{240} model.

The contour plot confirmed the effect of the initial feed composition on the conversion of oil discussed previously (Section 4.3.2). From the plots, it was also seen the significant effect of the temperature on the yield of biodiesel. The yield of biodiesel increased significantly at higher temperatures. Comparing the behaviour of the models at different temperatures (Figures 4.9 and 4.10), it was found that, at 70°C, the methanol to oil ratio dominated the yield of biodiesel, thus the operating condition with the highest methanol to oil ratio was found to be the optimum operating condition at 70°C. At 80°C, the effect of methanol to oil ratio on the yield of biodiesel was affected by other factors, such as acid concentration and temperature and thus was more complex.

A region of $X_{max} \geq 1$ (practically X_{max} can only =1) was found in the contour plots of the X_{max} model at 80°C (Figure 4.9). An experiment carried out in our design (Exp#15, Table 4.2) was found to be inside the optimum region of the contour plot of 80°C, and the oil conversion finally reached at 240 min was 98.92%. It was very constructive that a region of $X_{240} \geq 100\%$ was also found in the contour plot of the X_{240} model at 80°C. Thus it effectively predicted that it was possible to obtain 100% oil conversion with acid-catalyzed transesterification during a reaction time of 4hrs. The temperature still had a key impact on the yield of biodiesel at 240 min. At 70°C, a region of $X_{240} \geq 100\%$ was not found in the contour plot of X_{240} model, indicating the effect of temperature was significant. It was also found that the methanol to oil ratio dominated the yield at 240 min in the X_{240} model at 70°C, which was very similar to the results obtained from the X_{max} model at 70°C. An experiment carried out (Exp #15, Table 4.2) with a feed composition of 96.9 mol% MeOH, 2.5% acid and 0.6% oil at 80°C was also found to highest model predicted conversion, its actual X_{240} was found to be 0.989. Another experiment (Exp#11,

(a)

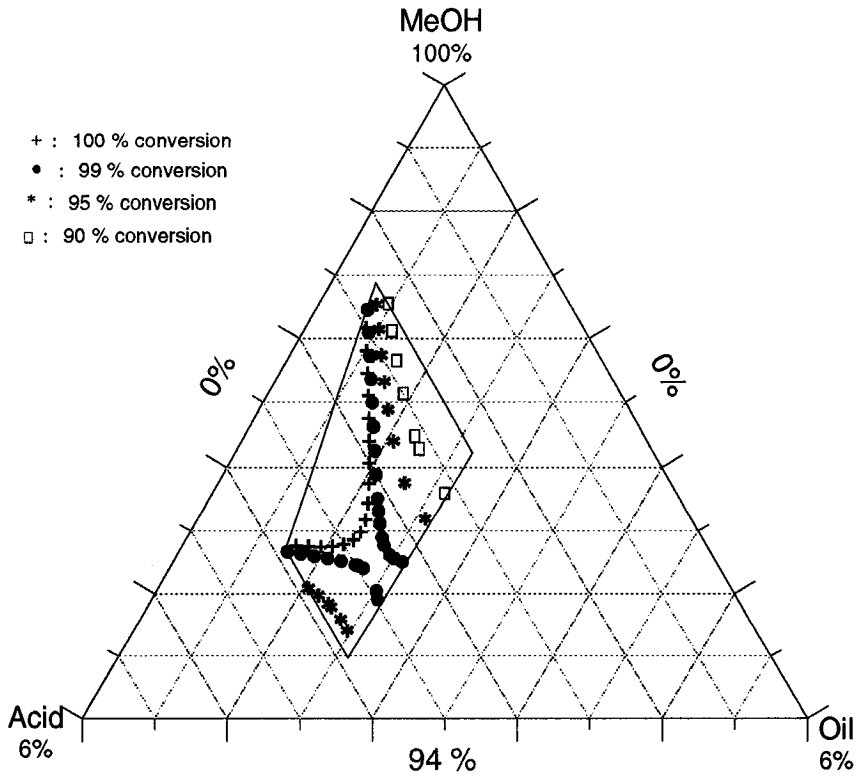

(b)

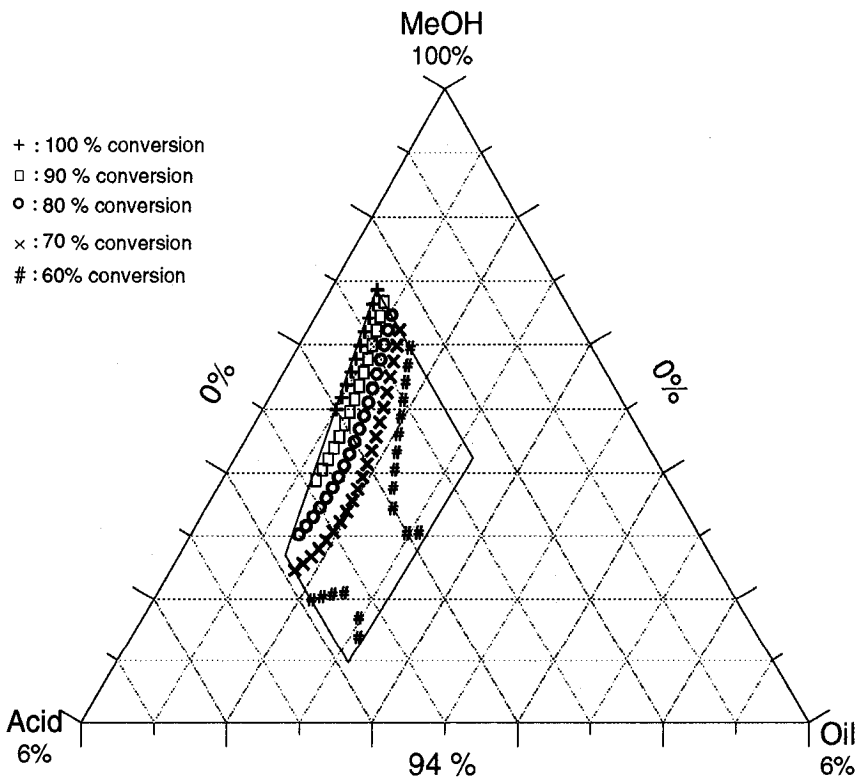

Figure 4.9 Model prediction of the reduced 2nd order X_{max} model at 80°C (a) and 70°C (b).

(a)

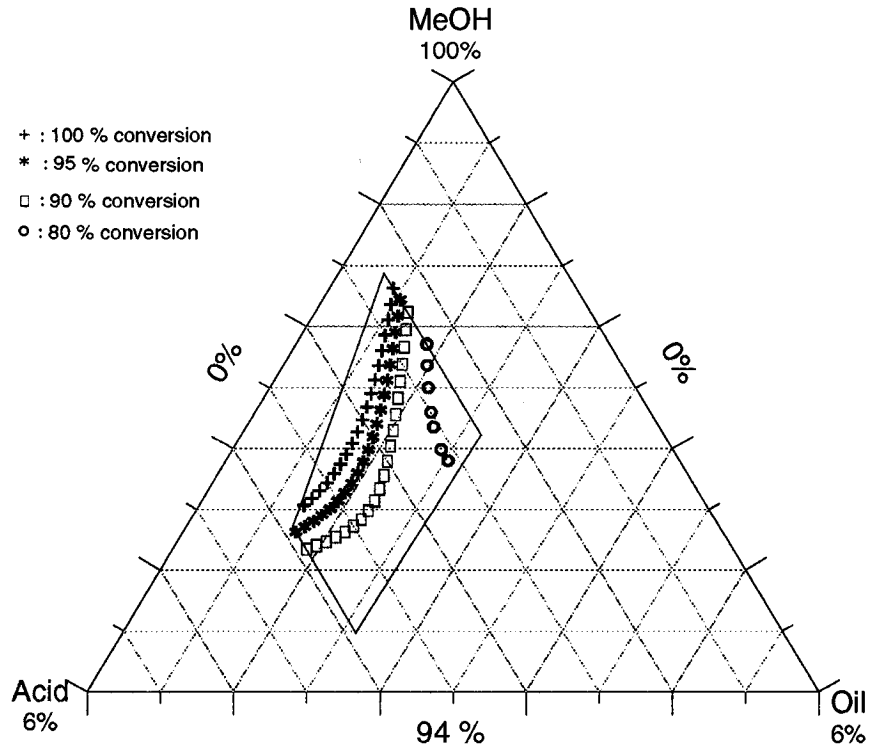

(b)

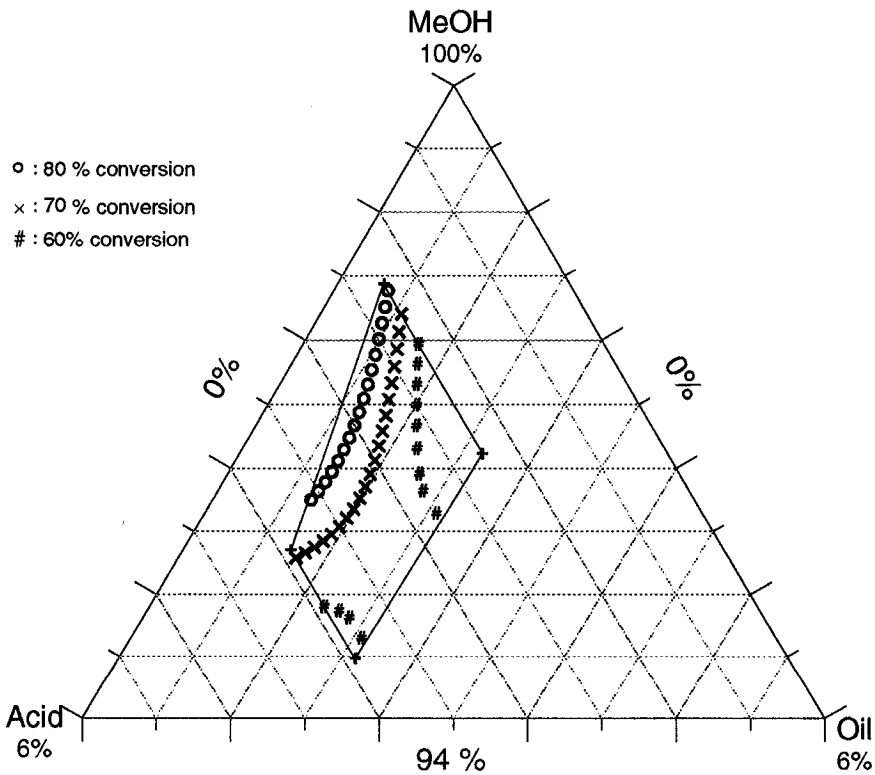

Figure 4.10 Model prediction of the reduced 2nd order X_{240} model at 80°C (a) and 70°C (b).

Table 4.2) with a feed composition of 98.1 mol % 1.5% acid and 0.4% oil at 80°C was fount to have the highest experimental conversion (X_{240} = 0.994). The two points were all in the optimum operating region.

4.4 Conclusions

The acid-catalyzed transesterification reached high conversion values with methanol to oil ratios in the range of 50:1 to 250:1 at temperatures of 70°C and 80°C. The free fatty acid present in the waste oils was found to be converted into FAME immediately in the acid-catalyzed transesterification when a large excess of methanol was used, thus it did not interfere with reaction.

There was no significant difference in conversion between runs using the 3 mixing rates (100, 400 and 600 rpm) used in the study, mainly because the large excess of methanol used in the study decreased the viscosity of the reaction mixture. Thus the mixing intensity was not a significant factor under the operating conditions in this work.

The reaction temperature had a significant effect on the reaction rate of the transesterification, higher temperatures resulting in higher conversions after a 4 hr reaction time. The conversion at the end of transesterification increased substantially on increasing the temperature from 70°C to 80°C.

The effect of feed composition on the yield of biodiesel was plotted at different temperatures. It was found that the methanol to oil ratio was an important factor, the yield of biodiesel increasing generally with increasing methanol to oil ratio. However, the influence of the feed composition and temperature on the yield of biodiesel was complex.

Empirical models were built to describe these complex combined effects of temperature and feed composition on four responses. An optimal feed composition region was determined using contour plots of conversion based on fitted models (see Figure 4.9 and 4.10).

A run with feed composition of 96.9 mol% MeOH, 2.5% acid and 0.6% oil and a temperature of 80°C (Exp #15, Table 4.2) gave the highest model predicted conversion, and another run with feed composition of 98.1 mol% MeOH, 1.5% acid and 0.4% oil and a temperature of 80°C (Exp #11, Table 4.2) gave the highest experimental conversion. Both of the runs were found in the optimal feed composition region.

4.5 References

Box, G. E. P., W.G. Hunter and J. S. Hunter, "Statistics for experimenters : an introduction to design, data analysis, and model building", Wiley, New York (1978).

Canakci, K. and J. Van Gerpen, "Biodiesel Production via Acid Catalysis", Transactions of the ASAE **42**, 1230-1210 (1999).

Coltrain, D., "Biodiesel: Is It Worth Considering", 2002 Risk and Profit Conference, Manhattan, Kansas (2002).

Freedman, B., E.H. Pryde and T.L. Mounts, "Variables Affecting the Yields of Fatty Esters from Transesterified Vegetable Oils", J. Am. Oil Soc. Chem.**61**, 1638-1643 (1984).

Liu, K., "Preparation of Fatty Acid Methyl Esters for Gas Chromatographic Analysis of Lipids in Biological Materials", J. Am. Oil Chem. Soc. **71**, 1179-1187 (1994).

McBride, N., "Modeling the Production of Biodiesel from Waste Frying Oil", B.A.Sc graduate thesis, unpublished (1999).

Mittelbach, M. and Gangl, S., "Long Storage Stability of Biodiesel Made from Rapeseed and Used Frying Oil", J. Am. Oil Soc. Chem.**78**, 573-577 (2001).

Noureddini, H. and D. Zhu, "Kinetics of Transesterification of Soybean Oil", J. Am. Oil Soc. Chem.**74**, 1457-1463 (1997).

Peterson, C.L., M. Feldman, R. Korus, and D.L. Auld, "Batch Type Transesterification Process for Winter Rape Oil", ASAE **91**, 711-716 (1991).

Ripmeester, W., "Modeling the Production of Biodiesel from Waste Frying Oil", B.A.Sc graduate thesis, unpublished (1998).

Zhang, Y., M.A. Dubé, D. D. McLean and M. Kates, "Biodiesel Production from Waste Cooking Oil: Economic Assessment and Sensitivity Analysis", Bioresource Technol., to be submitted (2002).

Zheng, S., M.A. Dubé, D. D. McLean and M. Kates, "Monitoring Biodiesel Production Using ATR-FTIR spectroscopy and GPC", J. Am. Oil Soc. Chem., to be submitted (2003).

CHAPTER 5

GENERAL DISCUSSION AND CONCLUSIONS

5.1 Discussion

5.1.1 In-line Monitoring of the Transesterification Reaction

ATR-FTIR spectroscopy used for the in-line monitoring of the acid-catalyzed transesterification, was found not to be practically useful (Chapter 3). Mixtures of methanol and sulfuric acid were used as the background for monitoring at the operating temperature (70°C or 80°C). The spectra of the reaction mixtures was taken every 2 minutes for a total of 240 minutes, and were plotted as a function of reaction time (Z axis) in a 3-D graph (Figure 5.1).

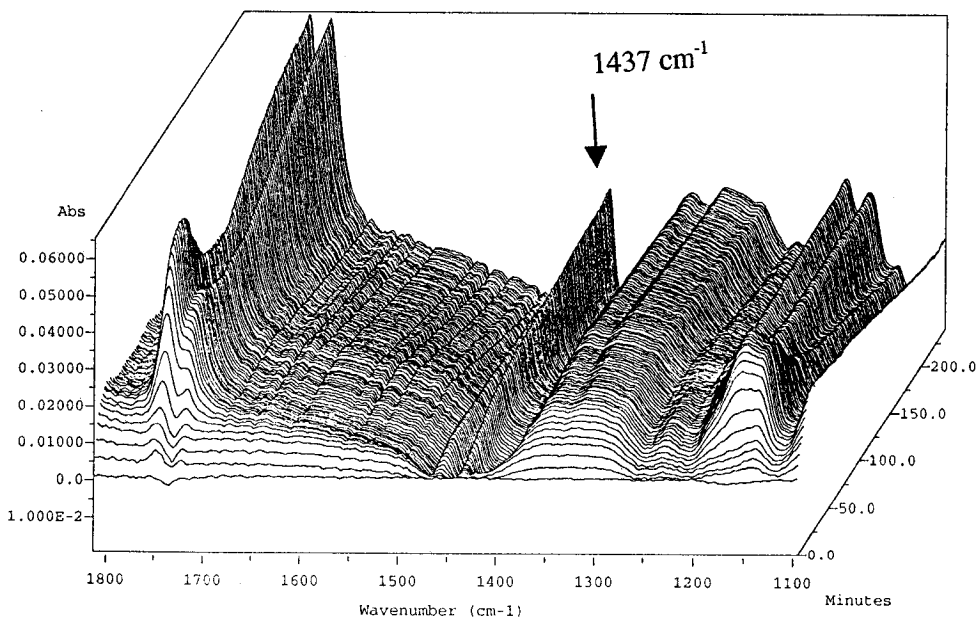

Figure 5.1 Typical ATR-FTIR spectra of a transesterification reaction as a function of time at 80°C with feed composition: 96.2 mol% MeOH, 2.5% acid and 1.3% oil.

The band at 1437 cm^{-1} was chosen for in-line monitoring of the reaction, which represented the CH_3-O- group in FAME. As discussed in Chapter 3, the absorbance peak height of this band is proportional to the concentration of FAME in the reactor and increased during the reaction (Figure 5.1). To convert the profiles of peak height into oil to FAME conversion data, 2 sets of calibrations using two methanol concentrations were carried out. For each calibration, mixtures of different compositions of waste frying oil and FAME in methanol (the methanol concentration was constant) was heated to 80°C, the peak height at 1437cm^{-1} was recorded against the background of methanol and plotted as a function of concentration of FAME. Sulfuric acid was not added to avoid reaction with components. The basic idea was to check whether the calibration was affected by the change of methanol concentration, so that the calibration could be used for all the experiments. Unfortunately, the calibration curves with different methanol concentrations differed from each other. Therefore, in order to determine the conversion of oil to FAME, for experiments with different methanol concentration, a separate calibration would have to be carried out for each methanol concentration, which was not practical. ATR-FTIR was also very sensitive to changes in temperature. Thus, if the set point of the operating temperature was changed, a new calibration would have to be done.

Some other difficulties were also encountered in the in-line monitoring. In our studies, since the operating temperature was above the boiling point of methanol, the evaporation of methanol resulted in variation of the methanol concentration during the reaction. This might affect the absorbance of the characteristic peak at 1437cm^{-1}. However, the effect can be reduced by operation of the water-cooled condenser. In-line monitoring still might be used for other purposes, such as checking the equilibrium of the

transesterification, indicated by the peak height at 1437 cm^{-1} reaching a constant. It is still possible to monitor transesterification at one methanol concentration once the optimum conditions have been determined.

For the off-line monitoring, since the methanol and sulfuric acid were removed from the reaction samples, spectra could be taken on the resulting oil, thus avoiding any problem caused by variation in methanol concentration.

5.2 Summary

In this thesis, an empirical study of the acid-catalyzed transesterification of waste frying oil was carried out, and two analytical methods GPC and ATR-FTIR spectroscopy were investigated for their suitability and accuracy in our kinetic study.

The two analytical methods were both found to be highly accurate and reproducible; the standard error of both methods was less than 10^{-4}. A series of nested designs were used to evaluate the reproducibility of procedures in both methods, the sources of variability were also characterized. None of the procedures was found to contribute to the total variability. The analyses by the two analytical methods were compared and were found to be in good agreement with each other.

The effect of rate of mixing, feed composition and temperature on the reaction was investigated. Because of the large excess of methanol, the intensity of mixing was not a contributing factor to the transesterification when the stirring speed was 100 rpm or higher. The yield of biodiesel increased generally with increasing methanol to oil ratio and operating temperature, but the combined effect of the feed composition and temperature on the yield of biodiesel was found to be complex. A mixture design was

thus used in the study. Empirical models were built on four responses: the maximum obtainable conversion (X_{max}), conversion at 240 min (X_{240}), overall reaction rate (k), and the time to reach 50% of maximum obtainable conversion ($t_{1/2}$). The second order X_{max} and X_{240} models were further reduced, and the reduced X_{max} and X_{240} models found to be the best fitted models. Using the conversion contour plots of the two models, the optimum feed composition region was determined (see Chapter 4, Figure 4.14 and 4.15). An experiment carried out (Exp #15, Table 4.2) with a feed composition of 96.9 mol% MeOH, 2.5% acid and 0.6% oil at 80°C was also found to highest model predicted conversion, its actual X_{240} was found to be 0.989. Another experiment (Exp#11, Table 4.2) with a feed composition of 98.1 mol % 1.5% acid and 0.4% oil at 80°C was fount to have the highest experimental conversion ($X_{240} = 0.994$). The two points were all found to be in the optimum operating region.

5.3 Recommendations

Based on the results of these studies and some assumptions we have made, the following recommendations are proposed to our kinetic study.

A study should be carried out to better understand the mechanism of the 3-step acid-catalyzed transesterification.

Efforts should be made to improve the separation of triglycerides and diglycerides in the GPC analyses, although the current results were adequate. Other GPC columns should be examined as well as lower column temperatures to improve the separations of triglycerides and diglycerides.

Replication of the analyses of the transesterification reactions in the experimental design should be carried out to validate the modelling. In order to validate the optimum feed composition region, some experiments should be carried out within the optimum region.

Based on the modeling of the acid-catalyzed transesterification, further increasing the reaction temperature may result in higher yields of biodiesel. For example, a higher temperature, such as 90°C, might result in higher yield of biodiesel at a lower methanol to oil ratio.

The design of the reactor might be altered to increase the contact area of methanol phase and oil phases, thus increasing the reaction rate. The transesterification reaction should also be scaled up to check its suitability for industrial use. A continuous process using the acid-catalyzed transesterification should be carried out and studied in connection with development of an industrial purpose.

APPENDIX

A-1 Acid Removal in Sample Preparation

It was important to remove all the residual catalyst in the samples to prevent any possible further reaction. A pH test was done to check for removal of acid in our sample preparation. We found that the oil after the methanol/water wash was neutral, however, the oil before the wash was slightly acidic. A second methanol/water washing was done to check the efficiency of first methanol/water washing. The oil layer was neutral after both the first and second washing. The methanol-water layer of the first washing was slightly acidic, but that of the second washing was found to be neutral, showing that one methanol/water washing was adequate to remove all the residual acid in the samples. Table A.1 shows the results of the extraction and methanol/water washing.

Table A.1 pH test results of petroleum ether extraction and methanol/water washing

	pH of upper layer (oil layer)	pH of bottom layer (water layer)	Necessity of wash
Samples extracted with petroleum ether	Acidic	Acidic	Yes
1st wash with methanol/water mixture	7	Slightly acidic	Yes
2nd wash with methanol/water mixture	7	7	No

A-2 GPC Calibration

Six standards were calibrated, the calibration curves are shown in Figure A.1, and the calculation of injection mass are shown in Table A.2.

Table A.2 Calibrations of standard solutions, injection mass (mg)=*a*+*b*×Peak Area

Component	*a*	*b*	Standard error	R^2
Glycerol	-0.0143	4.43×10^{-8}	0.002855	0.9965
Oleic acid	-0.00232	3.37×10^{-8}	0.004773	0.9904
Methyl oleate	-0.00018	5.44×10^{-8}	0.002151	0.9982
Monoolein	-0.00196	3.85×10^{-8}	0.002528	0.9989
Diolein	0.002469	4.29×10^{-8}	0.002931	0.9985
Triolein	0.001256	3.39×10^{-8}	0.002327	0.9991

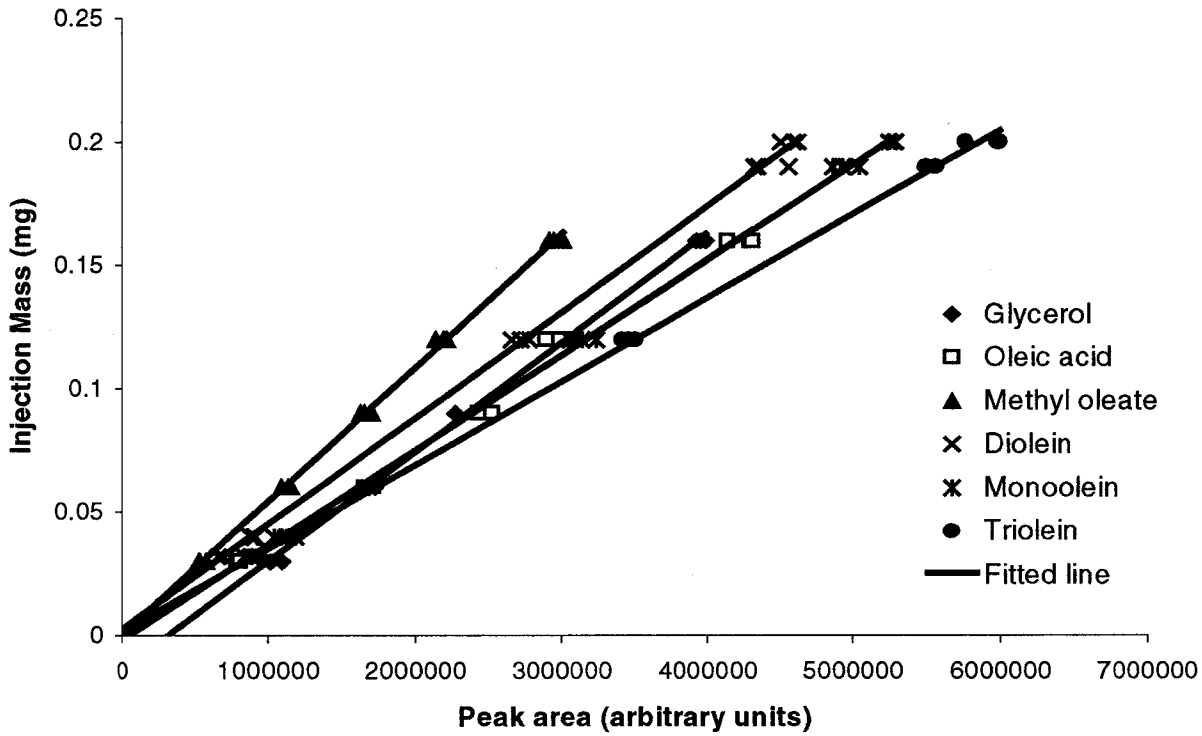

Figure A.1 Calibration curves of glycerol, oleic acid, methyl oleate (FAME), diolein, monoolein, and triolein.

A-3 Separations of TG and DG by GPC Analysis

Originally, all the injection concentrations were set at 1mg/mL; but we found that the separation of TG and DG was not complete at this concentration. Different concentrations of sample solutions were injected and different flow rates were used to improve the separations. The masses of samples injected were kept constant by varying the injection volumes (Table A.3).

Table A.3 Injections used to compare the separations.

Injection	Concentration (mg/mL)	Flowrate (mL/min)	Injection volume (μL)	Analysis time (min)
Inj#1	1	1	200	25
Inj#2	1	0.8	200	40
Inj#3	1	0.5	200	50
Inj#4	10	1	20	25
Inj#5	10	0.5	20	50
Inj#6	20	1	10	25

It was found that with the same concentration, lowering the flow rate would improve the separation. Inj#1, Inj#2, and Inj#3, Inj#3 had the best separation, however, the analysis time per sample doubled. And at the same flow rate, the more concentrated the sample, the better separation. In Inj#1, Inj#4, and Inj#6, Inj#6 had the best separation (Figure A.2). This could be explained because at the higher concentration, the sample would form a narrower band than at the lower concentrations, so that the eluted peak of each component would be sharper, thus helping the separation. Lowering the flow rate of mobile phase actually had the same effect as increasing the concentration. Theoretically, using a higher concentration and a lower flow rate at the same time would give the best separation, however, little differences were found between Inj#6 and Inj#5. Considering

the large amount of samples generated, 20 mg/mL injection concentration and 1mL/min flow rate were routinely used for all sample analyses in all experiments.

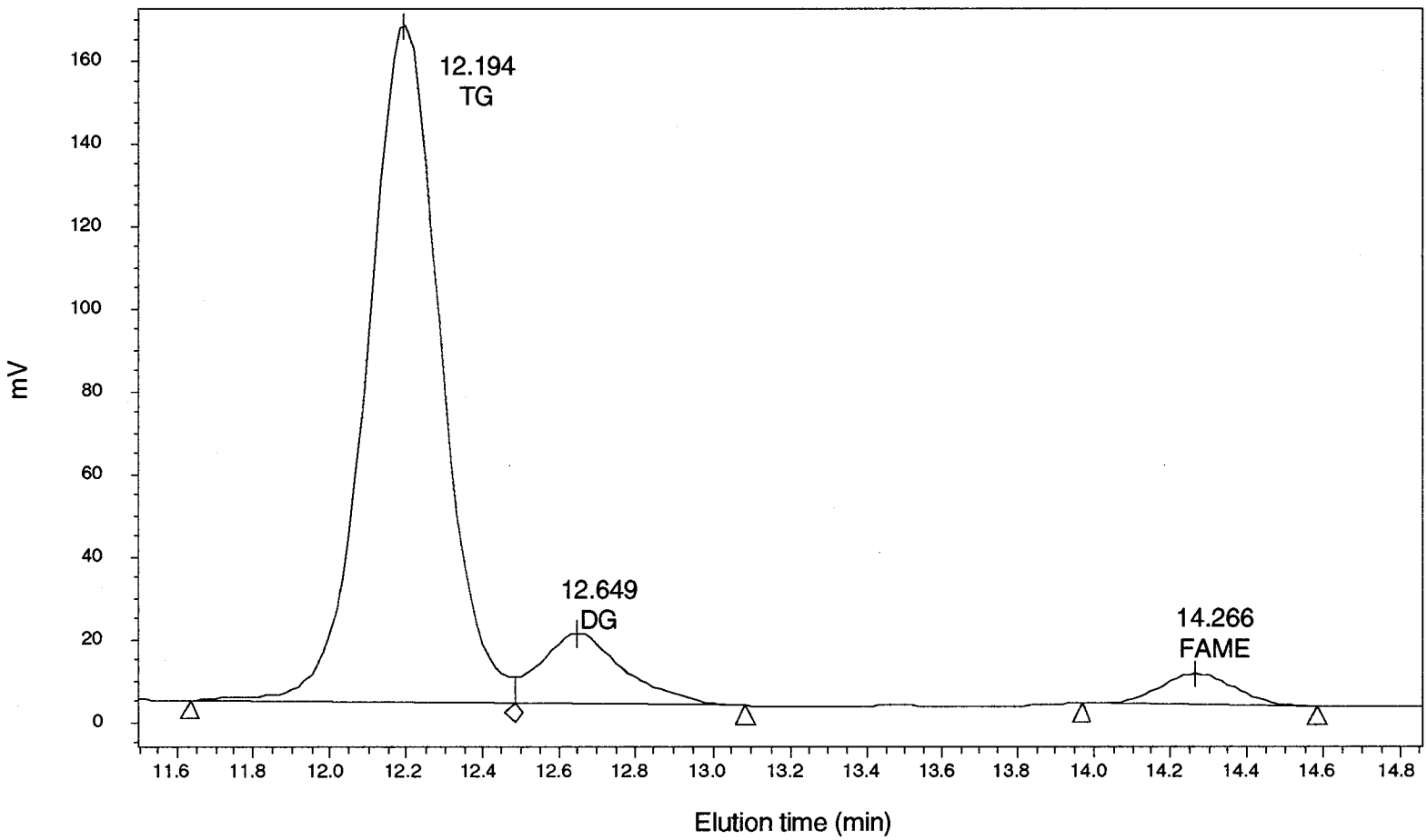

Figure A.2 GPC Separation of Inj#6, concentration, 20 mg/mL, flow rate of mobile phase, 1 mL/min, analysis time per sample: 25 min.

A-4 GPC Analysis of Standard of Mixtures

Table A.4 GPC analysis of the other 2 mixtures of standards*

		Weight fraction			
		Triolein	Diolein	Monoolein	Methyl oleate
Mixture 1	Inj#1	0.044	0.136	0.150	0.665
	Inj#2	0.046	0.138	0.150	0.665
	Inj#3	0.046	0.138	0.153	0.668
	Mean	0.046	0.137	0.151	0.666
	Actual	0.048	0.108	0.136	0.709
	Standard deviation	-0.002	0.030	0.015	-0.043
	Recovery	0.959	1.277	1.107	0.940
	Revised recovery	1.000	1.154	1.107	0.940
Mixture 2	Inj#1	0.205	0.063	0	0.722
	Inj#2	0.208	0.064	0	0.729
	Inj#3	0.214	0.064	0	0.732
	Mean	0.209	0.064	0	0.728
	Actual	0.234	0.053	0	0.713
	Standard deviation	-0.025	0.011	0	0.015
	Recovery	0.892	1.201	0	1.021
	Revised recovery	1.000	1.154	0	1.021

*Injection concentration used was 20 mg/mL, 10 μL of the solution was injected.

A-5 Experimental Results from Nested Designs.

A series of nested designs were used to try to identify the most significant sources of variability. Five mixtures of oil and FAME were used in the nested design. Three samples were taken from each of the mixtures and analyzed by both GPC and FTIR. For GPC analysis, 3 dilutions were made for each of the 5 mixtures, and for each dilution, 3 repeat injections were made for a total of 45 measurements. For ATR-FTIR spectroscopy, 3 samples were taken from each of the 5 mixtures, and 3 repeat measurements were carried out for each sample for a total of 45 measurements. The analysis results of the nested design are shown in Table A.5.

Table A.5 Analyses of ATR-FTIR spectroscopy and GPC in nested design

Composition	Sample/dilution	Measurement/injection	Off-line ATR-FTIR analysis	GPC analysis
1	1	1	0.117	0.120
1	1	2	0.114	0.121
1	1	3	0.110	0.123
1	2	1	0.114	0.123
1	2	2	0.116	0.125
1	2	3	0.112	0.126
1	3	1	0.107	0.126
1	3	2	0.110	0.129
1	3	3	0.113	0.129
2	1	1	0.232	0.246
2	1	2	0.229	0.246
2	1	3	0.230	0.246
2	2	1	0.230	0.247
2	2	2	0.230	0.247
2	2	3	0.229	0.247
2	3	1	0.232	0.248
2	3	2	0.226	0.249
2	3	3	0.226	0.250

(Continued next page)

Composition	Sample/dilution	Measurement/injection	Off-line ATR-FTIR analysis	GPC analysis
3	1	1	0.527	0.544
3	1	2	0.526	0.545
3	1	3	0.524	0.545
3	2	1	0.529	0.546
3	2	2	0.523	0.547
3	2	3	0.531	0.547
3	3	1	0.534	0.547
3	3	2	0.536	0.548
3	3	3	0.536	0.550
4	1	1	0.769	0.729
4	1	2	0.767	0.729
4	1	3	0.767	0.7320
4	2	1	0.771	0.742
4	2	2	0.770	0.743
4	2	3	0.768	0.757
4	3	1	0.753	0.760
4	3	2	0.756	0.762
4	3	3	0.754	0.765
5	1	1	0.891	0.894
5	1	2	0.888	0.895
5	1	3	0.893	0.897
5	2	1	0.895	0.898
5	2	2	0.889	0.899
5	2	3	0.889	0.899
5	3	1	0.886	0.901
5	3	2	0.886	0.901
5	3	3	0.887	0.904

A-6 Paired Comparison Results of All the Experiments.

Table A.6 Results from paired comparison of all the experiments.

Exp	Methanol	Acid	Oil	Temp	95% confidence interval of w*		0 included?	99% confidence interval of w		0 included?
1	98.1	1.5	0.4	70	0.0050	0.0264	No	0.0002	0.0312	No
2	95.6	3.5	0.9	70	-0.0031	0.0296	**Yes**	-0.0103	0.0368	**Yes**
3	94.6	3.5	1.9	70	-0.0004	0.0408	**Yes**	-0.0094	0.0498	**Yes**
4	96.5	1.5	2	70	0.0495	0.0980	No	0.0390	0.1086	No
5	96.9	2.5	0.6	70	-0.0099	0.0322	**Yes**	-0.0191	0.0414	**Yes**
6	95.1	3.5	1.4	70	-0.0195	0.0218	**Yes**	-0.0284	0.0308	**Yes**
7	97.3	1.5	1.2	70	0.0010	0.0393	**Yes**	-0.0074	0.0477	**Yes**
8	95.6	2.5	1.9	70	0.0042	0.0514	No	-0.0062	0.0618	**Yes**
9	96.2	2.5	1.3	70	0.0299	0.0814	No	0.0186	0.0927	No
10	96.2	2.5	1.3	70	0.0027	0.0548	**Yes**	-0.0086	0.0661	**Yes**
1	98.1	1.5	0.4	80	0.0009	0.0341	No	-0.0067	0.0242	**Yes**
2	95.6	3.5	0.9	80	0.0192	0.0633	No	0.0096	0.0729	No
3	94.6	3.5	1.9	80	-0.0319	0.0400	**Yes**	-0.0476	0.0557	**Yes**
4	96.5	1.5	2	80	0.0062	0.0745	No	-0.0087	0.0895	**Yes**
5	96.9	2.5	0.6	80	-0.0127	0.0224	**Yes**	-0.0204	0.0300	**Yes**
6	95.1	3.5	1.4	80	-0.0102	0.0681	**Yes**	-0.0273	0.0852	**Yes**
7	97.3	1.5	1.2	80	0.0425	0.1017	No	0.0296	0.1146	No
8	95.6	2.5	1.9	80	-0.0191	0.0669	**Yes**	-0.0379	0.0857	**Yes**
9	96.2	2.5	1.3	80	-0.0881	0.0055	**Yes**	-0.1085	0.0259	**Yes**
10	96.2	2.5	1.3	80	-0.0187	0.0408	**Yes**	-0.0309	0.0530	**Yes**

* w is the difference between off-line ATR-FTIR and GPC analyses (w = ATR-FTIR -GPC)

A-7 The Determination of the 95% Confidence Intervals of X_{max}, X_{240}, $t_{1/2}$ and k

The 95 % confidence interval of the X_{max} X_{240}, $t_{1/2}$ and k were estimated by

$$\hat{Y} - \frac{t_{v,0.025}\sqrt{Variance(\hat{Y})}}{\sqrt{n}} \leq Y \leq \hat{Y} + \frac{t_{v,0.025}\sqrt{Variance(\hat{Y})}}{\sqrt{n}} \quad \text{(A.1)}$$

where Y represent the estimated responses, v is the degree of freedom associated with the variance estimates and n is the numbers of observations. The variance of k and X_{max} were estimated by linearizing the non-linear conversion model approximately using covariance matrix of the parameter estimates, $(Z^TZ)^{-1}\hat{\sigma}^2$, and Z is defined as follows

$$Z = \left[\left.\frac{\partial X}{\partial X_{\max}}\right|_{\hat{X}_{\max},t} \quad \left.\frac{\partial X}{\partial k}\right|_{\hat{k},t} \right] \quad \text{(A.2)}$$

$$(Z^TZ)^{-1}\hat{\sigma}^2 = \begin{bmatrix} Variance(\hat{X}_{\max}) & Covariance(\hat{X}_{\max},\hat{k}) \\ Covariance(\hat{X}_{\max},\hat{k}) & Variance(\hat{k}) \end{bmatrix} \quad \text{(A.3)}$$

where $\hat{\sigma}^2$ can be estimated by SSres/n-2. The variance of $t_{1/2}$ can be estimated by

$$Variance(t_{1/2}) = \frac{\partial t_{1/2}}{\partial k} Variance(\hat{k}) \quad \text{(A.4)}$$

The variance of X_{240} was estimated by 7 replicates of X_{240} obtained at the center point of the design (feed composition: 95.6 mol%, 3.5% acid, 0.9% oil, temperature:80°C), and was found to be 0.0033.

A-8 The Maximum Obtainable Conversion (X_{max}) Model

The first order X_{max} model was first built according to Equation 4.6, the model was

$$E(Y) = 1.01 + 1.64\, x_{acid} - 24.28\, x_{oil} - 0.05\, T + 229.22\, x_{acid}\, x_{oil} + 1.94\, x_{acid}\, T + 10.79\, x_{oil} T - 244\, x_{acid}\, x_{oil} T \quad \text{(A.5)}$$

The observed Xmax were plotted against the model preditions in Figure A.3. The residuals were plotted as a funtion of X_{acid}, X_{oil}, T and the reaction order (Figure A.5) to examine the adequacy of the models . No time trend was detected in the residuals plot of reaction order. There was a trend in the residual plot of X_{acid}, X_{oil}, indicating that the first order model might not be adequate.

The second order model was then built according to Equation 4.7 and the model was

$$E(Y) = 0.46 + 69.60\, x_{acid} - 75.87\, x_{oil} + 0.023T - 6.34\, x_{acid}\, x_{oil} - 17.40\, x_{acid}\, T + 45.13\, x_{oil} T + 256\, x_{acid}\, x_{oil} T - 1242\, x_{acid}^2 + 2280\, x_{oil}^2 + 278\, x_{acid}^2 T - 1607\, x_{oil}^2 T \quad \text{(A.6)}$$

The observed X_{max} were plotted against the model preditions in Figure A.4. The second order model appeared to have a better fit than the first order model. The examination of the residuals plots (Figure A.5 and Figure A.6) also confirmed that the second order model was more significant than the first order model. Lack of fit test of the first, second and models was carried out using the R test. The value of R are given by

$$R = \frac{1}{\hat{\sigma}^2} \frac{\text{SSLF}}{\text{n - p - degree of freedom of } \hat{\sigma}^2} \quad \text{(A.7)}$$

where SSLF = SSres – $\hat{\sigma}^2 \times$ (degree of freedom associated with $\hat{\sigma}^2$), n is the number of observations, p is the number of parameter estimates in the model, and R values of the

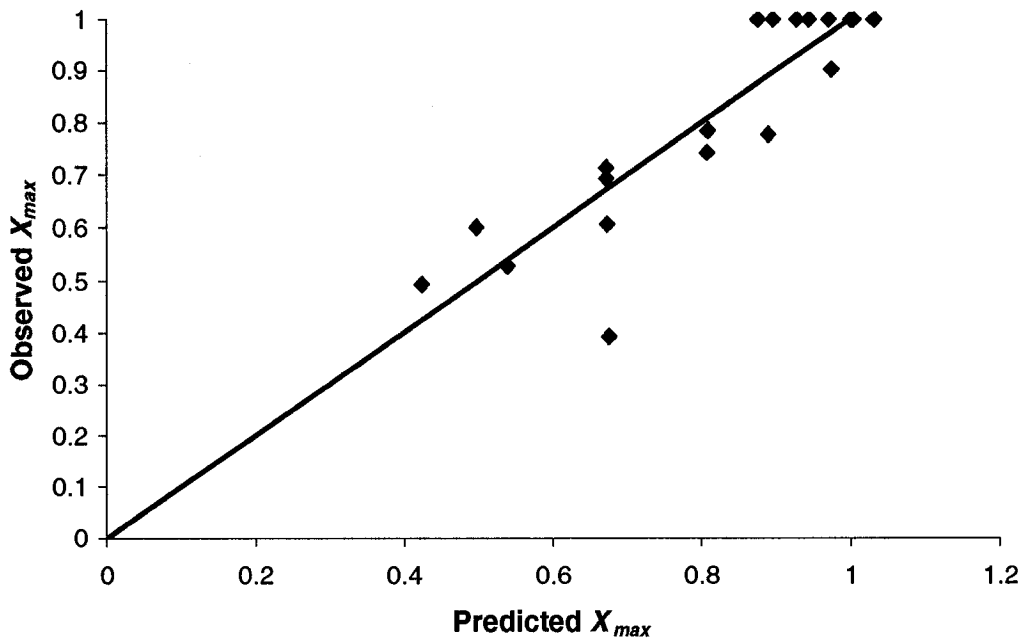

Figure A.3 Observed X_{max} vs. predicted X_{max} for the 1st order X_{max} model.

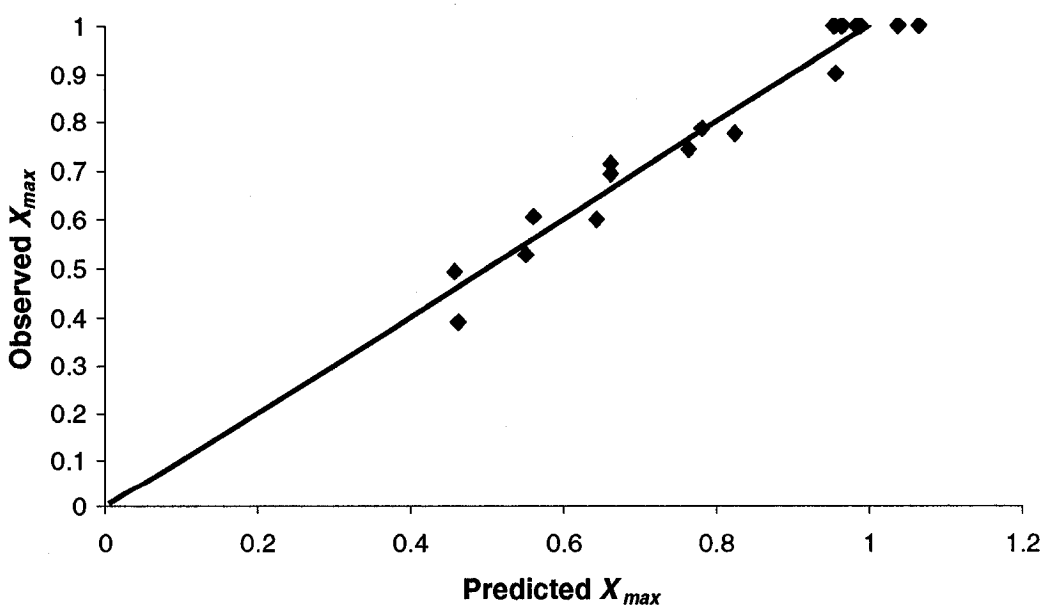

Figure A.4 Observed X_{max} vs. predicted X_{max} for the 2nd order X_{max} model.

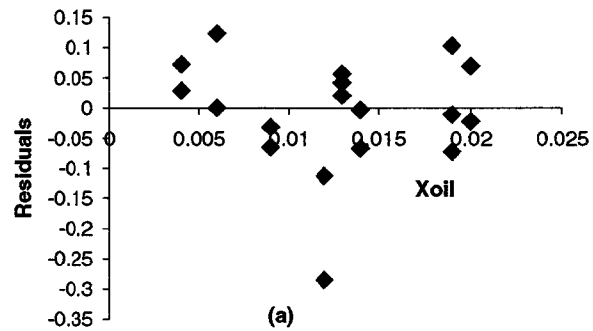

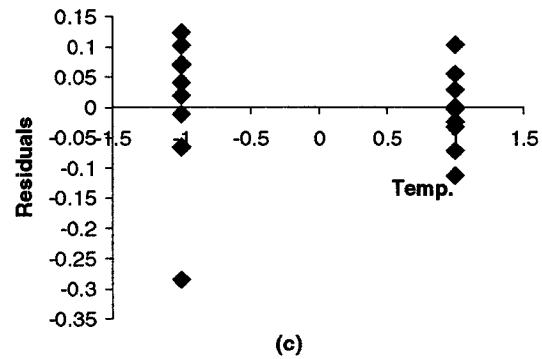

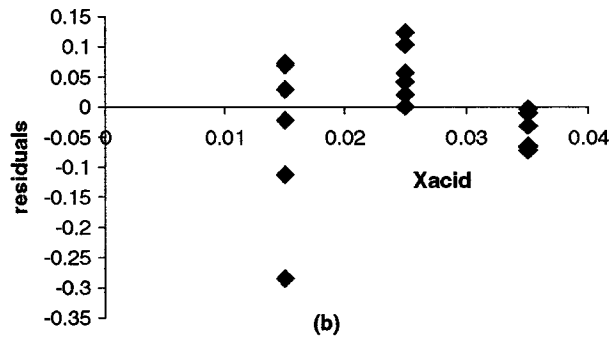

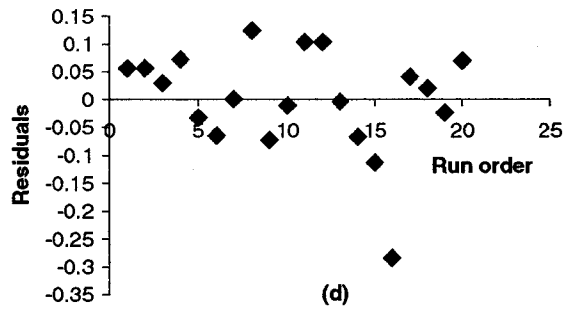

Figure A.5 Residuals plots of 1st order X_{max} model

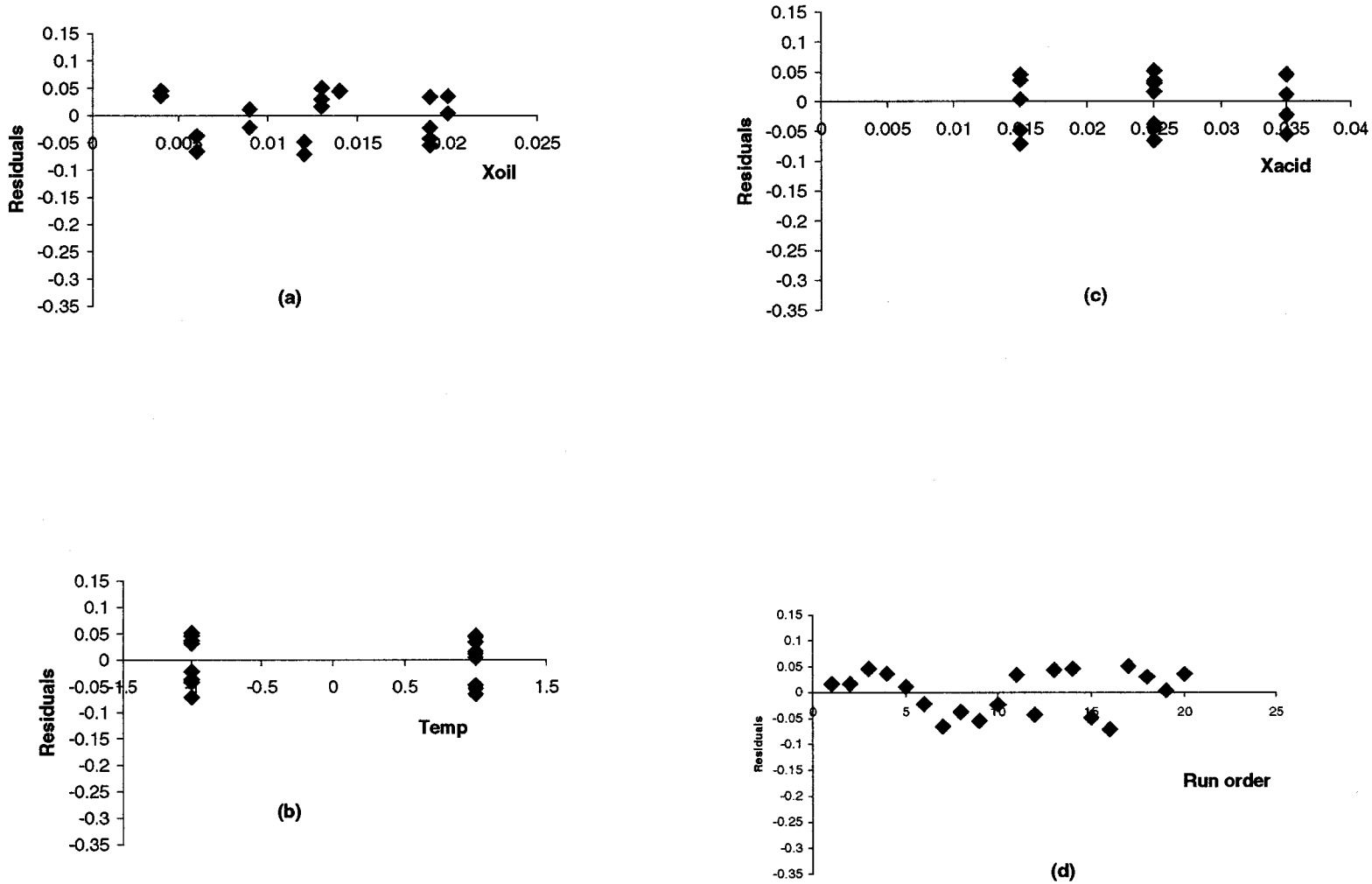

Figure A.6 Residuals plots of 2nd order X_{max} model

first and second order model were calculated

$$R\ (1^{st}\ \text{order}\ X_{max}\ \text{model}) = 155.58 > F_{2,\,10,\,0.05} = 19.40$$

and

$$R\ (2^{nd}\ \text{order}\ X_{max}\ \text{model}) = 51.66 > F_{2,\,6,\,0.05} = 19.34$$

Thus both of the models displayed lack of fit. One reason was that the X_{max} was obtained by fitting the first order non-linear model to the experimental data, a constraint of $X_{max} \leq 1$ was applied to the models, resulting in very small external pure error variance ($\hat{\sigma}^2 = 0.000106$). It was found that the lack of fit test might not be a good approach to assess the adequacy of the models. Thus an extra sum of squares test was carried out using external pure error variance estimation. The Q was calculated by

$$Q = \frac{1}{\hat{\sigma}^2} \frac{\text{SSres of } 1^{st} \text{ order model - SSres of } 2^{nd} \text{ order model}}{\text{No.of Parameters in } 2^{nd} \text{ order model - No.of Parameters in } 1^{st} \text{ order model}} \tag{A.8}$$

$$= 312.13 > F_{4,\,2,\,0.05} = 19.25$$

Combined with results from residuals plots, the second order X_{max} model was found to be the fitted model.

The second order X_{max} model was further reduced to simplify the modeling. A parameter correlation matrix (Figure A.7) was calculated for the model. It was found that most of the parameter estimates are highly correlated. 95% confidence intervals of the parameter estimates were examined and the parameter with the least correlation with other parameters was removed from the model. An extra sum of squares test was carried out between the reduced model and the full model to check the adequacy of reduced model. The process was repeated until the model could not be reduced (see Table A.7).

The fitted reduced model with least parameters was:

$$E(Y) = 0.46 + 69.53\, x_{acid} - 75.92\, x_{oil} - 0.182T + 45.21\, x_{oil}T + 1243\, x_{acid}^2 + 2277\, x_{oil}^2 - 1380\, x_{oil}^2 T \quad \text{(A.9)}$$

A lack of fit test was also carried out to check the adequacy of the reduced model, however, the model displayed lack of fit because of the small pure error variance.

$$R\ (2^{nd}\ \text{order reduced}\ X_{max}\ \text{model}) = 60.86 > F_{2,\,10,\,0.05} = 19.40$$

$\hat{\rho}(\hat{\beta}_i, \hat{\beta}_j) =$

1	-0.8937	-0.2551	-1×10^{-14}	0.4034	7×10^{-16}	3×10^{-14}	-9×10^{-15}	0.7788	0.0124	9×10^{-16}	-2×10^{-14}
-0.8937	1	-0.1640	7×10^{-16}	-0.2661	7×10^{-15}	-2×10^{-14}	1×10^{-14}	-0.933	0.3035	-9×10^{-15}	1×10^{-14}
-0.2551	-0.164	1	3×10^{-14}	-0.224	-2×10^{-14}	-3×10^{-14}	6×10^{-16}	0.2019	-0.846	2×10^{-14}	3×10^{-14}
-1×10^{-14}	7×10^{-16}	3×10^{-14}	1	-9×10^{-15}	-0.8937	-0.2551	0.4034	8×10^{-16}	-2×10^{-14}	0.7788	0.0124
0.4034	-0.266	-0.224	-9×10^{-15}	1	1×10^{-14}	6×10^{-16}	-1×10^{-15}	-0.0745	-0.302	-1×10^{-14}	-5×10^{-17}
7×10^{-16}	7×10^{-15}	-2×10^{-14}	-0.8937	1×10^{-14}	1	-0.164	-0.2661	-9×10^{-15}	1×10^{-14}	-0.9330	0.3035
3×10^{-14}	-2×10^{-14}	-3×10^{-14}	-0.2551	6×10^{-16}	-0.164	1	-0.2240	2×10^{-14}	3×10^{-14}	0.2020	-0.8464
-9×10^{-15}	1×10^{-14}	6×10^{-16}	0.4034	-1×10^{-15}	-0.2661	-0.224	1	-1×10^{-14}	-5×10^{-17}	-0.0746	-0.3019
0.7788	-0.9330	0.2019	8×10^{-16}	-0.0745	-9×10^{-15}	2×10^{-14}	-1×10^{-14}	1	-0.166	1×10^{-14}	-1×10^{-14}
0.0124	0.3035	-0.8464	-2×10^{-14}	-0.3019	1×10^{-14}	3×10^{-14}	-5×10^{-17}	-0.1658	1	-1×10^{-14}	-3×10^{-14}
9×10^{-16}	-9×10^{-15}	2×10^{-14}	0.7788	-1×10^{-14}	-0.9330	0.2020	-0.0745	1×10^{-14}	-1×10^{-14}	1	-0.1658
-2×10^{-14}	1×10^{-14}	3×10^{-14}	0.0124	-5×10^{-17}	0.3035	-0.8464	-0.3019	-1×10^{-14}	-3×10^{-14}	-0.1658	1

Figure A.7 The parameter correlation matrix of 2nd order X_{max} model

where $\hat{\rho}$ is the correlation matrix, $\hat{\beta}_i$ and $\hat{\beta}_i$ are the parameter estimates, and the parameters are: the intercept, x_{acid}, x_{oil}, T, $x_{acid}\,x_{oil}$, $x_{acid}\,T$, $x_{oil}T$, $x_{acid}\,x_{oil}T$, x_{acid}^2, x_{oil}^2, x_{acid}^2T and x_{oil}^2T, respectively.

Table A.7 Model reduction of 2nd order X_{max} model.

	Variables	95% confidence interval of the Coefficients	$\hat{\sigma}^2$	Lack of fit	SSres	Compared with 2nd order model
2nd order X_{max} full models	Intercept	0.46±0.45	0.000106	Lack of fit	0.0331	—
	x_{acid}	69.60±36.47				
	x_{oil}	-75.87±36.90				
	T	0.02±0.45				
	$x_{acid}*x_{oil}$	-6.34±883.55				
	$x_{acid}*T$	-17.40±36.47				
	$x_{oil}*T$	45.13±36.90				
	$x_{acid}*x_{oil}*T$	-1242.23±692.39				
	x_{acid}^2	2280.17±1483.95				
	x_{oil}^2	256.10±883.55				
	x_{acid}^2*T	278.18±692.39				
	x_{oil}^2*T	-1607.05±1483.95				
Reduced X_{max} model 1	Intercept	0.46±0.36	0.000106	Lack of fit	0.0349	$Q = 8.7158$ $< F_{2,2,0.05} = 19$
	x_{acid}	69.53±31.22				
	x_{oil}	-75.93±31.93				
	T	-0.03±0.36				
	$x_{acid}*T$	-14.59±31.22				
	$x_{oil}*T$	47.53±31.93				
	x_{acid}^2	-1242.60±613.16				
	x_{oil}^2	2276.96±1256.34				
	x_{acid}^2*T	293.14±613.16				
	x_{oil}^2*T	-1477.22±1256.34				
Reduced X_{max} model 2	Intercept	0.46±0.34	0.000106	Lack of fit	0.0350	$Q = 6.1505$ $< F_{3,2,0.05} = 19.16$
	x_{acid}	69.53±29.45				
	x_{oil}	-75.93±30.12				
	$x_{acid}*T$	-16.78±13.34				
	$x_{oil}*T$	47.06±29.60				
	x_{acid}^2	-1242.60±578.40				
	x_{oil}^2	2276.96±1185.11				
	x_{acid}^2*T	336.07±267.68				
	x_{oil}^2*T	-1461.95±1171.01				

A-9 The Conversion at 240 min X_{240} Model

The first order X_{240} model was built (Equation 4.6) and the observed X_{240} was plotted as a function of prediction of the model, as shown in Figure A.8.

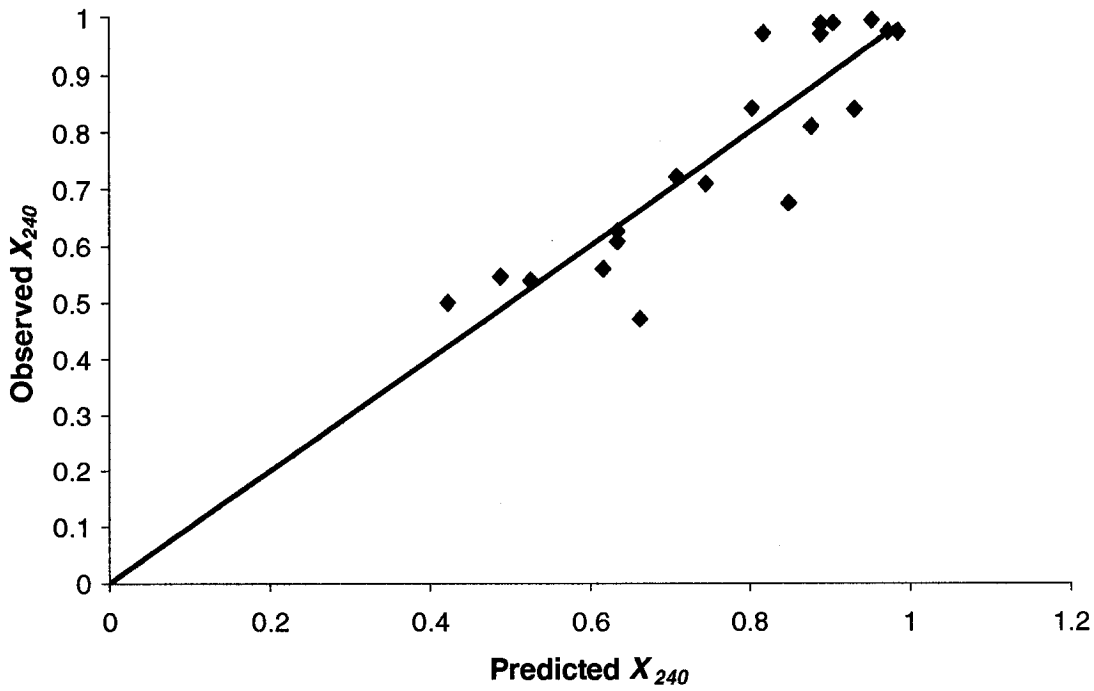

Figure A.8 Observed X_{240} vs. predicted X_{240} in the 1st order X_{240} model

And the model was found to be

$$E(Y) = 1.04 - 1.86\, x_{acid} - 26.8\, x_{oil} - 0.096\, T + 350\, x_{acid}\, x_{oil} + 5.75\, x_{acid}\, T + 12.2\, x_{oil} T - 244 x_{acid}\, x_{oil} T \quad \text{(A.10)}$$

The residuals of the first order model were examined (similar to those of the X_{max} model, omitted), and it was found that the first order model was not adequate. Thus the second order model was built and the response was plotted as a function of prediction of the model, as shown in Figure A.9.

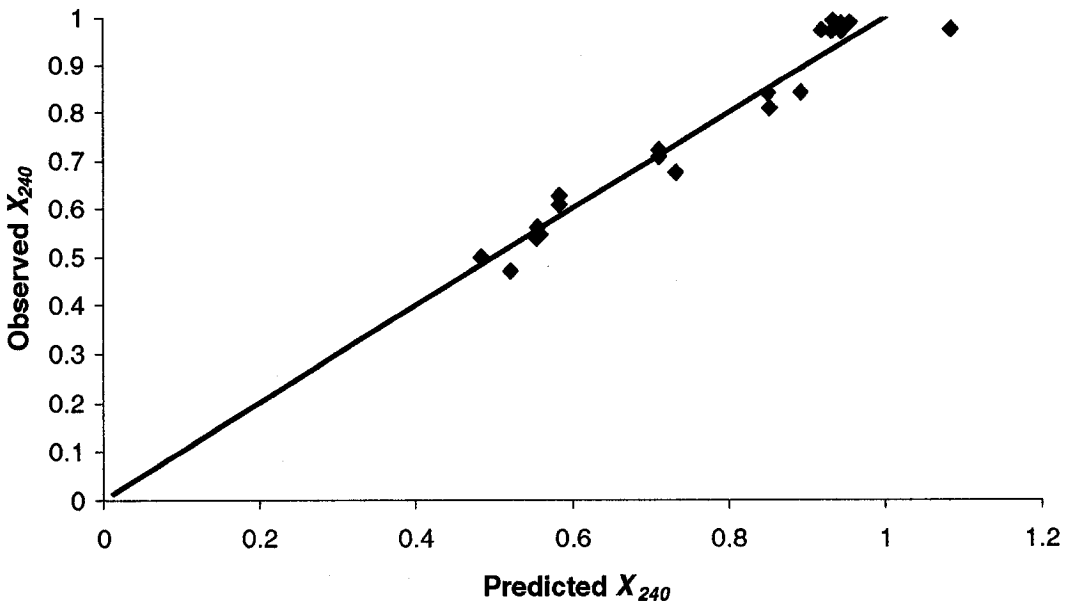

Figure A.9 Observed X_{240} vs. predicted X_{240} in the 2nd order X_{240} model

And the model was found to be

$$E(Y) = 0.46 + 69.6\, x_{acid} - 75.8\, x_{oil} + 0.024T - 6.34\, x_{acid}\, x_{oil} - 17.4\, x_{acid}T + 45.1\, x_{oil}T$$
$$+ 256\, x_{acid}\, x_{oil}T - 1242\, x_{acid}^2 + 2280\, x_{oil}^2 + 278\, x_{acid}^2T - 1607\, x_{oil}^2T \qquad \text{(A.11)}$$

Similarly, an extra sum of square test was done to compare the first order and second order model, and a lack of fit test was carried out to check the adequacy of the first and second order model. The Q and R values of these model were calculated

$$R\ (1^{st}\ \text{order}\ X_{240}\ \text{model}) = 26.83 > F_{2,\,10,\,0.05} = 19.40$$

$$R\ (2^{nd}\ \text{order}\ X_{240}\ \text{model}) = 8.18 < F_{2,\,6,\,0.05} = 19.34$$

$$Q\ (1^{st}\ \text{order vs.}\ 2^{nd}\ \text{order}) = 49.79 > F_{4,\,2,\,0.05} = 19.25$$

Thus the second X_{240} order model was more significant than the first order model. The residual plots were similar to those of the X_{max} model, thus were omitted.

Similarly, the second order model was further reduced as shown in Table A.8

Table A.8 Model reduction of 2nd order X_{240} model

	Variables	95% confidence interval of the Coefficients	$\hat{\sigma}^2$	lack of fit	SSres	Compared with 2nd order full model
2nd order X_{240} full models	Intercept	0.58 ± 0.41	0.00054	No lack of fit	0.0276	
	x_{acid}	56.15 ± 33.32				
	x_{oil}	-68.78 ± 33.71				
	T	-0.29 ± 0.41				
	$x_{acid}*x_{oil}$	248.15 ± 807.19				
	$x_{acid}*T$	17.41 ± 33.32				
	$x_{oil}*T$	27.59 ± 33.71				
	$x_{acid}*x_{oil}*T$	-1084.40 ± 632.55				
	x_{acid}^2	1756.04 ± 1355.70				
	x_{oil}^2	-111.45 ± 807.19				
	x_{acid}^2*T	-293.91 ± 632.55				
	x_{oil}^2*T	-716.65 ± 1355.70				
Reduced X_{240} model 1	Intercept	0.53 ± 0.34	0.00054	No lack of fit	0.0297	$Q = 1.93$ < $F_{2,2,0.05}$ =19
	X_{acid}	58.87 ± 28.78				
	X_{oil}	-66.46 ± 29.44				
	T	-0.27 ± 0.34				
	X_{acid}*T	16.18 ± 28.78				
	X_{oil}*T	26.55 ± 29.44				
	X_{acid}^2	-1069.91 ± 565.35				
	X_{oil}^2	1881.85 ± 1158.37				
	X_{acid}^2*T	-300.42 ± 565.35				
	X_{oil}^2*T	-773.15 ± 1158.37				

(Continued next page)

(continued from previous page)

	Variables	95% confidence interval of the Coefficients	$\hat{\sigma}^2$	Lack of fit	SSres	Compared with 2nd order full model
Reduced X_{240} model 2	Intercept	0.53 ± 0.36	0.00054	No lack of fit	0.0430	Q = 5.70 < $F_{4,2,0.05}$ =19.25
	X_{acid}	58.87 ± 30.92				
	X_{oil}	-66.46 ± 31.64				
	T	-0.02 ± 0.11				
	X_{acid}*T	2.10 ± 3.81				
	X_{oil}*T	7.13 ± 5.69				
	X_{acid}^2	-1069.91 ± 607.42				
	X_{oil}^2	1881.85 ± 1244.59				
Reduced X_{240} model 3	Intercept	0.53 ± 0.36	0.00054	No lack of fit	0.0481	Q = 6.34 < $F_{5,2,0.05}$ =19.30
	X_{acid}	58.87 ± 31.18				
	X_{oil}	-66.46 ± 31.89				
	T	0.02 ± 0.08				
	X_{oil}*T	7.60 ± 5.67				
	X_{acid}^2	-1069.91 ± 612.39				
	X_{oil}^2	1881.85 ± 1254.77				
Reduced X_{240} model 4	Intercept	0.53 ± 0.45	0.00054	No lack of fit	0.0792	Q = 13.64 < $F_{6,2,0.05}$ =19.33
	x_{acid}	58.87 ± 38.25				
	x_{oil}	-66.46 ± 39.13				
	T	0.12 ± 0.04				
	x_{acid}^2	-1069.91 ± 751.28				
	x_{oil}^2	1881.85 ± 1539.34				

A lack of fit test was carried out for the reduced second order X_{240} model and

$$R\ (2^{nd}\ \text{order reduced}\ X_{240}\ \text{model}) = 11.11 < F_{2,\,12,\,0.05} = 19.41$$

and thus the second order reduced X_{240} models is adequate.

A-10 The Overall Reaction Rate *k* Model

The first and second order *k* models were built (according to Equations 4.6 and 4.7) and the observed *k* was plotted as a function of prediction of the models, as shown in Figures A.10 and A. 11.

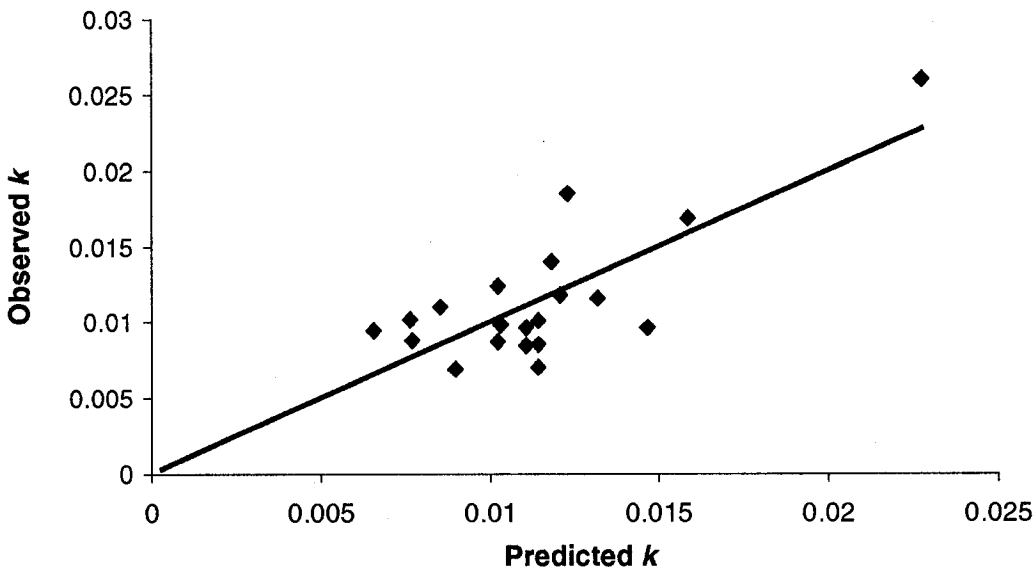

Figure A.10 Observed *k* vs. predicted *k* in the 1st order *k* model

The model form of the first order model was discussed in Chapter 4 (Equation 4.17), and the model was

$$E(Y) = 0.035 - 0.885\, x_{acid} - 1.69\, x_{oil} - 0.0304T + 22.5\, x_{acid} x_{oil} + 2.05\, x_{acid} T + 0.403\, x_{oil} T - 50\, x_{acid} x_{oil} T + 9.39\, x_{acid}^2 + 33.7\, x_{oil}^2 - 24.1\, x_{acid}^2 T + 29.6\, x_{oil}^2 T \quad \text{(A.12)}$$

A lack of fit test was done for the first order and second order *k* model and the *R* values were calculated

$$R\ (1^{st}\ \text{order}\ k\ \text{model}) = 4.47 < F_{2,\,10,\,0.05} = 19.40$$

$$R\ (2^{nd}\ \text{order}\ k\ \text{model}) = 4.32 < F_{2,6,0.05} = 19.34$$

where the value of $\hat{\sigma}^2$ is 2.63, thus the two models were adequate.

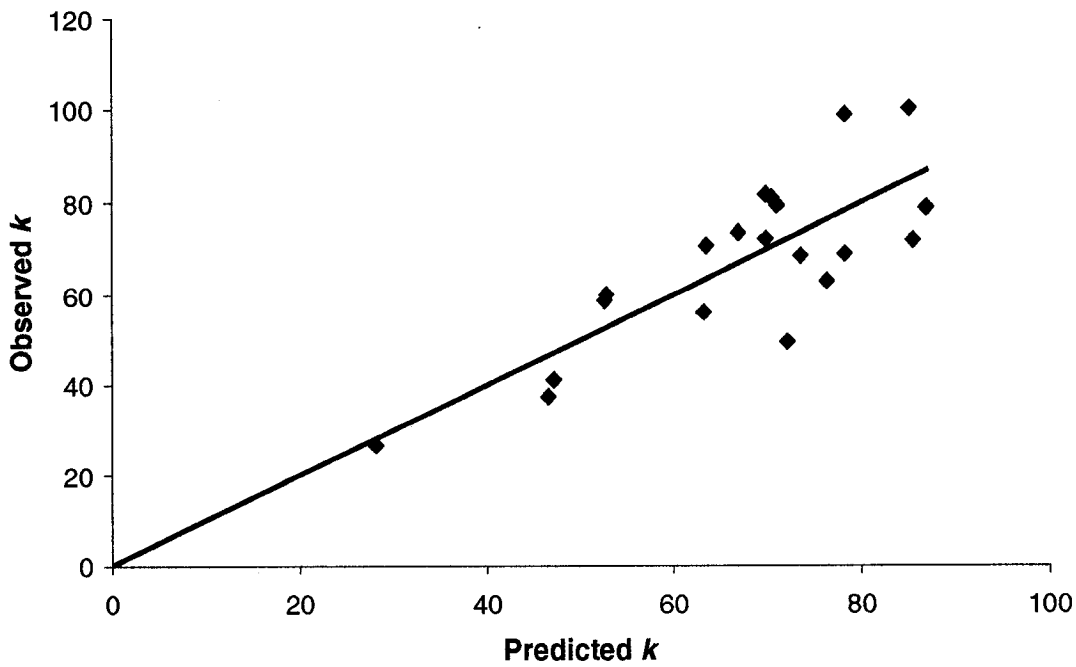

Figure A.11 Observed k vs. predicted k for the 2nd order k model.

And the comparison of first order and second order k models was carried out similar to that of the X_{max} model using extra sum square test, and the value of Q was calculated

$$Q = 4.63 < F_{4,2,0.05} = 19.25$$

Thus the first order k model is more significant than the second order k model. The residual plots of first order and second order models were omitted.

The 1st order k model was attempted to be further reduced and the correlation matrix was also calculated in Figure A.11, however, the parameters were highly correlated, and also the 95% confidence intervals of all the parameter estimates all included zero, thus it was very difficult to further reduce the model.

$\hat{\rho}(\hat{\beta}_i, \hat{\beta}_j) =$

1.0000	-0.9459	-0.9107	0.0000	0.8790	0.0000	0.0000	0.0000
-0.9459	1.0000	0.8611	0.0000	-0.9317	0.0000	0.0000	0.0000
-0.9107	0.8611	1.0000	0.0000	-0.9435	0.0000	0.0000	0.0000
0.0000	0.0000	0.0000	1.0000	0.0000	-0.9459	-0.9107	0.8790
0.8790	-0.9317	-0.9435	0.0000	1.0000	0.0000	0.0000	0.0000
0.0000	0.0000	0.0000	-0.9459	0.0000	1.0000	0.8611	-0.9317
0.0000	0.0000	0.0000	-0.9107	0.0000	0.8611	1.0000	-0.9435
0.0000	0.0000	0.0000	0.8790	0.0000	-0.9317	-0.9435	1.0000

Figure A.12 The parameter correlation matrix of the 1st order *k and* 1st order $t_{1/2}$ model

where $\hat{\rho}$ is the correlation matrix, $\hat{\beta}_i$ and $\hat{\beta}_i$ are the parameter estimates, and the parameters are: the intercept, x_{acid}, x_{oil}, T, x_{acid} x_{oil}, $x_{acid}T$, $x_{oil}T$ and x_{acid} $x_{oil}T$, respectively.

A-11 The Time to Reach 50 % Maximum Obtainable Conversion $t_{1/2}$ Model

The first and second order $t_{1/2}$ models were built (according to Equations 4.6 and 4.7) and the observed $t_{1/2}$ was plotted as a function of prediction of the models, as shown in Figures A.13 and A.14.

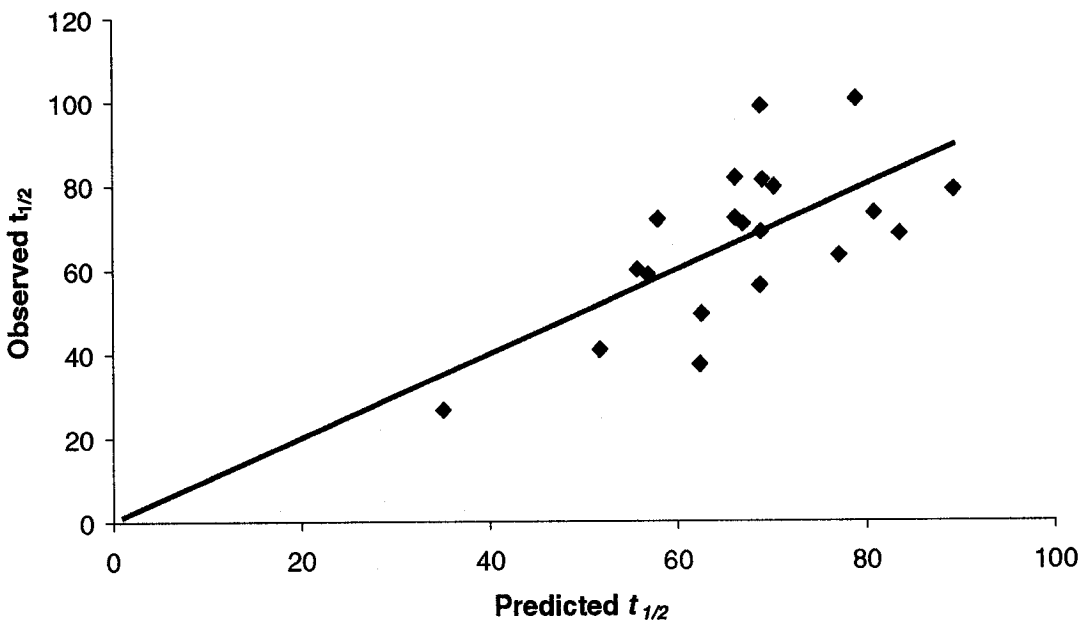

Figure A.13 Observed $t_{1/2}$ vs. predicted $t_{1/2}$ in the 1st order $t_{1/2}$ model

The model form of the first order $t_{1/2}$ was discussed (Equation 4.18) in Chapter 4, and the model form of the second order model was

$$E(Y) = 0.035 - 0.885\,X_{acid} - 1.69\,X_{oil} - 0.0304T + 22.5\,X_{acid}X_{oil} + 2.05\,X_{acid}T + 0.403\,X_{oil}T - 50\,X_{acid}X_{oil}T + 9.39\,X_{acid}^2 + 33.7\,X_{oil}^2 - 24.1\,X_{acid}^2T + 29.6\,X_{oil}^2T \quad \text{(A.3)}$$

A lack of fit test of the two models was carried out, and the R values of the first order and second order $t_{1/2}$ model were calculated

$$R\ (1^{st}\ \text{order}\ t_{1/2}\ \text{model}) = 1.24 < F_{2,\,10,\,0.05} = 19.40$$

$$R\ (2^{nd}\ \text{order}\ t_{1/2}\ \text{model}) = 1.29 < F_{2,\,6,\,0.05} = 19.34$$

where the value of $\hat{\sigma}^2$ is 246.5, thus the two models were adequate.

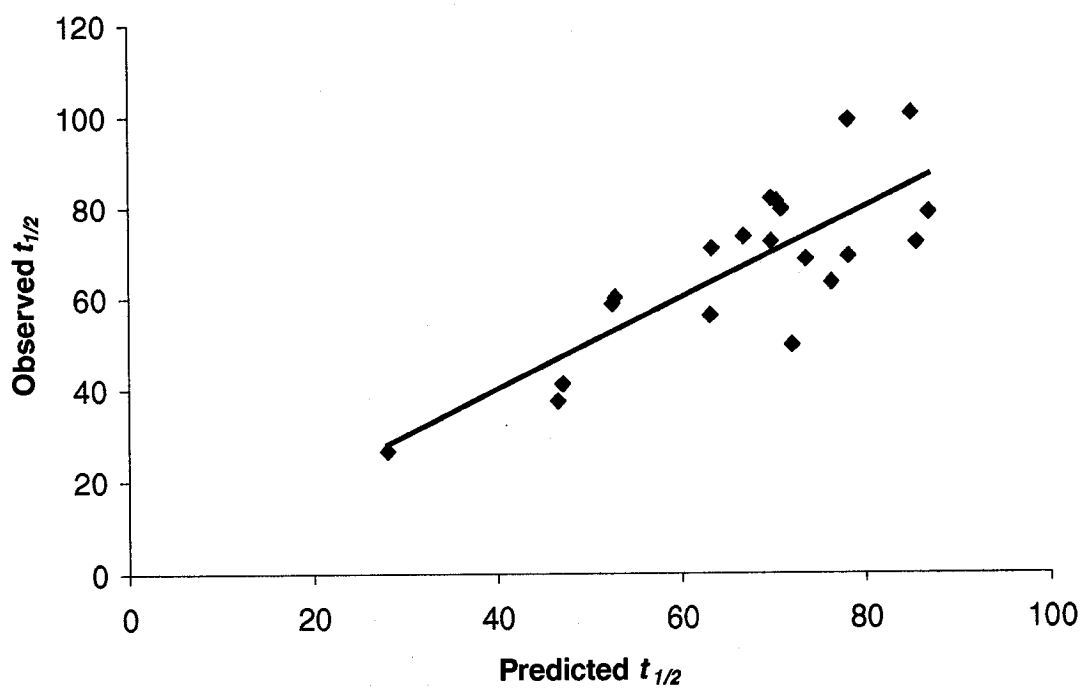

Figure A.14 Observed $t_{1/2}$ vs. predicted $t_{1/2}$ for the 2nd order $t_{1/2}$ model.

And the comparison of first order and second order $t_{1/2}$ models was carried out similar to that of the X_{max} model using extra sum square test, and the value of Q was calculated as follows

$$Q = 1.18 < F_{4,\,2,\,0.05} = 19.25$$

Thus the first order $t_{1/2}$ model is significantly better than the second order $t_{1/2}$ model.

The residual plots of first order and second order models were omitted.

The 1st order $t_{1/2}$ model was attempted to be further reduced and the correlation matrix was also calculated in Figure A.12, however, the parameters were highly correlated, and also the 95% confidence intervals of all the parameter estimates all included zero, thus it was very difficult to further reduce the model.